SUPERINTENDENCIA DE INDUSTRIA Y COMERCIO
DIRECCIÓN DE NUEVAS CREACIONES

2020
Bogotá, D.C.,

Abogada
LUZ CLEMENCIA DE PÁEZ

ASUNTO

Radicación	08-133446
Trámite	11
Evento	379
Actuación	519
Oficio	11 07 08
Folios	7

Patente de Invención	☒	Patente de Modelo de Utilidad	☐
Vía Nacional	☐		
Vía PCT (Fase Nacional)	☒	Capítulo I ☐	Capítulo II ☒

No. Solicitud Internacional	PCT/EP2007/005302
Fecha de Presentación Internacional	15/Junio/2007

Como resultado del Examen de Fondo realizado, con fundamento en el Artículo 45 de la Decisión 486 de la Comisión de la Comunidad Andina, se comunica:

1. Documentos estudiados

Descripción:	Folios 34 a 69	16/Diciembre/2008
Reivindicaciones:	Folios 70 a 74	16/Diciembre/2008
	Folios 96 a 99	24/Marzo/2009
Dibujos:	Folios 76 a 78	16/Diciembre/2008
Prioridad:	EP 06360027.4	20/Junio/2006
	US 60/861,452	29/Noviembre/2006

2. Análisis de la Prioridad

Se acepta la reivindicación de Prioridad porque esta solicitud fue presentada dentro del plazo establecido (Art. 9 D 486), y su contenido técnico corresponde con el de la prioridad reivindicada.

3. Modificaciones aceptadas

Se acepta el capítulo reivindicatorio modificado (Folios 96 a 99) porque no se amplía el objeto de la Solicitud.

4. Objeto de la invención

Título de la solicitud: "Proceso para producir poxvirus y composiciones de poxvirus".

El problema planteado en esta solicitud consiste en la necesidad de producir y purificar poxvirus para propósitos profilácticos o terapéuticos.

Para resolver este problema técnico la solicitud en estudio proporciona un poxvirus que es un EEV sin especificidad de infección objetivada y composiciones que lo contienen.

El objeto de la presente Solicitud se relaciona con la Clasificación Internacional de Patentes (CIP): A61K 48/00, 35/76, 39/00; C12N 15/863, 5/06, 7/02.

5. Reivindicaciones relativas a un uso o a un segundo uso (Art 14 y 21 D 486)

El uso de las reivindicaciones 17 – 19 no es patentable, de acuerdo con el Art 14.

6. De la Solicitud de Patente

Reivindicaciones (Art 30 D 486, Art 22 PCT)

Las reivindicaciones 1 – 7 carecen de concisión porque utilizan las expresiones "un virus vaccinia Ankara modificado recombinante", "una secuencia exógena que codifica una molécula que tiene directa o indirectamente una función citotóxica", "un gen suicida", "un antígeno Asociado a Tumor (TAA)", "una secuencia exógena que codifica un antígeno", "dicho antígeno se deriva de un virus", "comprende los elementos necesarios para la expresión de la secuencia exógena", lo cual dificulta determinar la extensión del objeto que se busca proteger. Se recuerda al solicitante que un polipéptido, un ácido nucleico (un vector recombinante) se caracterizan por la secuencia de aminoácidos y polinucleótidos, respectivamente. Por lo tanto se invita al solicitante para realizar una delimitación correcta de la invención, definir cada término de manera apropiada basándose en los ejemplos de la descripción (Folios 62 a 69), haciendo una generalización razonable de estos y de acuerdo a las definiciones establecidas en los Folios 40 a 44, como por ejemplo definir el antígeno asociado a tumor como MUC1 y definiendo la secuencia de los vectores recombinantes.

La reivindicación 8 carece no es clara ni concisa porque no se definen la naturaleza de las células de empaque, el período de tiempo de cultivo y las condiciones de recuperación de las partículas poxvíricas.

La reivindicación 13 no es clara porque no se define la proporción de los componentes dentro de la composición.

Debido a que la solicitud se refiere a material biológico, es necesario presentar el Certificado de Depósito para las cepas de virus recombinantes del que trata la invención.

La reivindicación 12 no es clara porque utiliza el término "benzonasa", el cual es una marca registrada (Benzonase®). Así mismo, la reivindicación hace referencia a que "no se utiliza nuecleasa", pero benzonasa es en sí una nucleasa. Se sugiere hacer la aclaración respectiva.

Se requiere al Solicitante hacer las aclaraciones necesarias.

7. Determinación del Estado de la Técnica

El estado de la técnica se determinó con base en la fecha de presentación de la solicitud de prioridad: Junio 20 de 2006, y se encontraron los siguientes documentos que anticipan el objeto de esta solicitud:

Ítem	Documento	Título	Fecha de Publicación
D1	Journal of Virology, Vol. 71, Pág. 3178-3187	The cytoplasmic and transmembrane domains of the vaccinia virus B5R protein target a chimeric human immunodeficiency virus type 1 glycoprotein to the outer envelope of nascent vaccinia virions	Abril/1997
D2	Journal of Virology, Vol. 71, Pág. 4032-4041	A novel virus binding assay using confocal microscopy: demonstration that the intracellular and extracellular vaccinia virions bind to different cellular receptors	Mayo/1997
D3	Cancer Immunology Immunotherapy, Vol. 50, Pág. 397-407	Transduction of human dendritic cells with a recombinant modified vaccinia Ankara virus encoding MUC1 and IL-2	22/Agosto/2001

D1 http://www.ncbi.nlm.nih.gov/pubmed?term=9060681 divulga un virus vaccinia recombinante que es un EEV sin especificidad de infección objetivada y que expresa la proteína quimérica B5R-HIV (Resumen y Pág. 3179, columna izquierda, último párrafo).

D2 http://jvi.asm.org/content/71/5/4032.full.pdf+html divulga un virus vaccinia recombinante que es un EEV sin especificidad de infección objetivada, porque no menciona que comprenda un ligando heterólogo localizado en la superficie del virus y que sirva de unión a una molécula localizada en la superficie de una célula blanco (Resumen y Pág. 4033-4034).

D3 http://www.ncbi.nlm.nih.gov/pubmed?term=11726134 divulga un virus vaccinia Ankara recombinante que codifica el antígeno asociado a tumor MUC1 y IL-2 (Resumen).

8. Examen de Patentabilidad (Art 14 D486)

Novedad (Art 16 D486)

La **reivindicación 1** consiste en un virus vaccinia Ankara modificado recombinante, en donde dicho virus vaccinia Ankara modificado recombinante es un EEV sin especificidad de infección objetivada.

Comparación de las características técnicas **esenciales**, con las del Estado de la Técnica:

Características **esenciales**	D1	D2	D3
Un virus vaccinia Ankara modificado recombinante, en donde dicho virus vaccinia	Un virus vaccinia recombinante que es un EEV sin	Un virus vaccinia recombinante que es un EEV sin	Un virus vaccinia Ankara recombinante que

Ankara modificado recombinante es un EEV sin especificidad de infección objetivada.	especificidad de infección objetivada y que expresa la proteína quimérica B5R-HIV (Resumen y Pág. 3179, columna izquierda, último párrafo).	especificidad de infección objetivada, porque no menciona que comprenda un ligando heterólogo localizado en la superficie del virus y que sirva de unión a una molécula localizada en la superficie de una célula blanco (Resumen y Pág. 4033-4034).	codifica el antígeno asociado a tumor MUC1 y IL-2 (Resumen).

Las características **esenciales** de la composición de la reivindicación 1 habían sido divulgadas previamente en D1, D2 y D3 porque:

D1 divulga un virus vaccinia recombinante que es un EEV sin especificidad de infección objetivada, porque no menciona que comprenda un ligando heterólogo localizado en la superficie del virus y que sirva de unión a una molécula localizada en la superficie de una célula blanco (Resumen y Pág. 3179, columna izquierda, último párrafo). D1 también enseña que el virus vaccinia expresa la proteína quimérica B5R-HIV (Resumen).

D2 divulga un virus vaccinia recombinante que es un EEV sin especificidad de infección objetivada, porque no menciona que comprenda un ligando heterólogo localizado en la superficie del virus y que sirva de unión a una molécula localizada en la superficie de una célula blanco (Resumen y Pág. 4033-4034). D2 también enseña que una composición que comprende 3% de EEV (Pág. 4034, párrafo 1).

D3 divulga un virus vaccinia recombinante que codifica el antígeno asociado a tumor MUC1 y IL-2 (Resumen).

En consecuencia, la reivindicación 1 carece de novedad, según lo divulgado en los documentos D1, D2 o D3.

Las reivindicaciones dependientes 2 – 7 no mencionan alguna característica que haga nueva al virus de la reivindicación 1, por lo cual se considera que no son nuevas.

La **reivindicación 13** consiste en una composición que comprende el virus vaccinia Ankara modificado recombinante de acuerdo con una cualquiera de las reivindicaciones 1 a 7 o se obtiene mediante un proceso de acuerdo con una de las reivindicaciones 8 a 12.

Comparación de las características técnicas **esenciales**, con las del Estado de la Técnica:

Características **esenciales**	**D2**
Una composición que comprende el virus vaccinia Ankara modificado recombinante de acuerdo con una cualquiera de las reivindicaciones 1 a 7 o se obtiene mediante un proceso de acuerdo con una de las reivindicaciones 8 a 12.	Una composición que comprende un virus vaccinia recombinante que comprende 3% de EEV (Resumen y Pág. 4034, párrafo 1)

Las características **esenciales** de la composición de la reivindicación 1 habían sido divulgadas previamente en D2, el cual divulga una composición que comprende un virus vaccinia recombinante que comprende 3% de EEV (Resumen y Pág. 4034, párrafo 1).

En consecuencia, la reivindicación 13 carece de novedad, según lo divulgado en el documento D1.

Las reivindicaciones dependientes 14 – 16 no mencionan alguna característica que haga nueva a la composición de la reivindicación 13, por lo cual se considera que no son nuevas.

Nivel Inventivo (Art18 D486)

Las **reivindicación 8** consiste en un proceso para producir un poxvirus intacto, un poxvirus atenuado y/o un poxvirus recombinante sin especificidad de infección objetivada que comprende las etapas de:

a) Preparar un cultivo de células de empaque
b) Infectar dicho cultivo celular
c) Cultivar dichas células infectadas durante un período de tiempo apropiado
d) Recuperar las partículas poxvíricas producidas a partir del sobrenadante de cultivo y/o las células de empaque
e) Una etapa de aclaración de la mezcla obtenida a partir de la etapa d), permitiendo el retiro de los residuos celulares, en donde dicha etapa de aclaración es una etapa de filtración profunda
f) Una etapa de concentración, en donde dicha etapa de concentración es una etapa de microfiltración, y
g) Una etapa de diafiltración

Y en donde dicho proceso está libre de productos animales.

Comparación de las características técnicas **esenciales**, con las del Estado de la Técnica:

Características **esenciales**	**D1**
Un proceso para producir un poxvirus intacto, un poxvirus atenuado y/o un poxvirus recombinante sin especificidad de infección objetivada que comprende las etapas de: (a) Preparar un cultivo de células de empaque	Un proceso para producir un poxvirus intacto, un poxvirus atenuado y/o un poxvirus recombinante sin especificidad de infección objetivada que comprende las etapas de: (i) Preparar un cultivo de células CV-1 (Pág. 3178, "Materials and methods")
(b) Infectar dicho cultivo celular	(ii) Infectar dicho cultivo celular (Pág. 3179, "Materials and methods")
(c) Cultivar dichas células infectadas durante un período de tiempo apropiado	(iii) Cultivar dichas células infectadas durante 2 días (Pág. 3179, "Isolation of recombinant viruses")
(d) Recuperar las partículas poxvíricas producidas a partir del sobrenadante de cultivo y/o las células de empaque	(iv) Recuperar las partículas poxvíricas producidas a partir del sobrenadante de cultivo y/o las células de empaque (Pág. 3179, "Purification of EEV and IMV")
(e) Una etapa de aclaración de la mezcla obtenida a partir de la etapa d), permitiendo el	(v) Una etapa de purificación en gradientes de densidad de CsCl

retiro de los residuos celulares, en donde dicha etapa de aclaración es una etapa de filtración profunda	(Pág. 3179, "Purification of EEV and IMV")
(f) Una etapa de concentración, en donde dicha etapa de concentración es una etapa de microfiltración, y	
(g) Una etapa de diafiltración Y en donde dicho proceso está libre de productos animales.	

El documento D1 se considera el estado de la técnica cercano a la invención definida en la reivindicación 8 porque divulga un proceso para producir un poxvirus intacto, un poxvirus atenuado y/o un poxvirus recombinante sin especificidad de infección objetivada que comprende las etapas de: (i) Preparar un cultivo de células CV-1 (Pág. 3178, "Materials and methods"), (ii) Infectar dicho cultivo celular (Pág. 3179, "Materials and methods"), (iii) Cultivar dichas células infectadas durante 2 días (Pág. 3179, "Isolation of recombinant viruses"), (iv) Recuperar las partículas poxvíricas producidas a partir del sobrenadante de cultivo y/o las células de empaque (Pág. 3179, "Purification of EEV and IMV") y (v) Una etapa de purificación en gradientes de densidad de CsCl (Pág. 3179, "Purification of EEV and IMV").

La diferencia entre la invención, definida en la reivindicación 8 y el proceso de D1 consiste en que la solicitud en las etapas (e) – (g) utiliza operaciones de filtración y diafiltración para purificar el producto.

Esta diferencia no parece conceder un efecto técnico inesperado o una ventaja al proceso reclamado en esta solicitud porque no permite mejorar la purificación del poxvirus de acuerdo a la descripción.

El problema técnico objetivo de esta solicitud consiste en suministrar un proceso para producir un poxvirus alternativo al ya conocido en D1.

Teniendo en cuenta que D1 ya divulgaba un proceso para producir un poxvirus intacto, un poxvirus atenuado y/o un poxvirus recombinante sin especificidad de infección objetivada que comprende las etapas de: (i) Preparar un cultivo de células CV-1 (Pág. 3178, "Materials and methods"), (ii) Infectar dicho cultivo celular (Pág. 3179, "Materials and methods"), (iii) Cultivar dichas células infectadas durante 2 días (Pág. 3179, "Isolation of recombinant viruses"), (iv) Recuperar las partículas poxvíricas producidas a partir del sobrenadante de cultivo y/o las células de empaque utilizando un homogenizador (Pág. 3179, "Purification of EEV and IMV") y (v) Una etapa de purificación en gradientes de densidad de CsCl (Pág. 3179, "Purification of EEV and IMV"), y que es bien conocido en el estado del arte que el proceso de diafiltración es una técnica que se utiliza para remover completamente, reemplazar o disminuir la concentración de sales y solventes de soluciones de proteínas, péptidos, ácidos nucleicos y otras biomoléculas, así como para concentrar la muestra, minimizando el riesgo de pérdida de la muestra o contaminación[1], la persona del oficio medianamente versada en la materia habría inferido sin mucho esfuerzo de su parte, optimizar la etapa de purificación del producto para obtener un proceso de preparación de poxvirus.

1. Pall Life Sciences Scientific and Technical Report. Diafiltration: A Fast, Efficient Method for Desalting, or Buffer Exchange of Biological Samples. 2003.

De manera que la solución propuesta por esta solicitud en la reivindicación 8 y sus dependientes 9 – 12, es obvia y no tiene Nivel Inventivo.

9. Conclusión

Los requisitos de Patentabilidad de la presente Solicitud están afectados así:

Ítem	Documento	Reivindicaciones afectadas	Requisito que afecta
D1	Journal of Virology, Vol. 71, Pág. 3178-3187	1 – 12	Novedad y Nivel Inventivo
D2	Journal of Virology, Vol. 71, Pág. 4032-4041	1 – 7 y 13 – 16	Novedad
D3	Cancer Immunology Immunotherapy. Vol. 50, Pág. 397-407	1 – 7	Novedad

En cumplimiento del artículo 45 de la Decisión 486 de la Comisión de la Comunidad Andina, se le indica que debe dar respuesta dentro del término de sesenta (60) días contados a partir de la fecha de notificación de la presente comunicación. En caso de no dar respuesta al presente requerimiento, o si a pesar de la respuesta subsistieran los impedimentos para la concesión, se denegará la patente.

Se invita al solicitante se sirva indicar, si así lo considera, su renuncia al término faltante para dar respuesta a este requerimiento y presentarla por escrito

Notifíquese el presente oficio conforme a lo dispuesto en el numeral 5.2, literal e), del capítulo quinto del título primero de la Circular Única No. 10 de 2001.

JOSÉ LUIS SALAZAR LÓPEZ
Director de Nuevas Creaciones (C)

El anterior requerimiento fue notificado por fijación en lista, de fecha

20 JUN. 2012

Elaborado por: Juan David Moncaleano
Revisado por: Consuelo Leguizamón.

JOURNAL OF VIROLOGY, Apr. 1997, p. 3178–3187
0022-538X/97/$04.00+0

Vol. 71, No. 4

The Cytoplasmic and Transmembrane Domains of the Vaccinia Virus B5R Protein Target a Chimeric Human Immunodeficiency Virus Type 1 Glycoprotein to the Outer Envelope of Nascent Vaccinia Virions

EHUD KATZ,† ELIZABETH J. WOLFFE, AND BERNARD MOSS*

Laboratory of Viral Diseases, National Institute of Allergy and Infectious Diseases, Bethesda, Maryland 20892-0445

Received 26 September 1996/Accepted 10 December 1996

The outer envelope of the extracellular form of vaccinia virus (EEV) is derived from the Golgi membrane and contains at least six viral proteins. Transfection studies indicated that the EEV protein encoded by the B5R gene associates with Golgi membranes when synthesized in the absence of other viral products. A domain swapping strategy was then used to investigate the possibility that the B5R protein contains an EEV targeting signal. We constructed chimeric genes encoding the human immunodeficiency virus (HIV) type 1 glycoprotein with the cytoplasmic and transmembrane domains replaced by the corresponding 42-amino-acid C-terminal segment of the B5R protein. Recombinant vaccinia viruses that stably express a chimeric B5R-HIV protein or a control HIV envelope protein with the original cytoplasmic and transmembrane domains were isolated. Cells infected with recombinant vaccinia viruses that expressed either the unmodified or the chimeric HIV envelope protein formed syncytia with cells expressing the CD4 receptor for HIV. However, biochemical and microscopic studies demonstrated that the HIV envelope proteins with the B5R cytoplasmic and transmembrane domains were preferentially targeted to the EEV. These data are consistent with the presence of EEV localization signals in the cytoplasmic and transmembrane domains of the B5R protein.

Poxviruses, of which vaccinia virus is the prototype, have double-stranded DNA genomes within complex core structures that are surrounded by multiple membranes (12, 43). The surface of intracellular mature virions (IMV) is composed of two tightly apposed membranes derived from the intermediate compartment between the endoplasmic reticulum and the Golgi complex (35, 61). Some IMV are subsequently wrapped by cellular cisternae derived from the trans Golgi network, thereby acquiring two additional membranes (11, 31, 42, 56, 64). The resulting four-membrane intracellular enveloped virions (IEV) are transported by actin-containing microfilaments to the periphery of the cell (10, 30, 63). The outermost viral membrane of the IEV fuses with the plasma membrane, producing two related forms of externalized virions: cell-associated enveloped virions (CEV) that mediate cell-to-cell infection (3) and released extracellular enveloped virions (EEV) that mediate long-range transmission (47).

The protein components of the IMV and EEV membranes are predominantly if not exclusively viral (46, 55). Viral genes encoding many of the proteins associated with the IMV and EEV membranes have been identified. The proteins associated with the IMV membrane or its precursors are nonglycosylated and are encoded by the A17L (35, 52, 66), A27L (37, 53), D8L (39, 44, 60), D13L (62), and L1R (50, 51, 67) genes. The EEV membranes contain one nonglycosylated protein encoded by the F13L gene (2, 32, 57, 58) and glycosylated proteins encoded by the A33R (54), A34R (4, 15, 41), A36R (45), A56R (6, 59), and B5R (22, 23, 33, 65) genes.

The detection of EEV proteins in the Golgi network, wrapping cisterna, and outer EEV membrane of infected cells suggests that some viral proteins possess Golgi network retention and EEV targeting signals (31, 56). It may not be necessary for all EEV proteins to have such signals, since some could be targeted by interaction with another protein that has one. Alternatively, Golgi network retention might require the formation of oligomeric structures composed of several proteins. Of the six known EEV proteins, A34R and A56R are not required for EEV formation, A36R enhances EEV formation only 2.5- to 5-fold (45), and no information is yet available for A33R. Deletion of the F13L (2) or B5R (23, 65) gene prevents wrapping of the IMV with Golgi network, indicating a key role for these proteins in EEV formation. Moreover, the latter proteins both concentrate in the trans Golgi network during vaccinia virus infection (56). The F13L product is not an integral membrane protein, and acylation is required for membrane association (31, 48, 58), whereas the B5R protein is a type 1 integral membrane glycoprotein (33). Based on the information presented above, we considered that the B5R protein was likely to have Golgi network retention and EEV targeting signals. Here, we report that the B5R protein localized in the Golgi network when expressed by itself in transfected cells and that the 42-amino-acid C-terminal segment of the B5R protein, which constitutes the transmembrane (TM) and cytoplasmic domains, was sufficient to target a chimeric HIV-1 envelope (*env*) glycoprotein to the EEV membrane in infected cells.

MATERIALS AND METHODS

Viruses and cells. HeLa S3 (ATCC CCL 2.2), BS-C-1 (ATCC CCL 26), CV-1 (ATCC CCL 70), Cos-7 (ATCC CRL 1651), and RK_{13} (ATCC CCL 37) cells were grown in Eagle minimum essential medium (Quality Biologicals, Gaithersburg, Md.) supplemented with 10% fetal calf serum. Vaccinia virus strains WR (ATCC VR-1354) and IHD-J (derived from ATCC VR-156) and recombinant viruses prepared from them were propagated as previously described (18). Recombinant vaccinia viruses were handled under BL-2 conditions by individuals

* Corresponding author. Mailing address: Laboratory of Viral Diseases, NIAID, NIH, Building 4, Room 229, 4 Center Dr., MSC 0445, Bethesda, MD 20892-0445. Phone: (301) 496-9869. Fax: (301) 480-1147. E-mail: bmoss@nih.gov.

† Permanent address: Department of Virology, Hebrew University-Hadassah Medical School, Jerusalem 91120, Israel.

who had recently received a smallpox vaccination, in accordance with recommendations of the Immunization Practices Advisory Committee (34).

Antibodies. Two human immunodeficiency virus (HIV)-specific antisera were kindly provided by P. Earl; mouse monoclonal antibody (MAb) D47 (17), which reacts with the V3 loop of HIV *env*, and rabbit polyclonal antiserum 2144, raised against purified gp140 (HIV-1 *env* protein lacking the TM and cytoplasmic domains). L. Payne and G. Hiller provided MAb 20 (48), which reacts with gp42 encoded by the vaccinia virus B5R open reading frame (ORF) (33), and a rabbit polyclonal antiserum against p37 encoded by the F13L ORF (29), respectively. MAbs to F13L and B5R were gifts of G. Griffiths (56). We prepared rabbit antisera to a 12-amino-acid peptide, CDKNNDQYKFHK, of the cytoplasmic tail of the gp42 (B5R) protein and to a 23-amino-acid peptide, RLVETLPENMDFR SDLHLITFEC, of the N terminus of the p37 (F13L) protein. A MAb to the influenza virus hemagglutinin (HA) (25) was provided by J. Yewdell.

Plasmid expression vectors containing the B5R and F13L ORFs. A copy of the B5R ORF flanked by *Bgl*II sites was generated by PCR with purified vaccinia virus strain WR DNA as a template and primers EW12, 5'-GGGAGATCTAA AATGAAAACGATTTCCGTTGTT-3', and EW13, 5'-GGGAGATCTAGATT ACGGTAGCAATTTATGGAA-3' (restriction endonuclease sites are underlined). In a similar fashion, a copy of the F13L ORF flanked by *Eco*RI sites was generated with primers EW22, 5'-GGGGAATTCAAAATGTGGCCATTTGC ATCGGTA-3', and EW23, 5'-GGGGAATTCTTTTTAAATTTTTAACGATT TACT-3'. The PCR products of 1,021 and 1,240 bp were cloned into either the *Bgl*II or *Eco*RI site of the simian virus 40 early promoter expression vector pSG5 (28) (provided by R. Rosales), generating pSG542.1 and pSG537.1, respectively. Correct orientation of the DNA inserts was determined by DNA sequencing.

Construction of a chimeric B5R–HIV-1 *env* gene. DNA encoding the ectodomain of the HIV-1 *env* protein (49) was derived from plasmid pPE15 (19), in which the *env* protein was modified to eliminate cryptic vaccinia virus transcriptional termination signals, and from pPE12CB (17), in which the codons for 12 amino acids surrounding the proteolytic cleavage site between gp120 and gp41 were replaced with codons for Ser-Arg. The *Sst*I-*Xba*I fragment from pPE15 was ligated with *Sst*I- and *Xba*I-cut pUC18 (that had been modified by deletion of the *Hin*dIII site). The resultant plasmid, pEK1, encodes the full-length cleavable HIV-1 *env* protein. The *Hin*dIII-*Sst*I fragment of the plasmid pPE12CB was exchanged with the parallel fragment from pEK1, giving rise to the plasmid pEK2 encoding the noncleavable HIV-1 *env* protein. A three-step recombinant PCR protocol was then performed. In the first step, DNA segments containing the *Hin*dIII site to the TM region of the HIV-1 *env* protein and the TM and cytoplasmic domains of B5R were synthesized separately. The primers for the HIV-1 *env* segment were as follows: A, 5'-CAATTACACAAGCTTAATACAC TCC-3' (the *Hin*dIII site is underlined), and B, 5'-*ATGATAAGTTGC*TTATAT ATACCACAG-3', containing nucleotides 985 to 974 of B5R (in italics) and 2034 to 2020 of the HIV-1 *env* gene. The B5R fragment was generated with primers C, 5'-GGTATATAAAA*GCAACTTATCATATAATC*, containing nucleotides 2024 to 2034 of HIV-1 *env* and nucleotides 974 to 991 of B5R (in italics), and D, 5' GGGGAGCTCGCGGCCGCTTA*CGGTAGCAATTTATG*-3', containing the restriction sites for *Sst*I and *Not*I (underlined), a stop codon, and nucleotides 1099 to 1085 of the cytoplasmic domain of B5R (in italics). The two DNA fragments formed by PCR were then recombined in a third amplification reaction, using primers A and D, to generate a 300-bp fragment containing the sequence encoding the chimeric B5R–HIV-1 *env* protein. The *Hin*dIII-*Sst*I fragments (encoding the C-terminal sequences of HIV-1 *env*) of pEK1 and pEK2 were replaced with the *Hin*dIII- and *Sst*I-cut DNA formed in the third PCR. The two plasmids formed (pEK3 and pEK4) were then digested with *Sal*I and *Not*I, and the ORFs were ligated to *Sal*I- and *Not*I-cleaved $pSC11_{S\text{-}B\text{-}A\text{-}K\text{-}N}$ (a vector provided by I. Bacik that contains *Sal*I, *Bgl*II, *Apa*I, *Kpn*I, and *Not*I sites inserted into the *Sma*I site of pSC11 [7]), giving rise to pEK5 (with cleavable *env*) and pEK6 (with noncleavable *env*).

Isolation of recombinant viruses. Recombinant vaccinia viruses were prepared as previously described (20). CV-1 cells were infected with vaccinia virus (WR or IHD-J strain) at 1 PFU/cell. After 2 h, calcium phosphate-precipitated pEK5 or pEK6 was added, and the infected-transfected cells were harvested after 2 days. Combined thymidine kinase-negative (TK^-) selection and β-galactosidase color screening were used for repetitive plaque purifications of the recombinants WR/EK5, WR/EK6, IHD/EK5, and IHD/EK6. The transfer vectors pPE16 and pPE12 (obtained from P. Earl [16, 19]) were used to construct the recombinant IHD viruses IHD/PE16 and IHD/PE12, containing genes encoding nonchimeric HIV-1 *env* proteins, with or without cleavage sites, respectively. A recombinant virus (IHD/SC11), containing the expression vector only (without any HIV *env* insert), was also constructed and isolated.

Purification of EEV and IMV. EEV and IMV were isolated from RK_{13} cells at 48 h after infection. EEV were collected by centrifugation of clarified culture medium in an SW28 rotor at 14,000 rpm for 1 h at 4°C. IMV were collected by sedimentation of the cytoplasm, from Dounce-homogenized cells, through a cushion of 36% sucrose in an SW28 rotor at 13,500 rpm for 80 min at 4°C. Both EEV and IMV were purified in CsCl density gradients (46). The virus suspensions (0.5 ml) were layered on preformed, discontinuous layers of CsCl (2.5 ml of 1.30 g/ml, 3.5 ml of 1.25 g/ml, and 4.5 ml of 1.20 g/ml) in 10 mM Tris, pH 9. Centrifugation was done in an SW41 rotor at 32,000 rpm for 1 h at 15°C. When EEV from clarified medium of infected cultures were purified, a single band at a refractive index of 1.357 appeared; when the cytoplasmic extract was sedimented, two bands with refractive indexes of 1.357 (containing IEV or CEV) and 1.360 (containing IMV) were detected. Virus bands were collected and used directly for immunogold staining or sedimented and kept at −70°C for immunoblotting.

Transient synthesis of the B5R and F13L proteins. Cos-7 cells were grown on coverslips in 24-well plates to approximately 75% confluency and then transfected with 2 μg of polyethylene glycol-precipitated pSG5, pSG542.1, or pSG537.1 in serum-free medium with Lipofectin reagent (Gibco Life Technologies, Gaithersburg, Md.) as recommended by the manufacturer. Transfected cells were incubated at 37°C for 4 to 5 h, at which time an equal volume of medium containing 20% fetal calf serum was applied to each well. The incubation was allowed to proceed for a further 40 h, and cells were fixed in 3% paraformaldehyde.

Indirect immunofluorescence microscopy. Indirect immunofluorescence microscopy of transfected Cos-7 cells was performed as previously described (33). Briefly, cell monolayers on coverslips were infected with 5 PFU of recombinant vaccinia virus per cell; after 8 h, the cells were washed with phosphate-buffered saline (PBS) and fixed in 3% paraformaldehyde. Permeabilization and subsequent washing steps were carried out in PBS with 0.05% saponin (Calbiochem, San Diego, Calif.). The cells were incubated with rat MAb 15B6 or 19C2 to F13L or B5R EEV protein, respectively (56); washed; and then incubated with fluorescein isothiocyanate-conjugated goat anti-rabbit antibody (DAKO Corp., Carpinteria, Calif.). Golgi apparatus colocalization was performed with rhodamine-conjugated *Ricinus communis* agglutinin I (Vector Laboratories).

Immunostaining of virus plaques. BS-C-1 cell monolayers were infected with a recombinant virus, fixed on the following day with an equal mixture of ethanol and acetone, and then incubated with rabbit polyclonal antiserum (1:1,000) to HIV gp140. Donkey antibodies prepared against rabbit immunoglobulin G conjugated to horseradish peroxidase (Amersham Life Science, Inc., Arlington Heights, Ill.), were then added, followed by the substrate 3,3' dimethoxybenzidine (*o*-dianisidine) (Sigma Chemical Co., St. Louis, Mo.) and H_2O_2. When the expected antigen was made, a brown color (the oxidized form of dianisidine) was visualized by light microscopy (27).

Immunoblotting. Polypeptides from cell extracts or purified virions were dissociated with 2% sodium dodecyl sulfate (SDS) and 5% mercaptoethanol at 100°C and resolved by electrophoresis in a 10% polyacrylamide gel (36). The proteins were transferred to a nitrocellulose membrane (NitroPure; Micron Separations Inc., Westborough, Mass.) by electrophoresis in 150 mM glycine–20 mM Tris-HCl (pH 8.0)–20% methanol at 70 mA for 15 h. The membrane was incubated with blocking buffer (0.5% gelatin, 0.15% Tween 20 in PBS) for 1 h and was then incubated with specific antibodies in the same buffer for 3 to 4 h. The membrane was extensively washed with 0.5% Tween 20 in PBS and immersed in blocking buffer supplemented with 1 μCi of ^{125}I-labeled protein A (30 mCi/mg; Amersham International, Amersham, United Kingdom) per ml. The membrane was washed again and exposed to X-ray film (BioMax MR; Eastman Kodak, Rochester, N.Y.).

Reprobing of blots. Blots that had previously been developed with ^{125}I-protein A were rehydrated and incubated with 1:500 dilution of antiserum in PBS containing 1% Tween 20 for 2 h. After being washed, the blots were incubated with a 1:2,000 dilution of goat anti-rabbit immunoglobulin G conjugated to alkaline phosphatase (Sigma Chemical Co.) for 45 min and washed, and bound antibody was detected with the BCIP (5-bromo-4-chloro-3-indolylphosphate toluidinium)-nitroblue tetrazolium phosphatase system (Kirkegaard & Perry Laboratories, Gaithersburg, Md.).

Syncytium assay (1). HeLa cell monolayers were infected with 10 PFU of either vaccinia virus recombinant vCB3 which contains the cDNA of the human CD4 gene (5), WR/EK5, or WR/EK6 per cell. After 2 h at 37°C, the cells were dispersed, suspended at 5×10^5 cells per ml of growth medium, and incubated for 15 h at 31°C in a polyallomer tube (to which the cells do not firmly adhere). After being washed and counted, 75,000 cells that had been infected with vCB3 were mixed with an equal number of cells that had been infected with WR/EK5 or WR/EK6. The cell mixtures (0.6 ml) were seeded in each well of a 24-well cell culture cluster (Costar Co., Cambridge, Mass.), incubated for 20 h at 37°C, and then fixed with methanol-acetone (1:1) and stained with crystal violet (0.1% in 0.1 M citric acid).

Immunogold labeling of thawed cryosections. RK_{13} cells were grown in 60-mm-diameter dishes, infected with 10 PFU of recombinant vaccinia virus per cell, fixed, and prepared for ultrathin cryosectioning as previously described (66) with a Leica/Reichert Ultracryomicrotome FCS. Thawed sections were incubated with serum (1:500) from rabbits that had been immunized against purified HIV gp140 followed by protein A conjugated to 10-nm-diameter colloidal gold (Department of Cell Biology, Utrecht University School of Medicine, Utrecht, The Netherlands) and then stained with 0.3% uranyl acetate (Electron Microscopy Sciences, Fort Washington, Pa.) in 1.8% methylcellulose and viewed with a Philips CM100 electron microscope.

Immunogold labeling of EEV. Carbon-coated grids were floated on a suspension of CsCl-purified EEV or IMV. After being blocked with 1% Teleostean gelatin (Sigma Chemical Co.) in PBS, the grids were layered successively on solutions containing MAb D47 (47.2 μg/ml) or the MAb to influenza virus HA (47.4 μg/ml) for 30 min and then on 10-nm-diameter colloidal gold conjugated to protein A. The grids were washed and fixed with 1% glutaraldehyde (Electron Microscopy Sciences) in PBS and then negatively stained with 2% uranyl acetate.

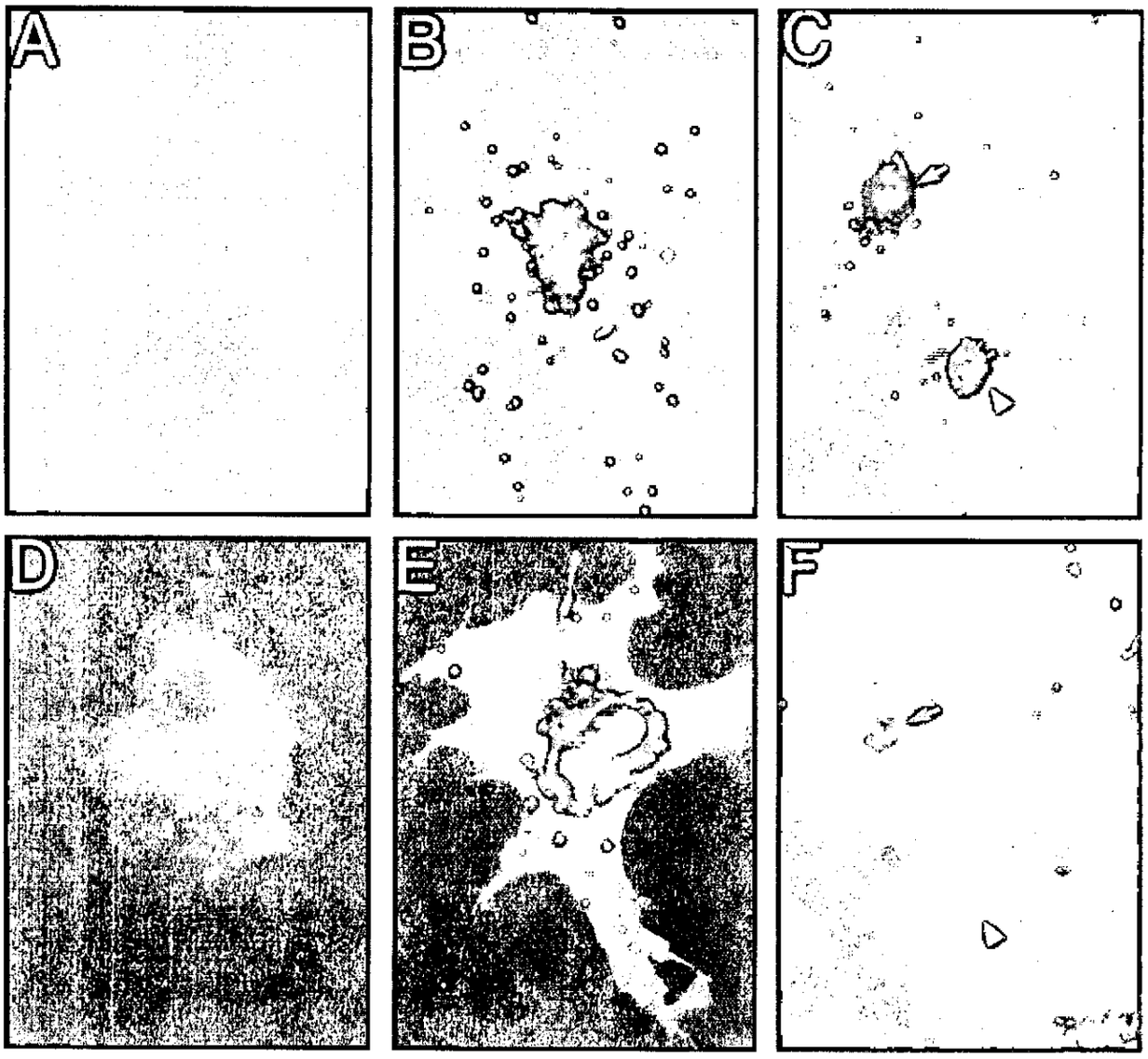

FIG. 1. Intracellular localization of the B5R and F13L proteins expressed separately in the absence of other viral proteins. Cos-7 cells were grown on coverslips and either untransfected (D) or transfected with the pSG5 vector (A) or pSG42.1 encoding the B5R gene (B, C, and F) or pSG37.1 encoding the F13L gene (E). After 45 h, the cells were examined by indirect immunofluorescence microscopy with antibody to the B5R protein (A, B, and C) or the p37 protein encoded by F13L (D and E) and fluorescein-conjugated anti-rabbit antibody. For Golgi apparatus localization (F), rhodamine-conjugated *R. communis* agglutinin was used. The arrows and arrowheads in panels C and F point to Golgi colocalization of antibody to B5R and *R. communis* agglutinin.

RESULTS

Intracellular localization of the B5R and F13L proteins. Plasmid expression vectors containing either the vaccinia virus B5R or F13L ORF were transfected into uninfected Cos-7 cells to determine the intracellular localization of the encoded proteins in the absence of other viral gene products. Immunofluorescence microscopy of B5R-transfected cells revealed an intensely staining juxtanuclear mass with the characteristic appearance of the Golgi apparatus as well as some punctate staining (Fig. 1B). The B5R Golgi staining (Fig. 1C) was confirmed by colocalization with *R. communis* agglutinin I (Fig. 1F). Apparent staining of the endoplasmic reticulum and plasma membrane were discerned in cells that highly expressed B5R (data not shown).

In cells transfected with the F13L gene, staining of F13L appeared brightest around the nucleus but was diffusely distributed throughout the cell (Fig. 1E). Untransfected cells or cells transfected with the vector alone showed low background staining (Fig. 1A and D). These data suggested that of the two proteins, B5R and F13L, the former was preferentially concentrated in the Golgi apparatus.

Construction of recombinant vaccinia viruses that express chimeric membrane glycoproteins. The TM domain, alone or together with the cytoplasmic domain, is necessary for the localization of several Golgi resident proteins (40). In view of the results discussed in the previous section, we decided to use a domain swapping strategy to determine whether the corresponding region of the B5R protein contains an EEV targeting signal.

The junction between the TM domain and ectodomain of

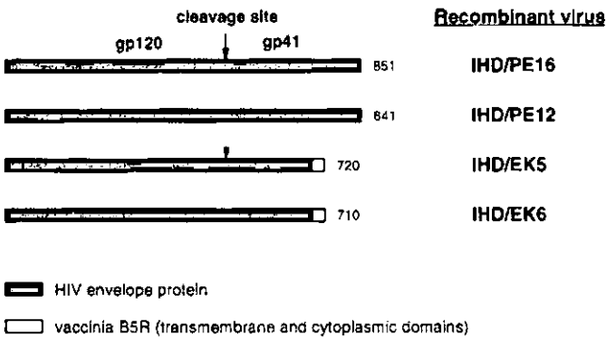

FIG. 2. Structures of chimeric B5R-HIV *env* proteins expressed by recombinant vaccinia viruses. The cytoplasmic and TM domains of the HIV-1 *env* protein are retained in the recombinant genes in vaccinia viruses IHD/PE16 and IHD/PE12, whereas they are replaced by the B5R cytoplasmic and TM domains in the recombinant genes encoded by IHD/EK5 and IHD/EK6. The site of cleavage between the gp120 and gp41 domains of the HIV-1 *env* protein was deleted in IHD/PE12 and IHD/EK6. Amino acid numbers are indicated. IHD refers to the strain of vaccinia virus used to construct the recombinant viruses. Corresponding WR strain recombinant vaccinia viruses are similarly named, with WR in place of IHD.

the vaccinia virus B5R protein had been determined by mutagenesis: when the predicted TM region was deleted, the B5R protein was secreted (33). The DNA encoding a 42-amino-acid segment, containing the cytoplasmic and TM domains of the B5R protein, was attached to the sequence encoding the ectodomain of the type 1 membrane glycoprotein encoded by HIV-1 (24). During transit through the Golgi complex, the HIV-1 *env* glycoprotein is normally cleaved into noncovalently linked gp120 and gp41 subunits that readily dissociate, resulting in the loss of gp120 from the plasma membrane or virion surface. For this reason, two chimeric genes were constructed: one with the normal, cleavable site between the gp120 and gp41 domains and the other with the cleavage site deleted.

The chimeric genes were inserted into a plasmid transfer vector so that the P7.5 promoter of vaccinia virus would regulate their expression (7). We chose a relatively weak promoter to prevent overexpression, which might perturb the normal process of EEV formation and possibly lead to premature retention of the recombinant protein in the wrong compartment. Conveniently, the vector directs recombination into the TK locus of the vaccinia virus genome, providing both TK selection and β-galactosidase color screening of recombinant viruses. Initially, the well-characterized WR strain of vaccinia virus was used for recombination. Subsequently, the same transfer vectors were used with the IHD-J strain of vaccinia virus because of the high proportion of EEV compared to CEV produced as a result of a point substitution in the A34R gene (4). The two viruses with chimeric genes retaining the gp120-gp41 cleavage sites were designated WR/EK5 and IHD/EK5; the two without cleavage sites were designated WR/EK6 and IHD/EK6 (Fig. 2). As controls, IHD-J recombinant viruses with full-length (nonchimeric) cleavable and noncleavable HIV-1 *env* genes were designated IHD/PE16 and IHD/PE12, respectively (Fig. 2).

Expression of the chimeric HIV-1 *env* glycoprotein in recombinant-vaccinia virus-infected cells. The plaques formed in BS-C-1 cells by recombinant vaccinia viruses expressing the chimeric HIV *env* genes were indistinguishable from those formed by ordinary vaccinia virus (Fig. 3), indicating no adverse effect on cell-to-cell virus spread due to an impairment in formation of extracellular virus. We also compared the spread of the recombinant viruses in monolayers of $CD4^+$ and $CD4^-$ HeLa cells and found no difference due to the presence of the HIV *env* receptor (data not shown). Immunoperoxidase staining of recombinant virus plaques using antiserum to the HIV *env* protein provided initial evidence of expression of the chimeric genes (Fig. 3).

HeLa cells infected with recombinant viruses containing the chimeric (IHD/EK6) or nonchimeric (IHD/PE12) HIV *env* gene were examined by indirect immunofluorescence microscopy with the D47 MAb to the V3 loop of the gp120 domain of the HIV-1 *env*. In both cases, we observed apparent staining of the endoplasmic reticulum, Golgi apparatus, and plasma membrane (Fig. 4A and B). However, a comparison of the two

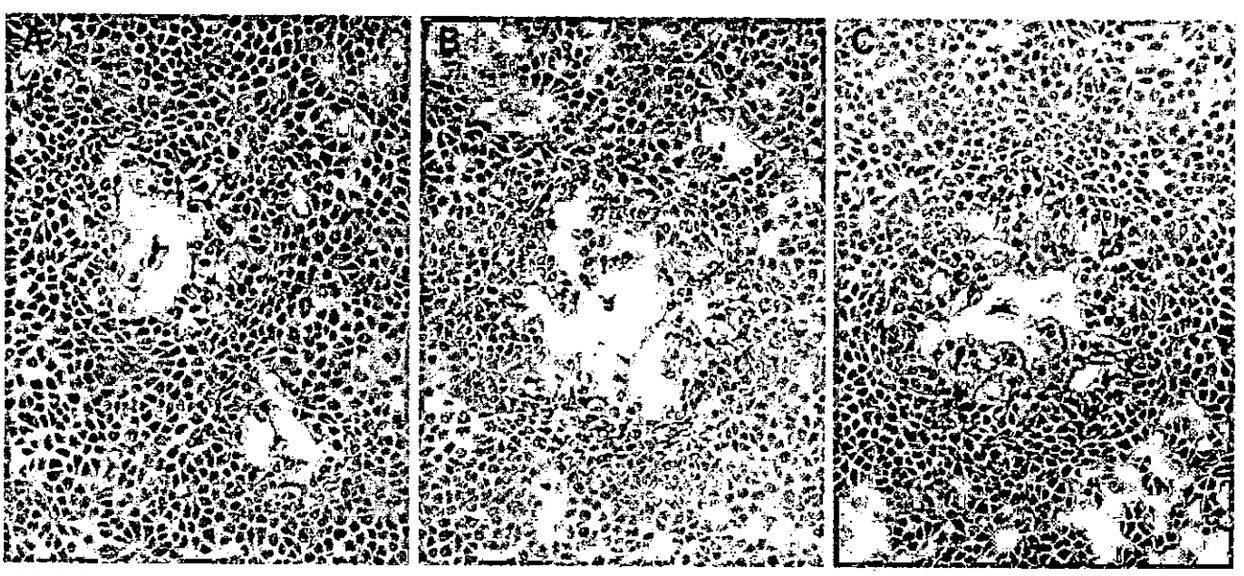

FIG. 3. Immunoperoxidase staining of recombinant virus-infected cells with antiserum against HIV-1 *env*. To show individual plaques, BS-C-1 cells were infected with a low multiplicity of vaccinia virus WR (A), WR/EK5 (B), and WR/EK6 (C). The cells were fixed on the following day, incubated with polyclonal antibody to HIV-1 *env*, and developed with an immunoperoxidase stain. Areas of the cell monolayers containing a virus plaque were photographed.

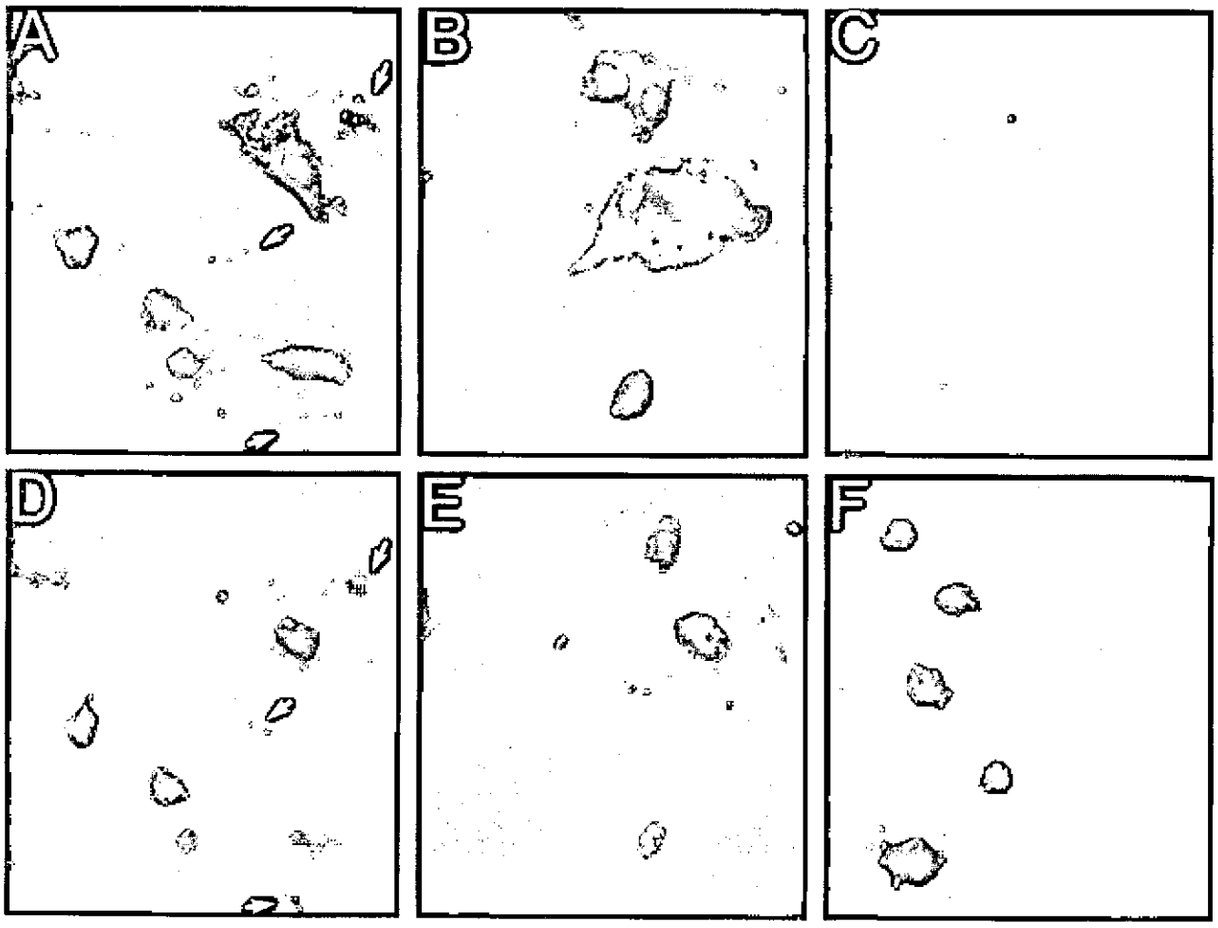

FIG. 4. Immunofluorescence microscopy of cells infected with recombinant vaccinia viruses. HeLa cells were infected with IHD/EK6 (A and D), IHD/PE12 (B and E), or IHD/SC11 (C and F) for 8 h. The cells were then fixed, permeabilized, and incubated first with mouse MAb D47 to HIV *env* (A, B, and C) or rabbit polyclonal antibody to the vaccinia virus P37 protein (D, E, and F) and then with rhodamine-conjugated rabbit anti-mouse antibody or fluorescein isothiocyanate-conjugated goat anti-rabbit antibody. The coverslips were mounted, and the cells were viewed with a fluorescence microscope. Arrows in A and D point to examples of colocalized punctate staining.

indicated an additional punctate staining pattern in cells expressing the chimeric *env* protein (Fig. 4A). Only background staining occurred in cells infected with a control vaccinia virus expressing β-galactosidase (Fig. 4C).

To investigate whether the punctate staining of the chimeric protein might represent enveloped virions, the infected cells were also incubated with antibody to the p37 EEV protein encoded by F13L. The F13L staining showed a characteristic juxtanuclear and punctate staining representing Golgi network and Golgi network-wrapped virus particles, respectively (Fig. 4D, E, and F). Some areas of p37 punctate staining colocalized with the chimeric HIV *env* protein (Fig. 4A and D), consistent with the association of the latter with enveloped vaccinia virions.

Fusion activity of the chimeric *env* glycoprotein. Infection of CD4-expressing human cells with HIV-1 or with recombinant vaccinia viruses that encode the HIV *env* protein results in syncytium formation (1, 38). HIV *env*-mediated fusion can be distinguished from vaccinia virus-mediated fusion (13, 26), as the former occurs at neutral pH, is CD4 dependent, and requires gp120-gp41 cleavage.

HeLa cells infected with WR/EK5 or WR/EK6 were mixed with HeLa cells infected with recombinant vaccinia virus vCB3 which expresses CD4. Cells infected with WR/EK5 formed syncytia (Fig. 5A), whereas cells infected with WR/EK6 (Fig. 5B) did not, since the gp120-gp41 cleavage site was deleted. In addition, cells infected with wild-type vaccinia virus instead of vCB3 did not fuse with cells infected with WR/EK5 (data not shown). These results demonstrated that some chimeric protein was properly folded and located on the cell surface, consistent with studies of B5R localization (56). Evidently the B5R cytoplasmic and TM domains could functionally substitute for those of the HIV *env* glycoprotein.

SDS-polyacrylamide gel electrophoresis (PAGE) analysis of recombinant HIV proteins. The size and glycosylation of the HIV *env* proteins were examined by immunoblotting of cytoplasmic extracts of cells infected in the absence or in the presence of tunicamycin, an inhibitor of N glycosylation. Polypeptides of approximately 160 kDa were detected with antibody to the HIV-1 *env* glycoprotein in extracts of cells infected with IHD/EK5 or IHD/EK6 (Fig. 6, left blot). Since gp120 is extensively shed into the medium after cleavage of the precursor (8), the glycosylated 160-kDa protein was the predominant band with IHD/PE12 as well as IHD/PE16 (Fig. 6, left blot). In the presence of tunicamycin, the chimeric polypeptides from IHD/EK5 and IHD/EK6 migrated as pre-

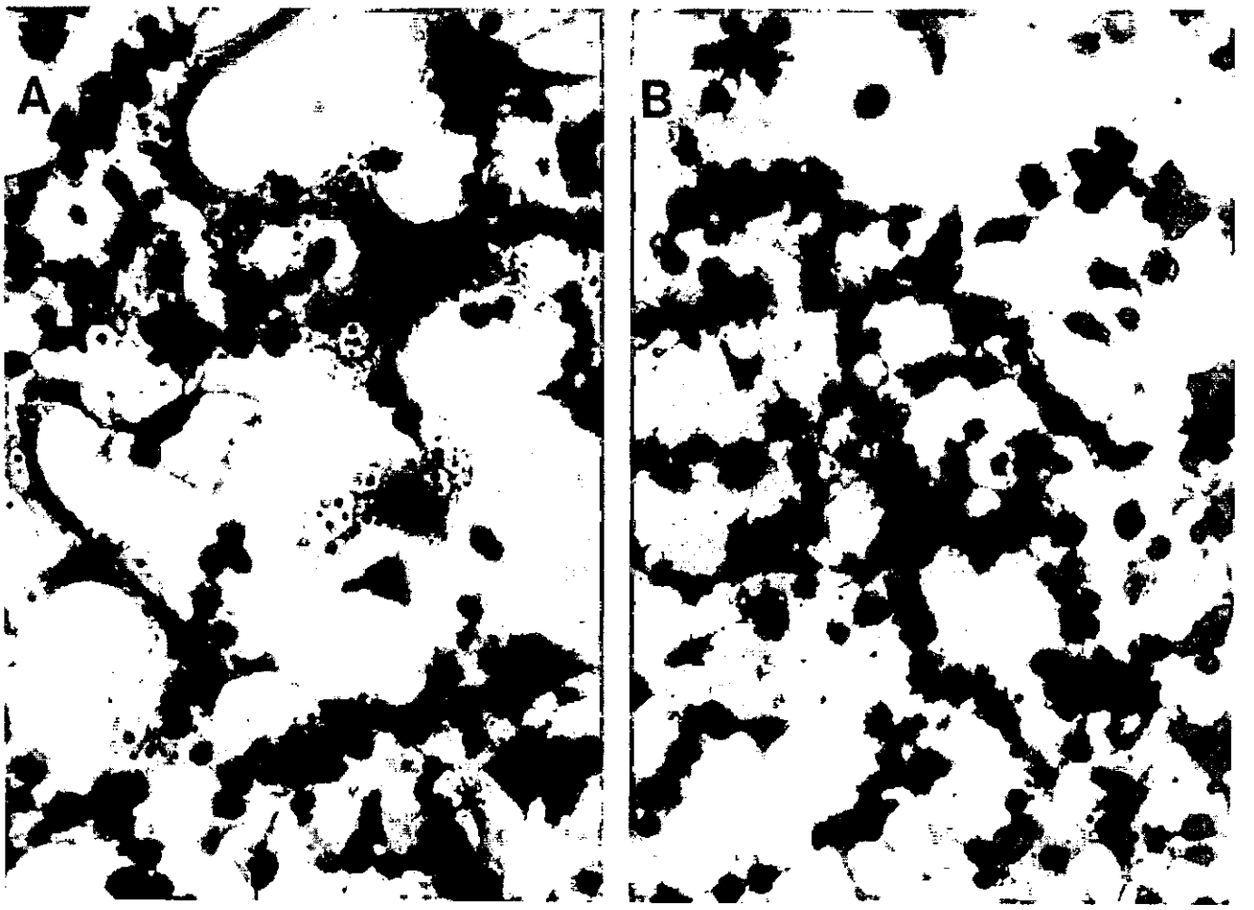

FIG. 5. HIV *env*-mediated syncytium formation. HeLa cells were infected separately with recombinant vaccinia virus vCB3 (which expresses the cDNA of the human CD4 gene) and either WR/EK5 or WR/EK6 for 15 h. At this time, cells infected with vCB3 were mixed with cells infected with WR/EK5 (A) or WR/EK6 (B) and incubated for an additional 20 h before being stained with crystal violet.

dicted for 80-kDa bands (Fig. 6, right blot). The slower mobilities of the unglycosylated, nonchimeric polypeptides expressed by IHD/PE16 and IHD/PE12 are consistent with the longer cytoplasmic domain of the HIV-1 *env* protein compared to that of B5R. The absence of the cleavage site of *env* in IHD/EK6 and IHD/PE12 appeared to increase the amounts of *env* detected particularly in the presence of tunicamycin, possibly by increasing protein stability.

The cytoplasmic domain of B5R is common to both the authentic B5R protein and the chimeric B5R/HIV *env* protein. We immunized rabbits with a peptide derived from the cytoplasmic domain and used the antisera to probe blots containing proteins from cells infected with IHD/EK5 and IHD/EK6. After incubation with ^{125}I-protein A, the relative amounts of B5R and B5R/HIV *env* protein were determined with a PhosphorImager. The results indicated that the chimeric protein from cells infected with IHD/EK5 and IHD/EK6 represented approximately 5 and 7%, respectively, of authentic B5R. The relatively small amount of chimeric protein was consistent with the weak promoter used for expression.

Association of the chimeric glycoprotein with EEV. The crucial experiment was to determine whether the chimeric glycoproteins were specifically incorporated into EEV. Similar amounts of EEV were purified by CsCl gradient centrifugation from the medium of cells infected with the various recombinant viruses. EEV proteins were analyzed by SDS-PAGE and immunoblotting with polyclonal antibody to the HIV *env* protein or with MAb D47 to the V3 loop of the gp120 portion (Fig. 7). Both antibodies reacted with a 160-kDa polypeptide present in EEV derived from cells infected with IHD/EK5 and IHD/EK6 (which express HIV *env* with B5R cytoplasmic and TM domains) but not in EEV from cells infected with IHD/PE16 or IHD/PE12 (which express HIV *env* with HIV cytoplasmic and TM domains). Evidence that a similar amount of EEV protein was present in each lane was obtained by reprobing the blots in Fig. 7 with antibody to the p37 protein (data not shown). Only when the gel was overloaded, by electrophoresis of 10 times the amount of IHD/PE12 or IHD/PE16 EEV, was gp160 detected by immunoblotting. In contrast to the results obtained with EEV, gp160 was not detected by immunoblotting of CsCl-purified IMV from the cytoplasm of cells infected with any of the recombinant vaccinia viruses. We concluded that the cytoplasmic and TM domains of the B5R protein selectively targeted the chimeric HIV *env* protein to EEV.

The larger amount of EEV-associated *env* protein from cells infected with IHD/EK6 than IHD/EK5 (Fig. 7) was consistent with the removal of the gp120-gp41 cleavage site in the former and the lability of the gp120-gp41 association in the latter. Several other specific and nonspecific bands were noted: the

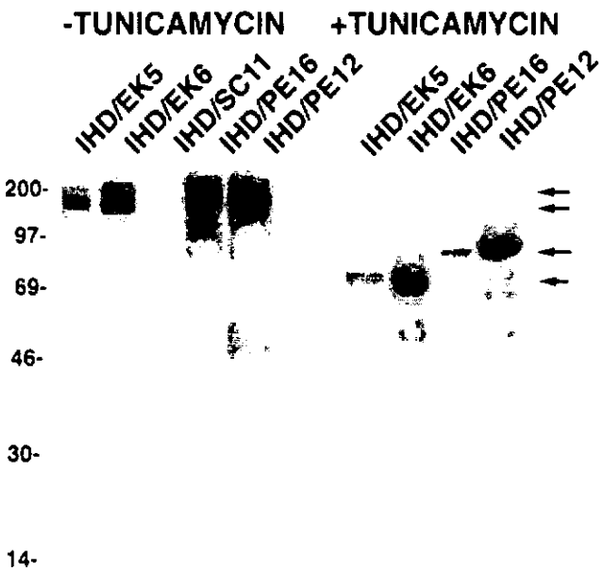

FIG. 6. SDS-PAGE analysis of glycosylated and nonglycosylated recombinant proteins. RK_{13} cells were infected with 1 PFU of the recombinant viruses described in the legend to Fig. 2 or IHD/SC11 (which expresses β-galactosidase) per cell. Tunicamycin (5 μg/ml) was added to one set of cultures (+tunicamycin) at 1 h after infection. The cells were harvested after 2 days and suspended in PBS. Immunoblotting with polyclonal antiserum (1:2,000) against HIV envelope antigen was performed following SDS-PAGE. An autoradiograph is shown. Arrows point to gp160, gp120, and unglycosylated *env* proteins. The numbers on the left are molecular masses (in kilodaltons).

HIV-specific protein of about 80 kDa was detected with polyclonal antibody but not with the V3 loop-specific MAb, because it represents a degradation product formed by cleavage within the V3 loop of the HIV *env* protein; the protein of approximately 60 kDa apparently reacts nonspecifically with protein A; lower-molecular-weight polypeptides were present in all lanes probed with the polyclonal antibody and evidently represent cross-reacting bands.

Immunogold labeling of the EEV surface. Further experiments were designed to determine whether the chimeric protein is displayed on the surface of the EEV. Two separate procedures were used. Thawed cryosections of cells infected with recombinant vaccinia virus IHD/EK6 were stained with MAb D47 and protein A-conjugated colloidal gold and then examined by electron microscopy. A field showing immunogold labeling of the outer membrane of EEV that have been released from infected cells but not of intracytoplasmic IMV is presented in Fig. 8A. Significant immunogold labeling of EEV from cells infected with IHD/PE12 was not detected (data not shown).

In the second procedure, CsCl gradient-purified EEV on carbon-coated grids were incubated with MAb D47 and then exposed to protein A-conjugated colloidal gold. An electron micrograph of an immunogold-labeled EEV from IHD/EK6-infected cells is shown in Fig. 8B. As controls, replicate grids were incubated with a MAb of the same isotype but to the influenza virus HA. The gold grains were visualized by electron microscopy, and their numbers per 100 EEV are indicated in Table 1. The largest number of grains was associated with EEV from cells infected with IHD/EK6 and IHD/EK5; the relatively few grains associated with EEV formed in cells that expressed nonchimeric HIV envelope (IHD/PE16 and IHD/PE12) were comparable to the background obtained with EEV from cells infected with a recombinant vaccinia virus that expressed β-ga-

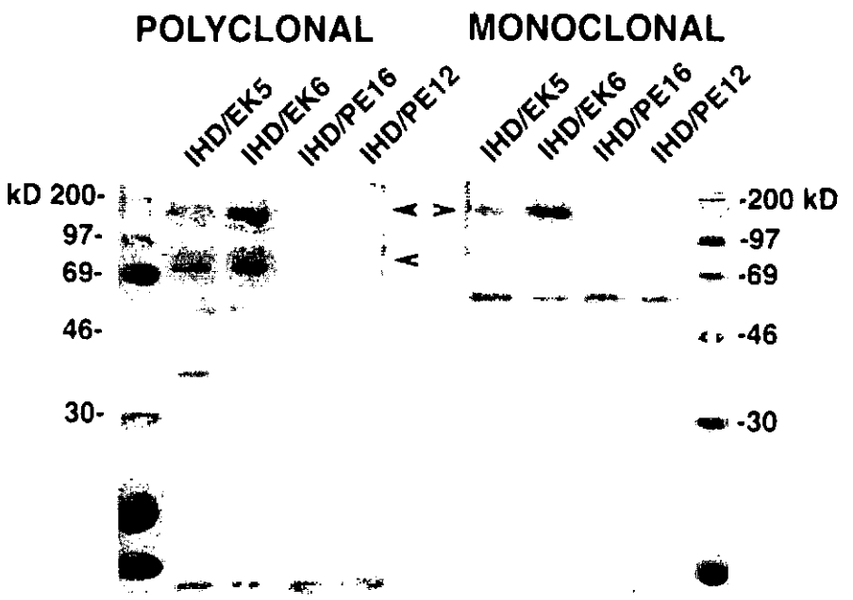

FIG. 7. Detection of chimeric proteins in EEV. EEV were purified by CsCl gradient centrifugation from the media of cells infected with recombinant vaccinia viruses. Purified EEV (0.04 optical density unit at 260 nm) were dissociated with SDS, and the component proteins were resolved by PAGE. The proteins were transferred to a nitrocellulose membrane and probed with a polyclonal antibody to the HIV-1 *env* protein (1:1,000) or with V3 loop-specific MAb D47 (1:500) followed by ^{125}I-labeled protein A. An autoradiograph is shown. The upper arrowheads point to full-length *env* proteins, and the lower one points to a proteolytically degraded form. The lane on the extreme left contains radioactively labeled marker proteins.

FIG. 8. Immunogold labeling of EEV from cells infected with IHD/EK6. (A) Thawed cryosections of HeLa cells infected with IHD/EK6 were incubated with MAb D47 and then with 10-nm-diameter colloidal gold conjugated to protein A. (B) CsCl gradient-purified EEV, from the medium of IHD/EK6-infected RK_{13} cells, were adsorbed onto a carbon-coated grid and incubated with MAb D47. The grid was then layered on 10-nm-diameter colloidal gold conjugated to protein A, fixed, and stained in uranyl acetate. Electron micrographs are shown.

lactosidase alone (IHD/SC11) or when the MAb used was to the unrelated influenza virus HA.

DISCUSSION

The goal of this project was to identify a vaccinia virus membrane protein that contains EEV targeting signals. The following criteria were used in choosing a candidate protein: Golgi localization during a natural infection, presence in IEV and EEV membranes, and requirement for EEV formation. The type 1 membrane glycoprotein encoded by the B5R gene (23, 56, 65) and the acetylated protein encoded by the F13L gene (2, 31, 48, 58) have these characteristics. We then set another criterion: Golgi localization in the absence of other viral proteins. Immunocytochemical studies of transfected cells indicated that the B5R protein localized in the Golgi compartment even under these conditions, whereas the F13L protein did not appear to do so. Thus far, independent Golgi localization has not been demonstrated for any other vaccinia virus protein, although this property may not be unique to the B5R product.

We considered several experimental approaches to determine whether B5R contains an EEV targeting signal, including random and directed mutagenesis and domain swapping. The latter strategy was attractive, since the three domains of type 1 membrane proteins generally constitute independent folding units, and consequently, exchanging domains of heterologous proteins is frequently tolerated without global disruption of structure (14). Moreover, the ability to confer a novel EEV localization property to a heterologous protein represents a gain of function and is likely to be specific. In contrast, mutations within domains are often associated with misfolding, and a loss of function would not necessarily correlate with disruption of specific signals. In choosing the cytoplasmic and TM domains as sites of Golgi and EEV localization domains, we were guided by studies with other proteins resident in the trans Golgi network (40). No consensus Golgi localization sequences have been defined, but the TM and cytoplasmic domains are important for some proteins resident in the Golgi network.

TABLE 1. Immunogold labeling of EEV with MAb to HIV-1 gp120

Recombinant virus	No. of gold grains/100 EEV with:	
	Anti-gp120[a]	Anti-HA[b]
IHD/EK5	121	18
IHD/EK6	248	23
IHD/SC11	21	10
IHD/PE16	33	9
IHD/PE12	13	6

[a] D47 MAb to V3 loop of HIV-1 gp120.
[b] MAb to the influenza virus HA.

Many choices were available for the heterologous ectodomain. The HIV-1 *env* protein was selected in part because it is a well-characterized membrane glycoprotein, antibodies to it are available, and it has specific and readily assayable biological activities such as CD4 binding and induction of cell fusion. Another purpose, to be considered elsewhere, was based on an effort to enhance the immunological response to the HIV protein expressed by a recombinant vector. Recombinant vaccinia viruses expressing the natural HIV *env* have been constructed and safely used in phase 1 human studies (9). Although we did not think it likely that incorporation of a chimeric HIV *env* protein into EEV would extend the already broad host range of vaccinia virus, all studies were carried out under BL-2 conditions by investigators who had received a recent smallpox vaccination.

The biological properties of the chimeric HIV-1 *env* protein were examined as an indicator of intracellular trafficking and proper folding of the chimeric molecule. The chimeric protein was able to induce specific syncytium formation, which requires recognition of CD4 by gp120 and fusion by gp41. Although the B5R cytoplasmic and TM domains did not abrogate biological functions of the HIV-1 ectodomain, they did confer an additional property. The chimeric protein was associated with vaccinia virus EEV that were released into the medium and purified by CsCl gradient centrifugation. The association was EEV specific, as the chimeric protein was not detected in similarly purified IMV. Furthermore, purified EEV particles were decorated by antibodies to the ectodomain of the HIV-1 glycoprotein, whereas IMV particles were not. Greater amounts of chimeric protein were detected on EEV when the gp120-gp41 cleavage site was deleted, consistent with the greater stability of the covalently linked segments. By contrast, when the HIV-1 *env* protein cytoplasmic and TM domains were used, the gel had to be overloaded with EEV to detect the

HIV-1 *env* glycoprotein by immunoblotting, and the numbers of immunogold grains associated with EEV particles were close to background.

In planning these experiments, we had elected to use a relatively weak promoter for the expression of the chimeric protein so as not to perturb EEV formation or alter cellular trafficking. The amount of the chimeric protein was found to be approximately 6% of that of B5R by Western blotting of cytoplasmic extracts using antiserum to the common cytoplasmic domain. Although we attempted to compare the amounts of native and chimeric B5R proteins in purified EEV, the background and low signal intensity prevented this. Therefore, the targeting efficiency of the chimeric protein may be less than that of authentic B5R.

Although the simplest interpretation of our data is that the B5R TM or cytoplasmic domain contains an EEV targeting signal, there is also a possibility that the 42-amino-acid C-terminal sequence interacts with authentic B5R or other viral proteins that serve as chaperones. In this context, the B5R protein migrates as an oligomer under nonreducing conditions by SDS-PAGE (22, 33). The ectodomain of the HIV-1 *env* protein itself forms dimers and higher-order oligomers (21), and experiments with other ectodomains will be needed to determine whether this property contributed to EEV localization.

Another step in the analysis of the B5R targeting signal will be to determine whether both the cytoplasmic and TM domains are required for function. It will be of particular interest if Golgi network retention and EEV targeting signals can be separated. In this regard, the M protein of mouse hepatitis virus, which is resident in the trans Golgi network and is expressed by a recombinant vaccinia virus, was detected on IMV wrapping membranes but could not be detected in the majority of EEV particles (56).

ACKNOWLEDGMENTS

We appreciate the expert microscopy and photography provided by Andrea Weisberg, the advice and materials received from Pat Earl, and the technical assistance of Danielle Ompad, Norman Cooper, and Jerry Sisler.

REFERENCES

1. **Ashorn, P., E. A. Berger, and B. Moss.** 1990. Human immunodeficiency virus envelope glycoprotein/CD4-mediated fusion of nonprimate cells with human cells. J. Virol. **64**:2149–2156.
2. **Blasco, R., and B. Moss.** 1991. Extracellular vaccinia virus formation and cell-to-cell virus transmission are prevented by deletion of the gene encoding the 37,000-dalton outer envelope protein. J. Virol. **65**:5910–5920.
3. **Blasco, R., and B. Moss.** 1992. Role of cell-associated enveloped vaccinia virus in cell-to-cell spread. J. Virol. **66**:4170–4179.
4. **Blasco, R., J. R. Sisler, and B. Moss.** 1993. Dissociation of progeny vaccinia virus from the cell membrane is regulated by a viral envelope glycoprotein: effect of a point mutation in the lectin homology domain of the A34R gene. J. Virol. **67**:3319–3325.
5. **Broder, C. C., D. S. Dimitrov, R. Blumenthal, and E. A. Berger.** 1993. The block to HIV-1 envelope glycoprotein-mediated membrane fusion in animal cells expressing human CD4 can be overcome by a human cell component(s). Virology **193**:483–491.
6. **Brown, C. K., P. C. Turner, and R. W. Moyer.** 1991. Molecular characterization of the vaccinia virus hemagglutinin gene. J. Virol. **65**:3598–3606.
7. **Chakrabarti, S., K. Brechling, and B. Moss.** 1985. Vaccinia virus expression vector: coexpression of β-galactosidase provides visual screening of recombinant virus plaques. Mol. Cell. Biol. **5**:3403–3409.
8. **Chakrabarti, S., M. Robert-Guroff, F. Wong-Staal, R. C. Gallo, and B. Moss.** 1986. Expression of the HTLV-III envelope gene by a recombinant vaccinia virus. Nature (London) **320**:535–537.
9. **Cooney, E. L., A. C. Collier, P. D. Greenberg, R. W. Coombs, J. Zarling, D. E. Arditti, M. C. Hoffman, S. L. Hu, and L. Corey.** 1991. Safety of and immunological response to a recombinant vaccinia virus vaccine expressing HIV envelope glycoprotein. Lancet **337**:567–572.
10. **Cudmore, S., P. Cossart, G. Griffiths, and M. Way.** 1995. Actin-based motility of vaccinia virus. Nature (London) **378**:636–638.
11. **Dales, S.** 1963. The uptake and development of vaccinia virus in strain L cells followed with labeled viral deoxyribonucleic acid. J. Cell Biol. **18**:51–72.
12. **Dales, S., and L. Siminovitch.** 1961. The development of vaccinia virus in Earle's L strain cells as examined by electron microscopy. J. Biophys. Biochem. Cytol. **10**:475–503.
13. **Doms, R. W., R. Blumenthal, and B. Moss.** 1990. Fusion of intra- and extracellular forms of vaccinia virus with the cell membrane. J. Virol. **64**: 4884–4892.
14. **Doms, R. W., R. A. Lamb, J. K. Rose, and A. Helenius.** 1993. Folding and assembly of viral membrane proteins. Virology **193**:545–562.
15. **Duncan, S. A., and G. L. Smith.** 1992. Identification and characterization of an extracellular envelope glycoprotein affecting vaccinia virus egress. J. Virol. **66**:1610–1621.
16. **Earl, P., S. Koenig, and B. Moss.** 1991. Biological and immunological properties of human immunodeficiency virus type 1 envelope glycoprotein: analysis of proteins with truncations and deletions expressed by recombinant vaccinia viruses. J. Virol. **65**:31–41.
17. **Earl, P. L., C. C. Broder, D. Long, S. A. Lee, J. Peterson, S. Chakrabarti, R. W. Doms, and B. Moss.** 1994. Native oligomeric human immunodeficiency virus type 1 envelope glycoprotein elicits diverse monoclonal antibody reactivities. J. Virol. **68**:3015–3026.
18. **Earl, P. L., N. Cooper, and B. Moss.** 1991. Preparation of cell cultures and vaccinia virus stocks, p. 16.16.1–16.16.7. *In* F. M. Ausubel, R. Brent, R. E. Kingston, D. D. Moore, J. G. Seidman, J. A. Smith, and K. Struhl (ed.), Current protocols in molecular biology, vol. 2. Greene Publishing Associates & Wiley Interscience, New York, N.Y.
19. **Earl, P. L., A. W. Hügin, and B. Moss.** 1990. Removal of cryptic poxvirus transcription termination signals from the human immunodeficiency virus type 1 envelope gene enhances expression and immunogenicity of a recombinant vaccinia virus. J. Virol. **64**:2448–2451.
20. **Earl, P. L., and B. Moss.** 1991. Generation of recombinant vaccinia viruses, p. 16.17.1–16.17.16. *In* F. M. Ausubel, R. Brent, R. E. Kingston, D. D. Moore, J. G. Seidman, J. A. Smith, and K. Struhl (ed.), Current protocols in molecular biology, vol. 2. Greene Publishing Associates & Wiley Interscience, New York, N.Y.
21. **Earl, P. L., and B. Moss.** 1993. Mutational analysis of the assembly domain of the HIV-1 envelope glycoprotein. AIDS Res. Hum. Retroviruses **9**:589–594.
22. **Engelstad, M., S. T. Howard, and G. L. Smith.** 1992. A constitutively expressed vaccinia gene encodes a 42-kDa glycoprotein related to complement control factors that forms part of the extracellular virus envelope. Virology **188**:801–810.
23. **Engelstad, M., and G. L. Smith.** 1993. The vaccinia virus 42-kDa envelope protein is required for the envelopment and egress of extracellular virus and for virus virulence. Virology **194**:627–637.
24. **Gallaher, W. R., J. M. Ball, R. F. Garry, A. M. Martin-Amedee, and R. C. Montelaro.** 1995. A general model for the surface glycoproteins of HIV and other retroviruses. AIDS Res. Hum. Retroviruses **11**:191–202.
25. **Gerhard, W., J. W. Yewdell, M. E. Frankel, and R. G. Webster.** 1981. Antigenic structure of influenza virus haemagglutinin defined by hybridoma antibodies. Nature (London) **290**:713–717.
26. **Gong, S. C., C. F. Lai, and M. Esteban.** 1990. Vaccinia virus induces cell fusion at acid pH and this activity is mediated by the N-terminus of the 14-kDa virus envelope protein. Virology **178**:81–91.
27. **Graham, R. C., Jr., and M. J. Karnovsky.** 1966. Glomerular permeability. Ultrastructural cytochemical studies using peroxidases as protein tracers. J. Exp. Med. **124**:1123–1134.
28. **Green, S., I. Issemann, and E. Sheer.** 1988. A versatile in vivo and in vitro eukaryotic expression vector for protein engineering. Nucleic Acids Res. **16**:369.
29. **Hiller, G., H. Eibl, and K. Weber.** 1981. Characterization of intracellular and extracellular vaccinia virus variants: N_1-isonicotinoyl-N_2-3-methyl-4-chlorobenzoylhydrazine interferes with cytoplasmic virus dissemination and release. J. Virol. **39**:903–913.
30. **Hiller, G., C. Jungwirth, and K. Weber.** 1981. Fluorescence microscopical analysis of the life cycle of vaccinia virus in chick embryo fibroblasts. Virus-cytoskeleton interactions. Exp. Cell Res. **132**:81–87.
31. **Hiller, G., and K. Weber.** 1985. Golgi-derived membranes that contain an acylated viral polypeptide are used for vaccinia virus envelopment. J. Virol. **55**:651–659.
32. **Hirt, P., G. Hiller, and R. Wittek.** 1986. Localization and fine structure of a vaccinia virus gene encoding an envelope antigen. J. Virol. **58**:757–764.
33. **Isaacs, S. N., E. J. Wolffe, L. G. Payne, and B. Moss.** 1992. Characterization of a vaccinia virus-encoded 42-kilodalton class I membrane glycoprotein component of the extracellular virus envelope. J. Virol. **66**:7217–7224.
34. **Katz, S. L., and C. V. Broome.** 1991. Vaccinia (smallpox) vaccine. Recommendations of the Immunization Practices Advisory Committee (ACIP). Morbid. Mortal. Weekly Rep. **40**:1–10.
35. **Krijnse-Locker, J., S. Schleich, D. Rodriguez, B. Goud, E. J. Snijder, and G. Griffiths.** 1996. The role of a 21-kDa viral membrane protein in the assembly of vaccinia virus from the intermediate compartment. J. Biol. Chem. **271**: 14950–14958.

36. **Laemmli, U. K.** 1970. Cleavage of structural proteins during the assembly of the head of bacteriophage T4. Nature (London) **227**:680–685.
37. **Lai, C. F., S. C. Gong, and M. Esteban.** 1990. Structural and functional properties of the 14-kDa envelope protein of vaccinia virus synthesized in *Escherichia coli*. J. Biol. Chem. **265**:22174–22180.
38. **Lifson, J. D., M. B. Feinberg, G. R. Reyes, L. Rabins, B. Bonapour, S. Chakrabarti, B. Moss, F. Wong-Staal, K. S. Steimer, and E. G. Engelman.** 1986. Induction of CD4-dependent cell fusion by the HTLV-III/LAV envelope glycoprotein. Nature (London) **323**:725–728.
39. **Man, J.-S., J. F. Rodriguez, and M. Esteban.** 1990. Structural and functional characterization of a cell surface binding protein of vaccinia virus. J. Biol. Chem. **265**:1569–1577.
40. **Machamer, C. E.** 1993. Targeting and retention of Golgi membrane proteins. Curr. Opin. Cell Biol. **5**:606–612.
41. **McIntosh, A. A. G., and G. L. Smith.** 1996. Vaccinia virus glycoprotein A34R is required for infectivity of extracellular enveloped virus. J. Virol. **70**:272–281.
42. **Morgan, C.** 1976. Vaccinia virus reexamined: development and release. Virology **73**:43–58.
43. **Moss, B.** 1996. *Poxviridae*: the viruses and their replication. *In* B. N. Fields, D. M. Knipe, and P. M. Howley (ed.), Fields virology, 3rd ed., vol. 2. Lippincott-Raven Publishers, Philadelphia, Pa.
44. **Niles, E. G., and J. Seto.** 1988. Vaccinia virus gene D8 encodes a virion transmembrane protein. J. Virol. **62**:3772–3778.
45. **Parkinson, J. E., and G. L. Smith.** 1994. Vaccinia virus gene A36R encodes a Mr 43-50 K protein on the surface of extracellular enveloped virus. Virology **204**:376–390.
46. **Payne, L. G.** 1978. Polypeptide composition of extracellular enveloped vaccinia virus. J. Virol. **27**:28–37.
47. **Payne, L. G.** 1980. Significance of extracellular virus in the in vitro and in vivo dissemination of vaccinia virus. J. Gen. Virol. **50**:89–100.
48. **Payne, L. G.** 1992. Characterization of vaccinia virus glycoproteins by monoclonal antibody preparations. Virology **187**:251–260.
49. **Ratner, L., W. Haseltine, R. Patarca, K. J. Livak, B. Starcich, S. F. Josephs, E. R. Doran, J. A. Rafalski, E. A. Whitehorn, K. Baumeister, L. Ivanoff, S. R. Petteway, M. L. Pearson, J. A. Lautenberger, T. S. Papas, J. Ghrayeb, N. T. Chang, R. C. Gallo, and F. Wong-Staal.** 1985. Complete nucleotide sequence of the AIDS virus, HTLV-III. Nature (London) **313**:277–284.
50. **Ravanello, M. P., and D. E. Hruby.** 1994. Characterization of the vaccinia virus L1R myristyl protein as a component of the intracellular virion envelope. J. Gen. Virol. **75**:1479–1483.
51. **Ravanello, M. P., and D. E. Hruby.** 1994. Conditional lethal expression of the vaccinia virus L1R myristylated protein reveals a role in virus assembly. J. Virol. **68**:6401–6410.
52. **Rodríguez, D., M. Esteban, and J. R. Rodríguez.** 1995. Vaccinia virus A17L gene product is essential for an early step in virion morphogenesis. J. Virol. **69**:4640–4648.
53. **Rodriguez, J. F., E. Paez, and M. Esteban.** 1987. A 14.000-M_r envelope protein of vaccinia virus is involved in cell fusion and forms covalently linked trimers. J. Virol. **61**:395–404.
54. **Roper, R. L., L. G. Payne, and B. Moss.** 1996. Extracellular vaccinia virus envelope glycoprotein encoded by the A33R gene. J. Virol. **70**:3753–3762.
55. **Sarov, I., and W. K. Joklik.** 1972. Studies on the nature and location of the capsid polypeptides of vaccinia virions. Virology **50**:579–592.
56. **Schmelz, M., B. Sodeik, M. Ericsson, E. J. Wolffe, H. Shida, G. Hiller, and G. Griffiths.** 1994. Assembly of vaccinia virus: the second wrapping cisterna is derived from the trans Golgi network. J. Virol. **68**:130–147.
57. **Schmutz, C., L. G. Payne, J. Gubser, and R. Wittek.** 1991. A mutation in the gene encoding the vaccinia virus 37,000-M_r protein confers resistance to an inhibitor of virus envelopment and release. J. Virol. **65**:3435–3442.
58. **Schmutz, C., L. Rindisbacher, M. C. Galmiche, and R. Wittek.** 1995. Biochemical analysis of the major vaccinia virus envelope antigen. Virology **213**:19–27.
59. **Shida, H.** 1986. Nucleotide sequence of the vaccinia virus hemagglutinin gene. Virology **150**:451–462.
60. **Sodeik, B., S. Cudmore, M. Ericsson, M. Esteban, E. G. Niles, and G. Griffiths.** 1995. Assembly of vaccinia virus: incorporation of p14 and p32 into the membrane of the intracellular mature virus. J. Virol. **69**:3560–3574.
61. **Sodeik, B., R. W. Doms, M. Ericsson, G. Hiller, C. E. Machamer, W. van't Hof, G. van Meer, B. Moss, and G. Griffiths.** 1993. Assembly of vaccinia virus: role of the intermediate compartment between the endoplasmic reticulum and the Golgi stacks. J. Cell Biol. **121**:521–541.
62. **Sodeik, B., M. Griffiths, M. Ericsson, G. Hiller, C. E. Machamer, W. van't Hof, G. van Meer, B. Moss, and G. Griffiths.** 1994. Assembly of vaccinia virus: effects of rifampin on the intracellular distribution of viral protein p65. J. Virol. **68**:1103–1114.
63. **Stokes, G. V.** 1976. High-voltage electron microscope study of the release of vaccinia virus from whole cells. J. Virol. **18**:636–643.
64. **Tooze, J., M. Hollinshead, B. Reis, K. Radsak, and H. Kern.** 1993. Progeny vaccinia and human cytomegalovirus particles utilize early endosomal cisternae for their envelopes. Eur. J. Cell Biol. **60**:163–178.
65. **Wolffe, E. J., S. N. Isaacs, and B. Moss.** 1993. Deletion of the vaccinia virus B5R gene encoding a 42-kilodalton membrane glycoprotein inhibits extracellular virus envelope formation and dissemination. J. Virol. **67**:4732–4741.
66. **Wolffe, E. J., D. M. Moore, P. J. Peters, and B. Moss.** 1996. Vaccinia virus A17L open reading frame encodes an essential component of nascent viral membranes that is required to initiate morphogenesis. J. Virol. **70**:2797–2808.
67. **Wolffe, E. J., S. Vijaya, and B. Moss.** 1995. A myristylated membrane protein encoded by the vaccinia virus L1R open reading frame is the target of potent neutralizing monoclonal antibodies. Virology **211**:53–63.

JOURNAL OF VIROLOGY, May 1997, p. 4032–4041
0022-538X/97/$04.00+0

Vol. 71, No. 5

A Novel Virus Binding Assay Using Confocal Microscopy: Demonstration that the Intracellular and Extracellular Vaccinia Virions Bind to Different Cellular Receptors

ALAIN VANDERPLASSCHEN AND GEOFFREY L. SMITH*

Sir William Dunn School of Pathology, University of Oxford, Oxford OX1 3RE, United Kingdom

Received 6 December 1996/Accepted 30 January 1997

Vaccinia virus (VV) produces two antigenically and structurally distinct infectious virions, intracellular mature virus (IMV) and extracellular enveloped virus (EEV), which bind to unidentified and possibly different cellular receptors. Studies of VV binding have been hampered by having two infectious virions and by the rupture of the EEV outer membrane in the majority of EEV virions during purification. To overcome these problems, we have developed a novel approach to study VV binding that is based on confocal microscopy and does not require EEV purification. In this assay, individual virus particles adsorbed to the cell are simultaneously distinguished and quantified by double immunofluorescence labelling with antibody markers for EEV and IMV. By this method, we show unequivocally that IMV and EEV bind to different cellular receptors. Three independent observations allow this conclusion. First, the efficiencies with which IMV and EEV bind to different cell lines are unrelated; second, cell surface digestion with some enzymes affects IMV and EEV binding differently; and third, the binding of a monoclonal antibody to cells prevents IMV binding but not EEV binding. This technique may be widely applicable for studying the binding of different viruses.

Vaccinia virus (VV) is a poxvirus and produces large (250- by 350-nm) and complex virions that contain a double-stranded DNA genome and more than 100 polypeptides (8). There are two morphologically distinct infectious forms of virions, intracellular mature virus (IMV) and extracellular enveloped virus (EEV) (2, 10). IMV represents the majority of infectious progeny and remains within the cytoplasm of the infected cell until cell lysis. EEV is released from the cell and possesses an extra lipid envelope with at least 10 associated proteins which are absent from IMV (14, 15). These proteins endow EEV with different biological and immunological properties (2–4, 19). Despite the fact that EEV constitutes only a very minor fraction of total infectivity, it has two important biological properties. First, it mediates long-range dissemination of virus both in vitro and in vivo (15); second, it is the form of virus against which immune responses that are necessary for protection against infection by orthopoxviruses are induced (1, 3, 15).

Because EEV has an extra lipid envelope containing proteins absent from IMV, it is possible that each form of VV binds to distinct cellular receptors and consequently could have different tropisms. Surprisingly, this question, which is important for the understanding of VV pathogenesis and for the use of VV as a live recombinant vaccine, has not been investigated so far. Recently, Chang et al. described the isolation of a mouse immunoglobulin M (IgM) monoclonal antibody (MAb), B2, which reacts with a trypsin- and pronase-sensitive and neuraminidase-resistant cell surface epitope (5). When bound on the cell surface, MAb B2 was shown to prevent IMV binding, but its effect on EEV binding or infectivity was not tested.

Binding studies require purified virus, and this is particularly true for VV, which produces two forms of infectious virions. Despite the fact that EEV is the only form actively released from the cell, the supernatant of infected cells cannot be used as a source of pure EEV because it contains contaminating IMV released from lysed cells. Furthermore, because IMV is much more abundant than EEV (≥100-fold for the Western Reserve strain), breakage of only a minor proportion of cells produces overwhelming contamination. Recently, Ichihashi has shown that biophysical methods to separate EEV from IMV cause damage to the outer envelope of EEV virions, as demonstrated by their sensitivity to MAbs that neutralize IMV (9). Once the EEV membrane is ruptured, the particle retains full infectivity as an IMV. Similarly, if the EEV envelope presents a defect which reduces the specific infectivity of EEV virions, the rupture of the EEV membrane increases the specific infectivity (12). Because damaged EEV could bind to the cell via an EEV or IMV protein, purified EEV should not be used for binding studies.

To overcome these difficulties, we have developed a novel binding assay based on confocal microscopy which does not require purified virions. By this assay, we demonstrate that IMV and EEV bind to different cellular receptors. This method should be applicable for studying many different viruses.

MATERIALS AND METHODS

Cells and viruses. BS-C-1 cells (African green monkey kidney cells; ATCC CCL-26) and RK_{13} cells (rabbit kidney cells; ATCC CCL-37) were grown in minimum essential medium (MEM) (Gibco) supplemented with 10% fetal bovine serum (FBS). HeLa cells (ATCC CCL-10) were grown as suspension cultures as described elsewhere (6).

The International Health Department-J VV strain, which produces large amounts of EEV, was grown in RK_{13} cells infected with 1 PFU per cell. Three virus preparations were produced from the infected cultures. For fresh EEV, the culture supernatant was harvested at 24 h after infection and centrifuged to remove detached cells and cell debris (1,000 × *g*, 20 min, 4°C). A fresh EEV preparation was produced before each experiment. Alternatively, 48 h after infection, IMV and EEV were purified as described previously (13). Purified IMV and EEV were stored at −70°C and were sonicated at 40 μm for 30 s before use. Virus infectivity was titrated by plaque assay with BS-C-1 cells. Unless otherwise specified, cells were incubated with serial dilutions of the virus in phosphate-buffered saline (PBS) (3 mM KCl, 1.5 mM KH_2PO_4, 0.14 M NaCl, 6.5 mM Na_2HPO_4 [pH 7.2]) containing 2% FBS (0.5 ml per well of 6-well cluster

* Corresponding author. Mailing address: Sir William Dunn School of Pathology, University of Oxford, South Parks Rd., Oxford OX1 3RE, United Kingdom. Phone: 44-1865-275521. Fax: 44-1865-275501. E-mail: geoffrey.smith@path.ox.ac.uk.

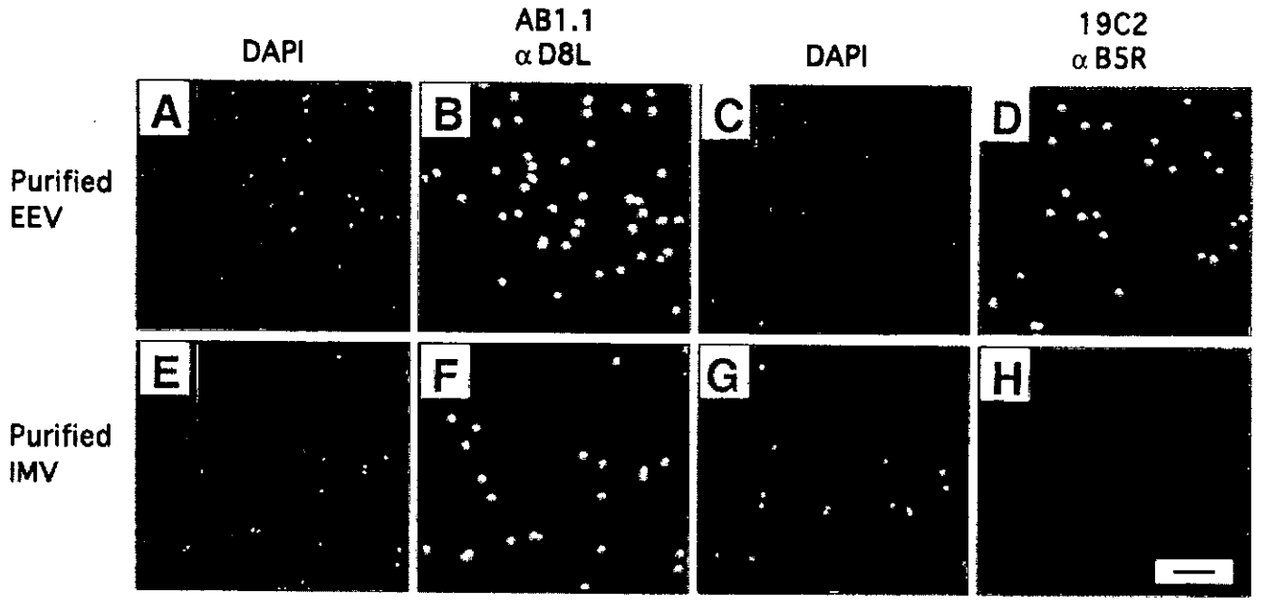

FIG. 1. Visualization of IMV and EEV by conventional fluorescent microscopy. Purified EEV (A through D) and IMV (E through H) (10^7 PFU/ml in PBS) were incubated for 30 min at 37°C on the surface of glass coverslips coated with fibronectin. After being washed with PBS, the virions adsorbed to fibronectin were treated as described in Materials and Methods for indirect immunofluorescent staining. MAb AB1.1 (B and F) and MAb 19C2 (D and H) were used as primary antibodies and were revealed by FITC-GAM and FITC-RAR secondary antibodies, respectively. The samples were then examined with a conventional fluorescent microscope (magnification, ×1,000; Axioplan microscope; Zeiss). Panel pairs (A and B, C and D, E and F, and G and H) represent the same field examined for DAPI and FITC fluorescent emissions, respectively. Bar, 2 μm. αD8L, anti-D8L; αB5R, anti-B5R.

dishes) for 1 h at 4°C, washed with PBS–2% FBS, and overlaid with 1.5% carboxymethyl cellulose (CMC) in MEM with 2.5% FBS (11). After 2 days, cells were stained with 0.1% crystal violet in 15% ethanol and the plaques were counted. To determine only the infectivity associated with EEV, any contaminating IMV infectivity was neutralized by the addition of MAb 5B4/2F2 (final dilution, 1/2,560) against the 14-kDa fusion protein (A27L gene product) of IMV (7).

MAbs. Culture supernatant from a murine hybridoma secreting the IgM MAb B2 was kindly provided by W. Chang (5). Murine MAb AB1.1 (13), raised against the D8L IMV surface protein, and rat MAb 19C2 (18), raised against the B5R EEV surface protein, were also used.

Capping of the MAb B2-reactive epitope. Capping of the MAb B2-reactive epitope was induced in HeLa cells grown as suspension cultures. Cells (10^6) were incubated for 1 h on ice with 0.2 ml of MAb B2-undiluted supernatant. Then cells were washed with cold PBS–10% FBS (PBSF) and further incubated for 30 min on ice with a rabbit antiserum to mouse IgM (RAM-IgM; Serotec) (16 μg/10^6 cells in 0.2 ml of PBSF). After washing with cold PBSF, capping was induced by incubation at 37°C for 10 min followed by cooling to 0°C to stop the process.

Cell surface enzymatic digestions. Trypsin (1.25 mg/ml; from bovine pancreas; Boehringer Mannheim), pronase (1 mg/ml; from *Streptomyces griseus*; Boehringer Mannheim), and neuraminidase (40 mU/ml; from *Vibrio cholerae*; Boehringer Mannheim) digestions were carried out in PBS for 30 min on ice. Cells were then washed extensively with cold PBS–2% FBS.

Indirect immunofluorescent staining for conventional microscopy and confocal microscopy. Virus particles bound to fibronectin-coated coverslips or cells were fixed in PBS containing 4% paraformaldehyde (wt/vol) for 20 min on ice. After being washed with PBS, samples were permeabilized in ethanol-PBS (90:10 [vol/vol]) at 0°C for 2 min. Then samples were extensively washed with PBS and incubated in PBSF containing the appropriate concentration of the primary MAb at 37°C for 45 min. MAb AB1.1 (diluted 1/300), biotinylated MAb AB1.1 (diluted 1/100), or MAb 19C2 (diluted 1/16) was used as the primary antibody. After being washed with PBSF, samples were incubated in PBSF containing the appropriate secondary reagent at 37°C for 30 min. Fluorescein isothiocyanate (FITC)-conjugated $F(ab')_2$ goat anti-mouse IgG (GAM) (8 μg/ml) (Sigma), rhodamine-conjugated streptavidin (Rd-Strep) (3.3 μg/ml) (Serotec), and FITC (10 μg/ml) (Serotec)- or *R*-phycoerythrin (PE) (10 μg/ml) (Serotec)-conjugated $F(ab')_2$ rabbit anti-rat IgG (RAR) were used as secondary conjugates, respectively. After extensive washing with PBSF and a final wash step with distilled water, samples were mounted in Mowiol-DAPI (6-diamin-2-phenylindole-dihydrochloride) mounting medium as described elsewhere (17). This mounting medium contained 1 μg of DAPI per ml.

Quantification of cell surface MAb B2-reactive epitope by indirect immunofluorescent staining and flow cytometry. HeLa cells (10^6) grown as suspension cultures were incubated for 1 h on ice in 0.2 ml of MAb B2 pure supernatant or in 0.2 ml of PBSF containing a mouse isotype IgM negative control (10 μg/10^6 cells) (Serotec). After being washed with cold PBSF, cells were further incubated with a FITC-conjugated sheep antiserum to mouse IgM (SAM-IgM) (Serotec) (16 μg/10^6 cells in 0.2 ml of PBSF) on ice for 30 min. After being washed with cold PBSF, cells were fixed in PBS containing 4% formaldehyde (vol/vol) and analyzed by flow cytometry.

Confocal-microscopy analysis. Cells were analyzed with a Bio-Rad MRC 1000 confocal microscope (run with Comos software) by using appropriate filters, the full dynamic range of grey scale, and Kalman filtration. Optical sections perpendicular to the z axis were performed every 0.6 μM throughout the sample. The confocal pictures were reconstructed by projection of sections.

Flow cytometry analysis. Flow cytometry analysis for FITC emission signal was performed with a FACScan flow cytometer (Becton Dickinson) as described previously (20).

Statistical analysis. Student's *t* test was used to test the significance of results ($P < 0.05$).

RESULTS

IMV and EEV particles can be visualized by conventional fluorescent microscopy. VV is a very large virus (approximately 250 by 350 nm); therefore, we investigated whether indirect immunofluorescent staining could be used as a novel assay to study VV binding to cells. Purified IMV and EEV (10^7 PFU/ml in PBS) were first incubated for 30 min at 37°C on the surface of glass coverslips coated with fibronectin. After being washed with PBS, adsorbed virions were treated as described in Materials and Methods for indirect immunofluorescent staining with MAb AB1.1 (anti-D8L gene product) (Fig. 1B and F) or MAb 19C2 (anti-B5R gene product) (Fig. 1D and H). Staining of viral DNA with DAPI enabled each isolated IMV and EEV particle to be visualized (Fig. 1A, C, E, and G). A much brighter signal was observed when virions (IMV or EEV) were revealed by indirect immunofluorescent staining. As expected, both IMV and EEV permeabilized particles were stained by MAb AB1.1 directed against the IMV surface protein D8L. Importantly, all the virions detected by DAPI staining were also revealed by staining with MAb AB1.1 (Fig. 1; compare

panels A and B and panels E and F). In contrast, MAb 19C2, which recognizes only EEV particles (18), stained 3% of the purified IMV particles revealed by DAPI staining (n = 400), indicating that the majority of the virions of this preparation were IMV (Fig. 1; compare panels G and H). Consistent with this, 95% (n = 598 PFU in the absence of MAb 5B4/2F2) of the purified IMV PFU were neutralized by MAb 5B4/2F2. Taken together, these data indicate the reasonably high purity of the purified IMV preparation and the efficiency with which MAb 5B4/2F2 neutralizes IMV infectivity.

For the purified EEV preparation, 96% of virions were stained by MAb 19C2 (determined by observation of 400 DAPI-positive particles), indicating that the majority of the virions of this preparation were EEV. When purified EEV was submitted to neutralization assay with MAb 5B4/2F2, 65% (n = 453 PFU in the absence of MAb 5B4/2F2) of the PFU were neutralized. Taking into account that only 31% of the infectivity of the original culture supernatant used for EEV purification was neutralized by MAb 5B4/2F2, these data indicated that the purification procedure led to isolation of EEV with a damaged outer membrane, allowing access of IMV-neutralizing antibody. Despite several attempts using different protocols, we were not able to purify EEV without obtaining a large fraction of damaged particles. Therefore, all further investigations on EEV biology were carried out with fresh EEV prepared at 24 h postinfection from the cell supernatant. For EEV infectivity assays, any contaminating IMV was neutralized by the addition of MAb 5B4/2F2. For binding studies, we developed a double immunofluorescent staining which permits IMV and EEV bound on the cell surface to be counted and differentiated simultaneously.

Simultaneous identification of IMV and EEV on the cell surface by double immunofluorescent staining and confocal microscopy analysis. Fresh EEV contains 15 to 25% contaminating IMV; therefore, its use for binding studies requires an assay which permits differentiation of IMV and EEV. With that goal in mind, we used a double immunofluorescent staining with MAbs AB 1.1 and 19C2 against the D8L and B5R gene products, respectively, on fixed and permeabilized samples (Fig. 2). Biotinylated MAb AB1.1 and MAb 19C2 were used as primary MAbs and were subsequently revealed by Rd-Strep and FITC-RAR, respectively. By this staining procedure, EEV virions appeared as double (red and green) foci while IMV virions were single (red) fluorescent foci on the cell surface. Each fluorescent focus was shown to represent an isolated particle and not a virus cluster by measuring the sizes of spots. The mean diameter of Rd fluorescent foci was 409.3 nm (standard deviation [SD] = 13.1; n = 20), which is similar to the dimension of a single vaccinia virion. This also demonstrated that the virus preparations contained disaggregated particles.

Determination of physical particle/PFU ratios. The ability to visualize individual VV virions and to determine their phenotypes by double immunofluorescent staining provided a simple way to determine the numbers of EEV and IMV particles per volume unit. To do this, the VV preparation whose titer was to be determined was serially diluted in distilled water. One microliter of each dilution was then loaded in triplicate on the surface of a glass coverslip coated with fibronectin (washed with distilled water and dried beforehand). After being dried completely, virions were fixed to fibronectin with 4% paraformaldehyde in PBS for 30 min on ice. Then samples were permeabilized and treated for double immunofluorescent staining as described above. The numbers of EEV (double-positive) and IMV (single-positive) particles were then counted on the entire area corresponding to each drop from dilutions giving between 100 and 1,000 virions/drop. The mean number of the three measurements multiplied by the dilution factor enabled the number of EEV or IMV virions/ml to be calculated. Simultaneously, the total infectivity (EEV plus IMV) was determined by plaque assay with BS-C-1 cells in triplicate and the infectivity associated with EEV was determined by plaque assay in the presence of MAb 5B4/2F2. To ensure that all the infectious particles had sufficient time to bind to cells, the virus was adsorbed for 3.5 h at 37°C (0.5 ml per well of 6-well cluster dishes). The particle/PFU ratio of IMV was calculated from analyses of purified IMV and fresh EEV, while the EEV particle/PFU ratio was calculated by analysis of fresh EEV. The data given are the means from three independent virus preparations. The IMV particle/PFU ratios were 45 (SD = 11.1; n = 3) and 64.6 (SD = 16.5; n = 3) in fresh EEV and purified IMV, respectively. The EEV particle/PFU ratio of fresh EEV was 12.7 (SD = 6.1; n = 3). These data indicate that EEV has a higher specific infectivity than does IMV under the conditions tested and that the purification of IMV reduces the specific infectivity.

Cell surface protease treatment affects differently IMV and EEV binding. The binding assay described above enables the identification and differentiation of IMV and EEV bound to the cell surface and consequently allows the use of virus preparations containing both IMV and EEV for binding studies. Therefore, it can be applied to investigate simultaneously the effects of a specific treatment on IMV and EEV binding. We used this feature of the binding assay to investigate whether IMV and EEV bind to identical or separate receptors.

If IMV and EEV bind to separate cellular receptors and these receptors have different biochemical compositions, cell surface treatment with some enzymes might affect differently IMV and EEV binding. To test this hypothesis, we investigated whether treating cells with different enzymes affected differentially IMV and EEV binding and infectivity. Binding and infectivity assays were performed concurrently with RK_{13} and BS-C-1 cells. Binding assays were also performed with HeLa cells grown in suspension. Cell surface treatments with trypsin, pronase, and neuraminidase were carried out as described in Materials and Methods. It was not possible to use BS-C-1 cells for protease experiments due to their high sensitivities to these enzymes causing detachment from the culture vessel.

Trypsin digestion did not affect either IMV binding or infectivity (Table 1). Statistically similar numbers of IMV particles were counted on the surfaces of cells digested with trypsin and those that were mock treated (Table 1). This observation was made with both RK_{13} and HeLa cells and with both sources of IMV (purified IMV and fresh EEV). When RK_{13} cells were subjected to the infectivity assay with purified IMV as the inoculum, similar numbers of PFU were observed for mock- and trypsin-treated cells (Table 1). Surprisingly, and in contrast to IMV, EEV bound more efficiently to trypsin-treated cells than to normal cells. The number of EEV counted on trypsin-treated cells was 2.0 times that observed on control cells. Similarly, EEV generated 2.3 times more plaques on trypsin-treated RK_{13} cell monolayers than on mock-treated monolayers (Table 1).

Pronase treatment had opposite effects on IMV and EEV binding. Pronase treatment of RK_{13} and HeLa cells reduced the amount of IMV bound on the cell surface by 92 and 97%, respectively (Table 1 [purified IMV used as the inoculum]). Similarly, when RK_{13} cell monolayers were treated with pronase before infection, the number of IMV plaques was decreased by 90% in comparison with the control (Table 1). In contrast to IMV, cell surface pronase treatment enhanced EEV binding and infectivity. RK_{13} and HeLa cells treated with

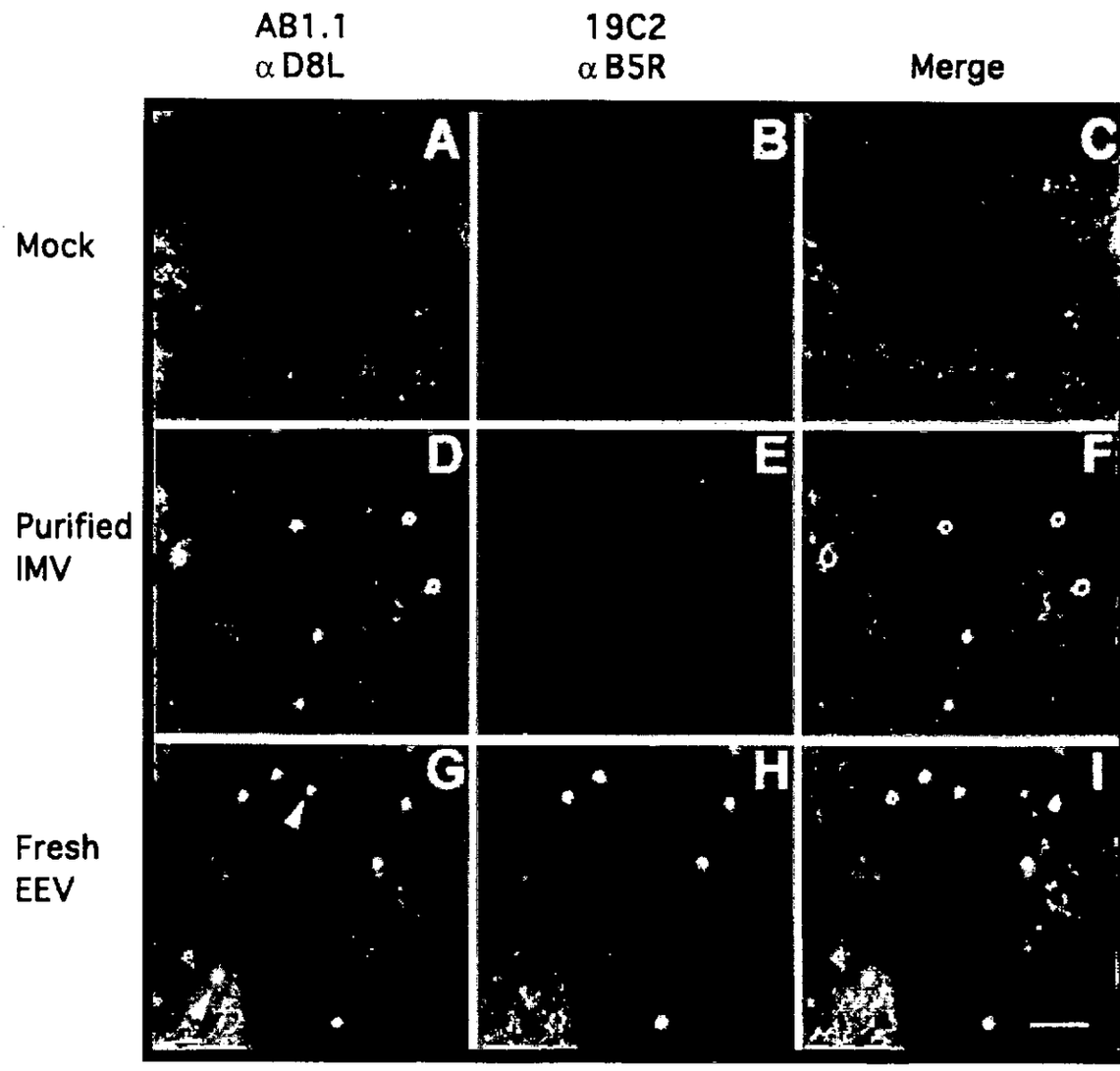

FIG. 2. Detection and identification of IMV and EEV on the cell surface by double immunofluorescent staining and confocal microscopy. RK_{13} cells were mock infected (A through C) or infected on ice with purified IMV (D through F) or fresh EEV (G through I). Cells were then treated as described in Materials and Methods for simultaneous detection of D8L and B5R gene products by double indirect immunofluorescent staining. Biotinylated MAb AB1.1 and MAb 19C2 were used as primary MAbs and were revealed by Rd-Strep and FITC-RAR, respectively. All three panels horizontally analyze the same cells. The first (A, D, and G) and second (B, E, and H) columns of panels are analyses for Rd and FITC fluorescent emissions, respectively. In the third (C, F, and I) column Rd and FITC signals are merged. The arrowheads in panel G identify particles (IMV) which were detected by MAb AB1.1 but not by MAb 19C2. Bar, 2 μm. αD8L, anti-D8L; αB5R, anti-B5R.

pronase bound 2.94 and 2.72 times more EEV, respectively, than did control cells (Table 1). The results of infectivity assays led to a similar conclusion; the number of PFU observed after EEV infection of pronase-treated monolayers was 3.17 times higher than that after infection of control cells (Table 1).

Cell surface treatment with neuraminidase enhanced slightly the binding of both IMV and EEV. Whereas IMV binding and infectivity were increased by about 15% (Table 1), a greater effect was observed with EEV, where both binding and infectivity were increased by about 50% (Table 1).

Treatment with each enzyme therefore produced different effects on IMV and EEV, suggesting that these virions bind to different receptors. In support of this, IMV and EEV also bound to different cell lines with various efficiencies (Table 1). In contrast to IMV, the efficiency of EEV binding was not constant for the cell lines tested. If IMV and EEV bind to an identical receptor, any variation in the expression of this putative receptor between different cell lines should affect IMV and EEV binding to the same extent. On the other hand, if IMV and EEV bind to separate receptors, the efficiency of IMV and EEV binding is expected to fluctuate independently between different cell lines. The results obtained with mock-treated cells showed that the numbers of IMV counted on the cell surface for the three cell lines tested were similar (Table 1). Both sources of IMV (purified IMV and fresh EEV) led to this observation. In contrast, the efficiency of EEV binding varied between cell lines. Statistically different numbers of EEV were detected on the surface of the three cell lines infected with fresh EEV (Table 1). For example, 4.9 times more EEV was detected on BS-C-1 cells than on RK_{13} cells. This

TABLE 2. Effects of MAb B2 on the abilities of cells to support IMV and EEV binding and plaque formation[a]

Cell line	Inoculum	Binding assay[b]				Infectivity assay[c]	
		Mock		MAb B2		Mock	MAb B2
		IMV	EEV	IMV	EEV		
BS-C-1	Purified IMV	2,057 ± 87 (100)	NA[d]	350 ± 34 (17)	NA	100 ± 4	23 ± 2
	Fresh EEV	241 ± 26 (100)	3,278 ± 122 (100)	46 ± 25 (19)	3,245 ± 87 (99)	100 ± 4	106 ± 7
RK_{13}	Purified IMV	2,103 ± 89 (100)	NA	878 ± 82 (42)	NA	100 ± 6	35 ± 5
	Fresh EEV	268 ± 20 (100)	687 ± 39 (100)	136 ± 43 (51)	701 ± 73 (102)	100 ± 4	96 ± 7
HeLa	Purified IMV	2,198 ± 110 (100)	NA	474 ± 22 (22)	NA	NA	NA
	Fresh EEV	294 ± 33 (100)	483 ± 62 (100)	55 ± 8 (19)	466 ± 35 (97)	NA	NA

[a] For binding and infectivity assays, adherent cells were grown in a 1-well culture chamber slide (Nunc) and 6-well cluster dishes (Falcon), respectively. For HeLa cells, both incubations (10^6 cells/0.2 ml) and infections (10^6 cells/ml) were performed in suspension. Before infection, cells were incubated with undiluted MAb B2 supernatant (450 μl per 1-well chamber slide or per well of 6-well cluster dishes) or with MEM–10% FBS (mock-treated cells) for 1 h on ice and then extensively washed with cold PBS–2% FBS.

[b] Mock- and MAb B2-treated cells were infected on ice for 1 h with either purified IMV (MOI of 10 PFU/cell) or fresh EEV (MOI of 4.6 PFU/cell, with 74% resistant to MAb 5B4/2F2 neutralization) diluted in PBS–2% FBS. After being washed, cells were treated as described in the text to reveal IMV and EEV virions by double immunofluorescent staining. The numbers of IMV and EEV virions bound on the surfaces of 200 cells were then determined by confocal-microscopy examination. The data are the averages ± SDs for triplicate measures. Parenthetical data are the results expressed as percentages of the control.

[c] Mock- and MAb B2-treated cell monolayers were infected on ice for 1 h with either purified IMV or fresh EEV (containing MAb 5B4/2F2; final dilution, 1/2,560) to obtain approximately 200 plaques per well on mock-treated monolayers. After being washed, cells were overlaid with CMC, and the plaques were counted 2 days later. The data are expressed as percentages of the control and are averages ± SDs for duplicate cultures.

[d] NA, not applicable.

HeLa cells grown in suspension by the protocol described in Materials and Methods.

To visualize and to control capping, cells were fixed before (Fig. 3A, panel b) or after (Fig. 3A, panel c) incubation at 37°C for 10 min. MAb B2/RAM-IgM complexes were then revealed by FITC-conjugated goat anti-rabbit IgG (GARB). Before the 37°C incubation period, the distribution of MAb B2-reactive epitope on the cell surface was mostly diffuse despite the presence of several small clusters (Fig. 3A, panel b). These clusters were artifacts of the three-step staining procedure (MAb B2, RAM-IgM, and FITC-GARB) as they were not observed when cells were subjected to indirect immunofluorescent staining with MAb B2 followed by FITC-SAM-IgM (data not shown). However, after 10 min at 37°C, all the FITC fluorescence was clustered, indicating capping of MAb B2-reactive receptor (Fig. 3A, panel c). The specificity of MAb B2 staining was controlled by using an irrelevant mouse IgM MAb as the primary antibody (Fig. 3A; compare panels a and b).

To address the effect of MAb B2-reactive receptor capping on EEV binding, the following three preparations of HeLa cells were subjected to the binding assay (Fig. 3B): (i) cells preincubated with an irrelevant mouse IgM MAb (negative control cells) (panel a), (ii) cells treated as described in Materials and Methods to induce MAb B2-reactive receptor capping but with omission of the 10-min incubation period at 37°C (MAb B2-labelled cells) (panel b), and (iii) cells treated to induce capping of MAb B2-reactive receptor (MAb B2-capped cells) (panel c).

Figure 3B shows that the capping of MAb B2-reactive receptor did not affect EEV binding, since similar numbers of EEV particles were observed on the surfaces of negative control, MAb B2-labelled, and MAb B2-capped cells. The capping of MAb B2-reactive receptor did not increase the degree to which IMV binding was inhibited by MAb B2, since similar numbers of particles were observed on cells whether or not capping was induced (Fig. 3B; compare panels b and c).

The capping of MAb B2-reactive receptor very probably reduces access to any part of this receptor by steric inhibition. The observation that EEV binding was not affected by the capping of MAb B2-reactive receptor might be explained in two ways. Either MAb B2-reactive receptor is not involved in EEV binding or EEV is able to bind to MAb B2-reactive receptor despite its capping. If the latter was true, EEV binding sites and MAb B2-reactive molecule clusters would colocalize on the surfaces of MAb B2-capped cells. To test this, we used a double immunofluorescent staining to visualize simultaneously MAb B2-reactive molecule clusters and EEV (Fig. 4). One hundred cells, containing 254 bound EEV, were examined by confocal microscopy to determine the relative localization of EEV binding sites and MAb B2-reactive molecule clusters. All but six EEV particles (which were observed at the periphery of MAb B2-reactive molecule clusters) were present at positions clearly isolated from the MAb B2 clusters, and three representative cells are shown in Fig. 4.

MAb B2 prevents IMV binding by steric inhibition. Chang et al. have shown that the MAb B2-reactive epitope is sensitive to trypsin digestion (5). However, these data did not determine the effect of trypsin digestion on IMV binding. Table 1 shows that cell surface trypsin digestion does not affect IMV binding, suggesting that the MAb B2-reactive epitope is not the IMV binding site and consequently that MAb B2 prevents IMV binding by steric inhibition. To be certain about this, it was necessary to demonstrate that trypsin digestion destroyed all of the MAb B2-reactive epitope present on the cell surface. To examine this, the MAb B2-reactive epitope on the surfaces of mock-digested and trypsin-digested cells was quantified by indirect immunofluorescent staining and flow cytometry (Fig. 5). Trypsin-treated cells had a relative fluorescence intensity identical to that of negative control cells (mock-treated cells stained with an irrelevant mouse IgM MAb as the primary antibody), indicating that the great majority of MAb B2-reactive epitopes were destroyed after trypsin treatment (Fig. 5). As this treatment has no effect on IMV binding, the mechanism by which MAb B2 prevents IMV binding must be steric inhibition.

DISCUSSION

VV produces two types of infectious particles, IMV and EEV. EEV is an IMV particle with an additional outer membrane that contains proteins that are absent from IMV. This EEV outer membrane explains why IMV-neutralizing antibodies fail to inhibit the infectivity of EEV particles (15). The EEV outer membrane has been described as a loose and extremely

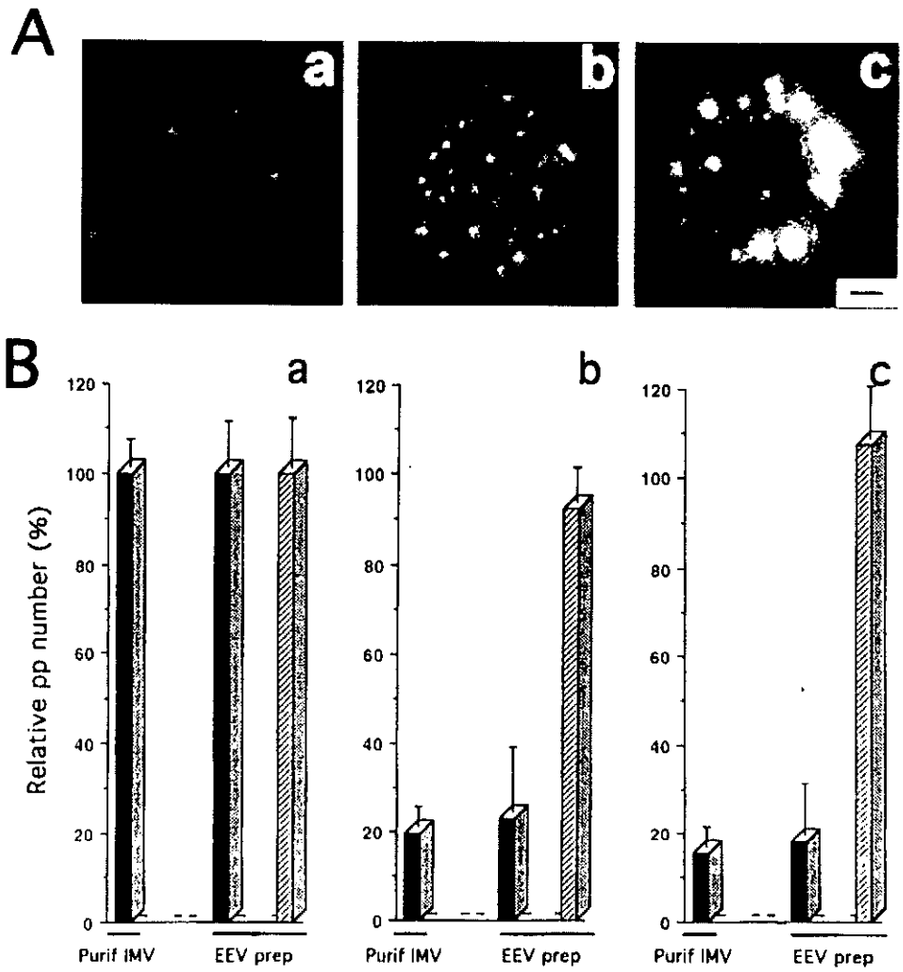

FIG. 3. (A) Capping of MAb B2-reactive receptor. HeLa cells grown as suspension cultures were processed as described in Materials and Methods to induce capping of MAb B2-reactive molecules (b and c). To visualize capping, cells were fixed before (b) or after (c) incubation at 37°C for 10 min and MAb B2/RAM-IgM complexes were revealed by FITC-GARB (12 μg/10^6 cells in 0.2 ml of PBSF). (a) Cell incubated with an irrelevant primary mouse IgM MAb and then treated as described for panel b. Bar, 2 μm. (B) Effect of MAb B2-reactive receptor capping on EEV binding. The following three preparations of HeLa cells were subjected to the binding assay: cells preincubated for 45 min at 0°C with an irrelevant mouse IgM MAb (Serotec) (10 μg/10^6 cells per 0.2 ml of PBSF) (negative control cells) (a), cells treated as described in Materials and Methods to induce MAb B2-reactive receptor capping without incubation at 37°C for 10 min (MAb B2-labelled cells) (b), and cells treated to induce capping of MAb B2-reactive receptor (MAb B2-capped cells) (c). These three cell preparations were then infected (10^6 cells/ml) on ice for 1 h with either purified (Purif) IMV (MOI of 10 PFU/cell) or fresh EEV (EEV prep) (MOI of 5.1 PFU/cell, with 79% resistant to neutralization by MAb 5B4/2F2) diluted in PBS–2% FBS. After being washed with PBS–2% FBS to remove unadsorbed virus, cells were treated as described in the text to reveal virions by double indirect immunofluorescent staining. The numbers of IMV (black bars) and EEV (hatched bars) virions bound on the surfaces of 200 cells were then determined by confocal-microscopy examination. Data are expressed as percentages of the control and are the averages ± SDs for triplicate measures. For control cells infected with purified IMV, a mean of 2,253 IMV virions was observed. For control cells infected with fresh EEV, means of 217 IMV virions and 509 EEV virions were observed. pp, physical particle.

fragile structure, and even when virions from the supernatant of infected cells were analyzed by cryoelectron microscopy, only a minority of particles had a complete and intact outer membrane (16). The data presented here show that the purification of EEV leads to the isolation of a majority of particles with a damaged outer membrane, as revealed by their sensitivity to a MAb that neutralizes IMV. Similar observations have been published recently by Ichihashi (9), who showed that treatments such as sonication and one cycle of freeze-thawing were sufficient to rupture the EEV membrane. Because damaged EEV could bind to the cell via an EEV or IMV protein, purified EEV should not be used for binding studies.

We took advantage of the fact that VV virions are very large to visualize them by fluorescent microscopy (conventional or confocal) after chemical (DNA labelling with DAPI) or indirect immunofluorescent labelling. The ability to visualize individual particles was then exploited to develop an original binding assay using double indirect immunofluorescence to differentiate and count IMV and EEV bound to the cell surface by confocal-microscopy analysis. This binding assay has several useful features. (i) By its capacity to reveal and identify simultaneously IMV and EEV, it enables unpurified preparations containing both forms of VV to be used. (ii) This assay does not require any prelabelling of the virus. (iii) The results generated are absolute numbers of virus particles/cell, not relative numbers representing the mean score of the cell culture; therefore, this assay could identify which cells in a heterogeneous culture bind IMV and/or EEV even if only a small fraction of cells do so. (iv) The assay gives steric information concerning the location of the virus binding site on the cell. (v)

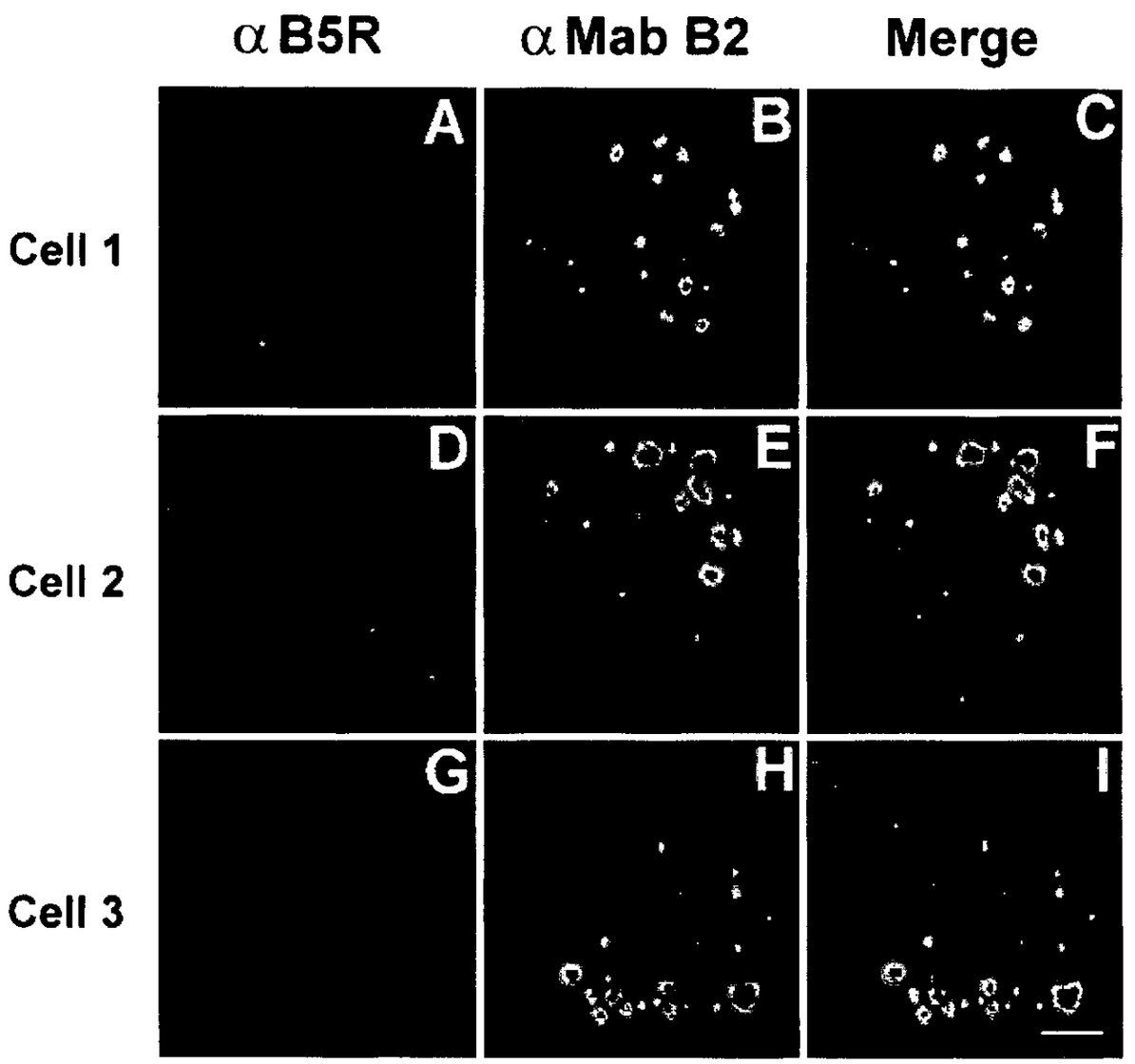

FIG. 4. Concomitant detection of EEV (red signal) and MAb B2-reactive molecule clusters (green signal) on the surfaces of HeLa cells. HeLa cells were grown as suspension cultures and were processed as described in Materials and Methods to induce capping of MAb B2-reactive molecules. Cells were then infected with fresh EEV at the MOI of 3.5 EEV PFU/cell (10^6 cells/ml) on ice for 1 h. After being washed with cold PBS–2% FBS, cells were fixed in PBS containing 4% paraformaldehyde (wt/vol) for 20 min on ice. MAb B2/RAM-IgM complexes were revealed by FITC-GARB. EEV were revealed by indirect immunofluorescent staining with MAb 19C2 as the primary antibody and PE-RAR as the secondary antibody. Cells were first incubated simultaneously with FITC-GARB and MAb 19C2 for 45 min at 37°C and after being washed were incubated with PE-RAR at 37°C for 30 min. After final washing, cells were mounted and examined by confocal microscopy. The three horizontal rows are analyses of three different cells. The first and second panels of each line are the emissions of red and green fluorescences, respectively, and the third panel is the merged image of the red and green emissions. Bar, 2 μm.

It enables staining with three or more antibodies, providing a way to investigate any correlation between the expression of a particular receptor and the capacity of a cell to bind EEV or IMV in a mixed cell population.

By this binding assay, we have shown that IMV and EEV bind to different cellular receptors. This conclusion is based on three observations. (i) The efficiencies with which different cell lines bind EEV and IMV are unrelated, (ii) cell surface treatments with some enzymes affect IMV and EEV binding differently, and (iii) MAb B2 bound on the cell surface does not affect EEV binding, even after capping of the unidentified molecule to which it binds.

In regard to the capacities of different cell lines to support EEV and IMV binding, we observed that while BS-C-1, RK_{13}, and HeLa cells bound IMV with similar efficiencies, these cells showed considerable variation in their capacities to bind EEV (Table 1), suggesting that the two forms of VV bind to different receptors. Theoretically, it should be possible to find cell lines which support exclusively IMV or EEV binding or cell lines which do not support the binding of IMV and EEV. These cell lines might be very useful in identifying IMV and EEV receptors by screening expression libraries of cDNA.

Cell surface treatments with trypsin, pronase, and neuraminidase affected IMV and EEV binding in different ways. The most spectacular effect was observed with pronase treatment, which nearly abolished IMV binding while EEV binding was

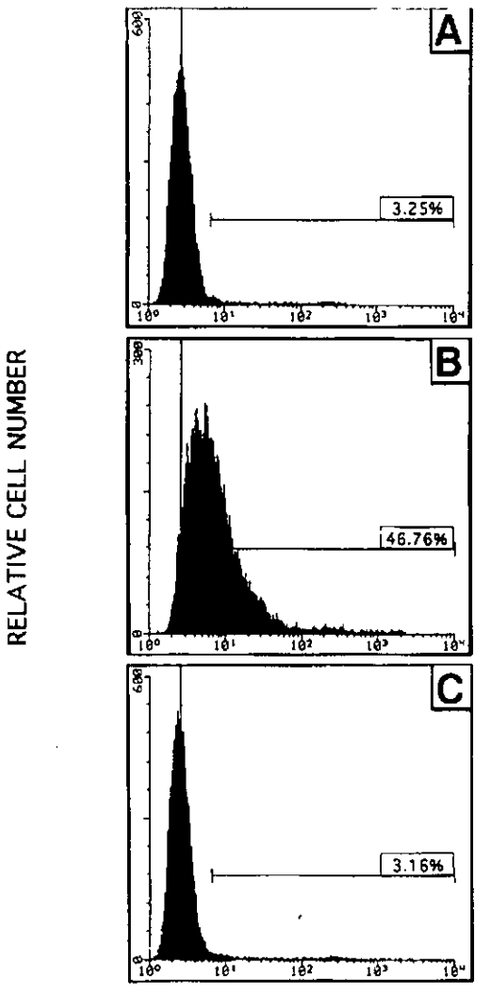

FIG. 5. MAb B2-reactive epitope is removed from the cell surface after trypsin treatment. HeLa cells grown as suspension cultures were mock (A and B) or trypsin (C) treated as described in Materials and Methods. Cell surface MAb B2-reactive epitope was quantified by flow cytometry. (A) Background staining of mock-treated cells stained with a mouse isotype IgM negative control and with secondary antibody. (B and C) Mock- and trypsin-treated cells stained for detection of MAb B2-reactive epitope, respectively.

enhanced (Table 1). This result showed that the IMV receptor must be composed of a peptide. The fact that pronase treatment seems to increase the accessibility of the EEV receptor does not prove that this receptor is not a protein; it could be a protein strongly resistant to protease treatment.

Lastly, the binding of MAb B2 to the cell surface, which inhibits IMV binding, has no effect on EEV binding, even after capping of the MAb B2-reactive molecule, indicating that this molecule is not a binding receptor for EEV. As to the inhibition of IMV binding by MAb B2, our results broadly confirm those published by Chang et al. (5), except that the degree to which IMV binding was prevented by MAb B2 was slightly different and that complete inhibition was not achieved. These results suggest that although the molecule recognized by MAb B2 is the major IMV receptor, it is not the only IMV receptor. Finally, our data demonstrate that MAb B2 prevents IMV binding by steric inhibition, because although trypsin treatment destroyed MAb B2 binding to cells, IMV binding was not affected.

Although saturation binding experiments were not possible due to the low concentration of EEV in fresh supernatants, we believe that the binding of virions to cells was specific. First, every bound IMV gave rise to a plaque, whereas for EEV only one in five virions did so. Second, the use of different cell types and the treatment of cells with three enzymes or MAb B2 affected the binding of IMV and EEV to cells and their infectivity to the same degree. If some binding was nonspecific, this would not have been so.

VV (and other orthopoxviruses) are unusual in that they produce two types of infectious virions, with different structures, antigenicity and biological properties. This is probably advantageous to the virus in enabling transmission in different ways but may also broaden the cell, tissue, or host tropism. The determination of the extent to which tropism may be broadened will require the identification of the IMV and EEV receptors and an analysis of their distribution. In vivo it may be that some cells express preferentially or exclusively IMV or EEV receptors. Consistent with this possibility, an analysis of only three cell lines has already shown considerable variation in EEV binding (Table 1). Another complication is that there is more than one IMV receptor, since MAb B2 only partially inhibited IMV binding (Table 2). Possibly EEV will also have several cellular receptors that are bound by different EEV glycoproteins.

In conclusion, we have described a novel method based on confocal microscopy to study virus binding. This assay has been applied to the study of VV binding, a field which has hitherto been complicated by the existence of two structurally and antigenically distinct forms of virus (IMV and EEV) which have not been physically purified from each other without damaging the outer envelope of EEV. Although the utility of this technique has been demonstrated here with VV, it should be applicable to any virus that is larger than 50 nm.

ACKNOWLEDGMENTS

We are most grateful to Christopher M. Sanderson for ideas and advice with capping experiments. MAb B2 was kindly provided by Wen Chang (Chinese Culture University, Republic of China). MAb 5B4/2F2 was a gift from Claus P. Czerny (Institute of Medical Microbiology, Infectious and Epidemic Diseases, Ludwig-Maximilians-University, Munich, Germany).

A. Vanderplasschen is a senior research assistant of the Fonds National Belge de la Recherche Scientifique (F.N.R.S.) and is the laureate of a NATO research fellowship. This work was supported by program grant PG8901790 from the U.K. Medical Research Council.

REFERENCES

1. **Appleyard, G., and C. Andrews.** 1974. Neutralizing activities of antisera to poxvirus soluble antigens. J. Gen. Virol. 23:197–200.
2. **Appleyard, G., A. J. Hapel, and E. A. Boulter.** 1971. An antigenic difference between intracellular and extracellular rabbitpox virus. J. Gen. Virol. 13:9–17.
3. **Boulter, E. A.** 1969. Protection against poxviruses. Proc. R. Soc. Med. 62: 295–297.
4. **Boulter, E. A., and G. Appleyard.** 1973. Differences between extracellular and intracellular forms of poxviruses and their implications. Prog. Med. Virol. 16:86–108.
5. **Chang, W., J.-C. Hsiao, C.-S. Chung, and C.-H. Bair.** 1995. Isolation of a monoclonal antibody which blocks vaccinia virus infection. J. Virol. 69:517–522.
6. **Cook, P. R., and I. A. Brazell.** 1975. Supercoils in human DNA. J. Cell Sci. 19:261–279.
7. **Czerny, C. P., and H. Mahnel.** 1990. Structural and functional analysis of orthopoxvirus epitopes with neutralizing monoclonal antibodies. J. Gen. Virol. 71:2341–2352.
8. **Essani, K., and S. Dales.** 1979. Biogenesis of vaccinia: evidence for more

than 100 polypeptides in the virion. Virology 95:385–394.
9. **Ichihashi, Y.** 1996. Extracellular enveloped vaccinia virus escapes neutralization. Virology 217:478–485.
10. **Ichihashi, Y., S. Matsumoto, and S. Dales.** 1971. Biogenesis of poxviruses: role of A-type inclusions and host cell membranes in virus dissemination. Virology 46:507–532.
11. **Mackett, M., G. L. Smith, and B. Moss.** 1985. The construction and characterization of vaccinia virus recombinants expressing foreign genes, p. 191–211. *In* D. M. Glover (ed.), DNA cloning: a practical approach. IRL Press, Oxford, United Kingdom.
12. **McIntosh, A. A. G., and G. L. Smith.** 1996. Vaccinia virus glycoprotein A34R is required for infectivity of extracellular enveloped virus. J. Virol. 70:272–281.
13. **Parkinson, J. E., and G. L. Smith.** 1994. Vaccinia virus gene A36R encodes a Mr 43-50K protein on the surface of extracellular enveloped virus. Virology 204:376–390.
14. **Payne, L. G.** 1979. Identification of the vaccinia hemagglutinin polypeptide from a cell system yielding large amounts of extracellular enveloped virus. J. Virol. 31:147–155.
15. **Payne, L. G.** 1980. Significance of extracellular enveloped virus in the *in vitro* and *in vivo* dissemination of vaccinia virus. J. Gen. Virol. 50:89–100.
16. **Roos, N., M. Cyrklaff, S. Cudmore, R. Blasco, J. Krijnse-Locker, and G. Griffiths.** 1996. A novel immunogold cryoelectron microscopic approach to investigate the structure of the intracellular and extracellular forms of vaccinia virus. EMBO J. 15:2343–2355.
17. **Sanderson, C. M., J. E. Parkinson, M. Hollinshead, and G. L. Smith.** 1996. Overexpression of the vaccinia virus A38L integral membrane protein promotes Ca^{2+} influx into infected cells. J. Virol. 70:905–914.
18. **Schmelz, M., B. Sodeik, M. Ericsson, E. J. Wolffe, H. Shida, G. Hiller, and G. Griffiths.** 1994. Assembly of vaccinia virus: the second wrapping cisterna is derived from the trans Golgi network. J. Virol. 68:130–147.
19. **Turner, G. S., and E. J. Squires.** 1971. Inactivated smallpox vaccine: immunogenicity of inactivated intracellular and extracellular vaccinia virus. J. Gen. Virol. 13:19–25.
20. **Vanderplasschen, A., M. Goltz, J. Lyaku, C. Benarafa, H.-J. Buhk, E. Thiry, and P.-P. Pastoret.** 1995. The replication *in vitro* of the gammaherpesvirus bovine herpesvirus 4 is restricted by its DNA synthesis dependence on the S phase of the cell cycle. Virology 213:328–340.

Cancer Immunol Immunother (2001) 50: 397–407
DOI 10.1007/s002620100214

ORIGINAL ARTICLE

Katrina T. Trevor · Evan M. Hersh · Jacquie Brailey
Jean-Marc Balloul · Bruce Acres

Transduction of human dendritic cells with a recombinant modified vaccinia Ankara virus encoding MUC1 and IL-2

Received: 30 March 2001 / Accepted: 7 June 2001 / Published online: 22 August 2001

Abstract The epithelial mucin MUC1 is considered an opportune target antigen for cancer immunotherapy, as it is over-expressed and exhibits aberrant glycosylation in malignant cells. Because dendritic cells (DC) are powerful initiators of immune responses, efforts have focused on tumor antigen-bearing DC as potent cancer vaccines. In this study we have characterized the transduction of monocyte-derived DC with a highly attenuated vaccinia virus vector [modified vaccinia Ankara (MVA)] encoding human MUC1 and the immunostimulatory cytokine IL-2. Analysis of transduced DC cultures generated from a number of donors revealed MUC1 expression in the range of 27–54% of the cells and a co-regulated secretion of bioactive IL-2. As shown by FACS analysis with MUC1-specific antibodies, the MVA-MUC1/IL-2-transduced DC predominantly expressed the fully processed glycoform of MUC1, typical of that displayed by normal epithelia. Over a 3-day period after transduction, transgene expression declined concurrent with an increase in MVA-induced cytopathic effects. The transduced DC stimulated allogeneic lymphocyte proliferation, indicating that DC immunostimulatory function is not impaired by vector transduction. In the presence of IL-2, MVA-transduced DC were able to enhance autologous lymphocyte proliferation. Also, vector expression was analyzed in DC cultures treated with TNF-α, a known DC maturation factor. As indicated by the up-regulation of several DC maturation markers, neither virus infection nor transgene expression influenced the maturation capacity of the cells. The MVA-MUC1/IL-2 vector effectively transduced both immature and TNF-α-matured DC. Overall, our results are encouraging for the clinical application of MVA-MUC1/IL-2-transduced DC.

Keywords Dendritic cells · Modified vaccinia Ankara · MUC1 · Immunotherapy · IL-2

K. T. Trevor (✉) · E. M. Hersh · J. Brailey
Arizona Cancer Center, 1515 N. Campbell Av.,
Tucson, AZ 85724, USA
E-mail: ktrevor@azcc.arizona.edu
Tel.: +1-520-6268467

J.-M. Balloul · B. Acres
Transgene S.A., Strasbourg, France

Introduction

The mucin MUC1 is a large, transmembrane glycoprotein localized to the apical membrane of normal epithelial tissue. Aberrant expression of the protein is observed in a number of different carcinoma types (prostate, lung, breast, ovarian, pancreatic, renal) [for reviews, see 39, 51] and certain hematopoietic neoplasms [52]. MUC1 is considered an opportune tumor-associated antigen (TAA) for immune targeting based on several novel features observed in the malignant state: (1) over-expression; (2) aberrant glycosylation, revealing novel epitopes for targeting; (3) loss of the normal apical distribution, allowing greater exposure to the immune system. Moreover, there is evidence of occasional antibody and cytotoxic T cell (CTL) immune responses to MUC1 in cancer patients, suggesting that MUC1 immunization has the potential to stimulate stronger anti-MUC1 responses [39, 51].

For pre-clinical testing, transgenic mice that express human MUC1 in a normal tissue distribution pattern have provided an opportunity to investigate novel vaccine approaches for generating human anti-MUC1 tumor immunity [2, 13, 25, 38, 44]. Of importance, tolerance to human MUC1 can be overcome without inducing autoimmunity. In several clinical trials, cancer patients have been vaccinated by direct administration of MUC1 polypeptides [22, 26, 33]. In general, anti-MUC1 antibody responses predominate with few, if any, MUC1-specific CTL responses detected. Although neither toxicity nor autoimmunity is evident, overt tumor regression has not been observed. Recently, a vaccinia virus (VV) vector containing both a MUC1 cDNA and a cDNA encoding the immunomodulatory cytokine

interleukin 2 (IL-2) was used in a phase I/II vaccine trial of breast cancer patients [47]. Intramuscular vaccination resulted in no serious side effects, and two of nine patients generated MUC1-specific CTL.

Because strong anti-tumor CTL responses are considered vital for tumor eradication [21], dendritic cell (DC)-based tumor vaccination has emerged as a promising approach to cancer immunotherapy [for reviews, see 21, 40, 41]. DC are the most potent antigen-presenting cells for stimulating naive and memory T cell responses, including both $CD4^+$ T helper cells and $CD8^+$ CTL [21, 41]. Strategies involve loading DC with specific TAA peptide/protein or RNA; pulsing DC with whole tumor cell products, such as RNA, apoptotic bodies and peptides eluted from major histocompatibility complexes (MHCs); and directly fusing DC with tumor cells [21, 25, 37, 40]. In a recent phase I study, vaccination with DC pulsed with MUC1-derived peptides induced CTL immune responses in at least some patients with metastatic breast or ovarian cancer [10].

A further approach for loading DC with TAA is the introduction of TAA transgenes into DC [for review see 34]. Advantages include prolonged duration of TAA presentation to the immune system by the gene-expressing DC and display of multiple TAA peptide epitopes by diverse HLA alleles, obviating the requirement to define the patient's HLA haplotype when pulsing with a TAA peptide. Both recombinant viral vectors (adenovirus, poxvirus, retrovirus, herpes virus) and plasmids have been used to introduce transgenes into DC [34].

MUC1 expression in DC has been obtained by transfection with MUC1-encoding plasmid DNA or RNA [35, 45], as well as by transduction with MUC1 recombinant viruses derived from murine retrovirus [27, 28] and adenovirus [24]. Limitations for the application of plasmid DNA and RNA include relatively low transfection efficiencies and lack of durable expression, especially with RNA molecules [34]. Transduction with murine retroviral vectors requires the isolation and transduction of dividing $CD34^+$ progenitors prior to cytokine-induced DC differentiation [27, 28]. This approach is not applicable to DC differentiated from non-dividing monocytes derived from peripheral blood, a common source of cells for ex vivo DC generation [6, 21].

In this report, we have investigated the in vitro transduction of monocyte-derived DC with a MUC1/IL-2 VV-type vector. Although direct administration of this vector type demonstrated CTL responses in at least some patients [47], our rationale is that improved MUC1-specific CTL responses would be observed upon immunization with gene-modified DC. For this study, the recombinant vector was prepared using the highly attenuated VV strain, modified vaccinia virus Ankara (MVA). In contrast to conventional VV strains, MVA exhibits limited replicative capacity in mammalian cells and has lost several functional cytokine receptors that may contribute to VV immune evasion and virulence [5, 7, 50]. We demonstrate that both immature and TNF-α-matured DC are effectively transduced with MVA-MUC1/IL-2, resulting in detectable expression of both MUC1 and bioactive IL-2. Although the MVA vector can induce virus-related cytopathic effects over time, the functional capacity and maturation status of DC are not overtly altered. Our results suggest that DC modified with this MVA recombinant vector may prove clinically relevant as a vaccine for the generation of anti-MUC1 tumor responses.

Materials and methods

Dendritic cells and cell culture

DC were generated from monocyte-derived peripheral blood mononuclear cells (PBMC). Briefly, peripheral blood was obtained from healthy donors, and PBMC were purified over Ficoll-Hypaque (Pharmacia Corp., Peapack, N.J.). The cells were washed three times with sterile phosphate-buffered saline [PBS (Nexell Therapeutics, Irvine, Calif.)] and plated in 25 ml of AIM-V medium (Gibco/BRL, Gaithersberg, Md.) at a concentration of $1.5–2\times10^8$ cells per T-75 flask (Corning Inc., Corning, N.Y.). Monocytes were allowed to adhere for 2 h at 37°C in a humidified 5% CO_2 incubator. The non-adherent PBMC were removed and frozen for future use in Origen Freezing Media (IGEN International Inc., Gaithersberg, Md.) at –80 °C. The plastic adherent cells were subsequently cultured in 25 ml of AIM-V media supplemented with 1000 U/ml GM-CSF (Immunex, Seattle, Wash.), 1000 U/ml Interleukin-4 (Schering-Plough, Kenilworth, N.J.) and 5×10^{-5} M 2-ME (Gibco/BRL). The cells were then incubated for 8 days (= day). For maturation, TNF-α (R&D Systems) was added at 200 IU/ml during the last 2 days of culture. The DC yield was typically 5–10% of the input PBMC. The MCF-7 human breast cancer cell line was obtained from the American Type Culture Collection (Rockville, Md.) and cultured in RPMI-1640 medium (GIBCO/BRL) supplemented with 10% heat-inactivated fetal bovine serum [FBS (HyClone, Logan, Utah)] and 2 mM L-glutamine. Cell viability was evaluated by trypan blue dye exclusion.

Monoclonal antibodies and FACS analysis

The DC phenotype was assessed by immunostaining followed by FACS analysis using fluorescent-conjugated monoclonal antibodies recognizing HLA-DR (MHC class II), CD1a, CD14 (monocyte lineage marker), the co-stimulatory molecules CD86 and CD80, and the CD83 DC maturation marker (BD Pharmingen, San Diego, Calif.). The monoclonal antibodies HMFG-1, HMFG-2 and SM-3, which recognize differentially glycosylated forms of MUC-1, were kindly provided by Dr. J. Burchell (Imperial Cancer Research Fund, London, England) [11, 12, 23]. FITC-conjugated goat anti-mouse antibody (Sigma Chemical Co., St. Louis, Mo.) was used as secondary antibody. Washes were performed in PBS. Cells were subsequently fixed in 2% paraformaldehyde/PBS. Apoptosis and necrosis were assessed by staining with FITC-Annexin V/propidium iodide using the Apoptosis Detection Kit (Caltag Laboratories, Burlingame, Calif.), as described by the manufacturer. Flow cytometry was performed on a FACScan (Becton Dickinson, San Jose, Calif.) with staining pattern analysis performed using the WinMDI software (J. Trotter, Scripps Institute, La Jolla, Calif.).

Viral vectors and gene transduction of target cells

The recombinant MVA-MUC1 vector encodes the human MUC1 containing 5 copies of the tandem repeat under the control of the early/late pH5R promoter. The vector MVA-MUC1/IL-2 addi-

tionally encodes the human IL-2 cDNA under the control of the vaccinia early/late p7.5 promoter, which is placed head-to-head with the MUC1 sequence. DC were plated in 6-well dishes (Corning) at 1–2×10^6 cells/well. Recombinant virus was added in a total of 2 ml of AIM-V media. Plates were spun at 1000 *g* for 1.5 h at room temperature. The co-centrifugation of MVA virus and DC improved transduction (data not shown), as previously reported for recombinant retrovirus and adenovirus vectors [36, 42]. Directly after the centrifugation period, the viral-containing medium was removed, and the cells were returned to AIM-V media containing 1000 IU/ml each of GM-CSF and IL-4. For DC maturation studies, TNF-α (R&D Systems, Minneapolis, Minn.) was added at 200 IU/ml to media containing GM-CSF and IL-4. With respect to the multiplicity of infection (MOI) with MVA virus, 1 plaque-forming unit (pfu) of MVA is composed of a clump of virus particles, unlike replicative VV strains [48]. Therefore, 1 pfu of MVA is likely to infect several cells.

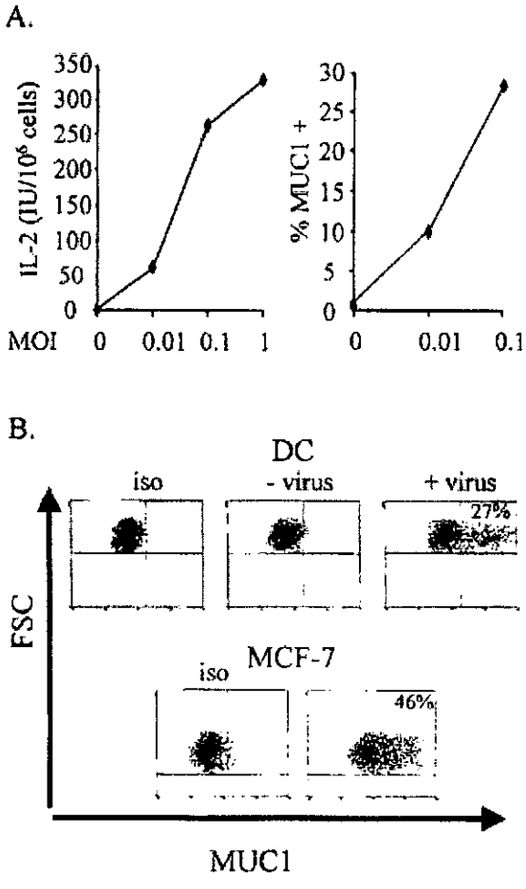

Fig. 1A, B Dose-response expression of MVA-MUC1/IL-2 vector by DC. **A** DC were transduced at the indicated MOI and analyzed for expression 24 h later. MUC1 expression was determined by immunostaining with the anti-MUC1 HMFG-1 antibody followed by FACS analysis. IL-2 levels were assessed by ELISA analysis of cell supernatants. **B** FACScan representation of MUC1 expression at 24 h post-transduction at the indicated MOI of 0.1 shown in **A**. *Panels* depict DC stained with the anti-HMFG-1 antibody with and without virus transduction and immunostaining with the control isotype (*iso*) antibody. Immunostaining of MCF-7 breast cancer cells is shown for comparison. Percent MUC1 positive cells are indicated

IL-2 cytokine analysis

Expression of IL-2 by transduced cells was determined by analyzing supernatants for levels of secreted IL-2. Cells were centrifuged at 1000 *g* for 5 min, and supernatants were removed and stored at –20 °C. Samples were thawed and analyzed for human IL-2 using a commercial enzyme-linked immunosorbent assay (ELISA) kit (Biosource International, Camarillo, Calif.). ELISA values (ng/ml) were converted to IU/ml according to the manufacturer. Standard deviations between duplicate samples were routinely less than 15%. IL-2 bioactivity was confirmed by determining whether the secreted protein supported the proliferation of activated peripheral blood lymphocytes [4]. PBMC were activated by plating cells at 1×10^6 cells/ml in AIM-V media in 24-well dishes that were pre-coated with a solution of 2 μg/ml murine anti-CD3 monoclonal antibody (BD Pharmingen) in PBS. PBMC were maintained for 3 days, washed and plated in triplicate at 1×10^5 cells in 96-well dishes in 100 μl of fresh AIM-V media and 100 μl of supernatant from individual DC cultures. Supernatants were derived from DC that had been transduced as described above and maintained for 3 days in AIM-V media without the addition of GM-CSF and IL-4 to avoid potential proliferative effects induced by these cytokines. Controls included supernatant from the same DC cultures that were not transduced or AIM-V media only and AIM-V media containing 100 IU/ml recombinant human IL-2 (Cetus, Emeryville, Calif.). After 5 days, PBMC proliferation was assessed by [^{3}H]-thymidine incorporation as described previously [43]. Mean counts per minute (cpm) values were calculated and standard deviations determined.

Mixed lymphocyte reaction (MLR) assays

Frozen, non-adherent PBMC that were obtained following monocyte adherence (described above) were thawed at 37 C and rested overnight in AIM-V media at 1×10^6 cells/ml in a 24-well culture dish. PBMC (2×10^5 cells) were added to 4×10^4 DC plated in triplicate in 200 μl of AIM-V media in a flat-bottom, 96-well culture dish. Autologous MLR assays were performed using DC and PBMC derived from the same donor. DC and PBMC obtained from separate donors were used for the allogeneic MLR assays. To those cultures receiving exogenous IL-2, recombinant human IL-2 (Cetus, Emeryville, Calif.) was added to 100 IU/ml. After 5 days, proliferation was determined by [^{3}H]-thymidine incorporation as previously described [43].

Results

Dose-response expression of the MVA-MUC1/IL-2 vector by DC

Monocyte-derived DC obtained from culturing in GM-CSF and IL-4 generally showed characteristic expression of HLA-DR class II, CD1a, CD54, CD86 and CD80 with < 15% of the cells displaying the monocyte lineage marker CD14 (data not shown). Viable staining of the cells at days 6–8 revealed the morphologic appearance of DC with veiled edges and multiple processes (data not shown). A dose-response experiment was initially performed comparing expression of the MVA-MUC1/IL-2 vector at increasing multiplicities of infection (MOIs). DC were transduced at three different MOIs and incubated for 24 h prior to determining IL-2 and MUC1 antigen expression. With respect to IL-2 secretion, increasing MOIs clearly resulted in higher levels of IL-2 (Fig. 1A). Similarly, there was a parallel increase in MUC1 expression, as determined by immunostaining

with the anti-MUC1 antibody HMFG-1, which recognizes a highly glycosylated form of MUC1 [12]. At the highest MOI tested (an MOI of 1), the DC culture contained extensive amounts of cellular debris and dead cells, based on microscopic examination, preventing accurate measurement of MUC1 expression. DC receiving lower doses of virus (MOIs of 0.01 and 0.1) were ~90% viable, as determined by trypan blue dye staining, similar to non-transduced DC. Figure 1B shows FACS analysis for MUC1 expression by DC cultures infected at an MOI of 0.1 and analyzed 24 h post-transduction. Non-transduced DC appeared negative for immunostaining with the HMGF-1 antibody. For comparison, anti-HMFG-1 staining of MUC1-expressing MCF-7 breast cancer cells is shown; the percentage of positive cells was routinely 45–55%.

MVA-MUC1/IL-2-transduced DC were further analyzed for expression of differentially glycosylated forms of MUC1. As detected by immunostaining with the HMFG-1 antibody, the cells primarily displayed highly glycosylated molecules (Table 1), which are exhibited most abundantly on normal epithelium [51]. A much lower percentage of cells was stained with the SM-3 or HMFG-2 anti-MUC1 antibodies, both of which recognize tumor-associated, under-glycosylated MUC1 molecules. Typical of the MCF-7 breast cancer cell line, a combination of all 3 glycoforms of MUC1 was expressed [11, 12]. As previously shown for MCF-7 cells, surface staining was heterogeneous with SM-3 epitopes displayed on ~50% fewer cells than HMFG-2 epitopes [31].

Expression of MVA-based MUC1 vectors by DC generated from different donors

To examine DC donor variation in the expression the MVA-MUC1/IL-2 vector, cultures of DC derived from five different blood donors were transduced at an MOI of 0.1 and analyzed for MUC1 and IL-2 expression at 24 h post-transduction. As shown in Fig. 2A, MUC1-positive cell expression varied between 27 and 54%. IL-2 secretion profiles correlated with the MUC1 levels in that higher amounts were detected in those cultures with higher numbers of MUC1-expressing DC. In addition, DC derived from three different donors were transduced with both the MVA-MUC1/IL-2 vector and an MVA-MUC1 virus, lacking the IL-2 cDNA insert. The percentages of MUC1-positive cells were comparable for the two vectors (Fig. 2 B). These results suggest that co-expression of IL-2 does not alter DC expression of the MUC1 transgene.

Table 1 DC expression of MUC1 glycoforms

Anti-MUC1 antibody	DC (% +)	MCF-7 (% +)
HMFG-1	28	57
HMFG-2	<1	27
SM-3	<1	14

Bioactivity of transgene-derived IL-2

The immunostimulatory activity of IL-2 was confirmed by determining whether the IL-2 secreted by DC transduced with the MVA-MUC1/IL-2 vector was capable of sustaining the proliferation of activated PBMC. Supernatants were removed from cultures 72 h after transduction with the MVA-MUC1 or MVA-MUC1/IL-2 vector (MOI 0.1) and subsequently added to previously activated PBMC cultures. As shown in Fig. 3, supernatants derived from non-transduced DC or DC transduced with MVA-MUC1 vector exhibited little, if any,

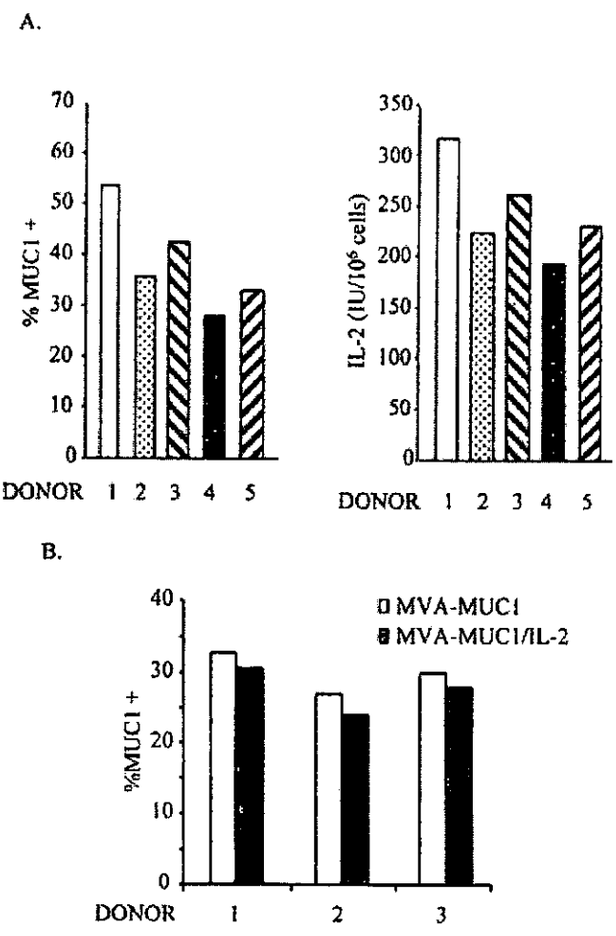

Fig. 2A, B Donor DC expression of MVA vectors encoding MUC1. DC cultures generated from separate donors were transduced at an MOI of 0.1 and analyzed 24 h later for vector expression. A Cells from five donors were immunostained with the anti-MUC1 HMFG-1 antibody, followed by FACS analysis. Supernatants were analyzed by ELISA for IL-2 expression. B Cells from three donors were transduced with either the MVA-MUC1 or MVA-MUC1/IL-2 vector. MUC1 expression was determined by HMFG-1 antibody immunostaining and FACS analysis

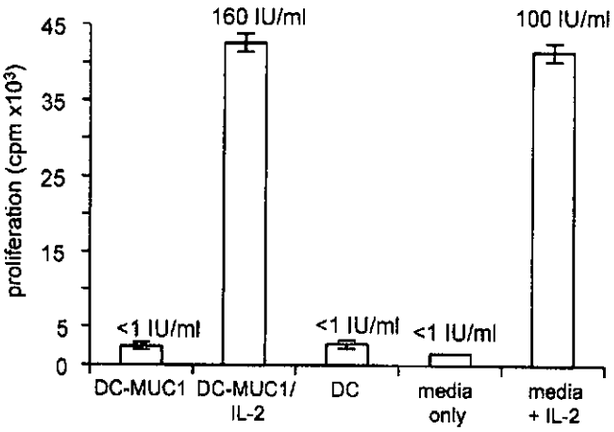

Fig. 3 Bioactivity of MVA-MUC1/IL-2 transgene-encoded IL-2. Supernatants derived from non-transduced DC or cells transduced with either MVA-MUC1 or MVA-MUC1/IL-2 were added to pre-activated PBMC, as described in the Materials and methods. ELISA values of IL-2 (IU/ml) added to each sample are indicated. Additional samples of PBMC received media only or media to which recombinant human IL-2 was added (100 IU/ml). PBMC proliferation was assessed 5 days later by measuring [^{3}H]-thymidine incorporation. Mean counts per minute (cpm) are given for triplicate samples; standard deviations are shown

IL-2, as determined ELISA analysis and failed to support high-level PBMC proliferation. In contrast, supernatant derived from DC transduced with MVA-MUC1/IL-2 and added at 160 IU/ml IL-2 maintained PBMC proliferation at levels comparable to PBMC receiving 100 IU/ml recombinant human IL-2. This data indicated that the MVA-encoded IL-2 is functionally active and capable of supporting PBMC expansion.

Time-course of MVA-MUC1/IL-2 expression and MVA-induced cytopathic effects

Expression levels of MVA-derived MUC1 and IL-2 were monitored at 24, 48 and 72 h post-transduction. As depicted in Table 2, the percentage of MUC1-positive cells declined over each consecutive 24-h time period, from 54% at 24 h post-transduction to only 10% by 72 h post-transduction. IL-2 secretion monitored over each time period was also reduced. Moreover, as determined by trypan blue dye exclusion, there was a concomitant decline in cell viability that appeared to correlate with the loss in MUC1-positive cells. Comparable results have been obtained for transduced DC generated from 2 other blood donors (data not shown).

Table 2 Time course of MUC1 expression and DC viability. DC were plated at 2×10^6 cells/well and infected at an MOI of 0.1. Medium was exchanged daily and analyzed for IL-2

Time post-transduction	% MUC1 +	IL-2 (IU/well)	% Viability
24 h	54	660	89
48 h	36	401	58
72 h	10	123	39

The cell death observed over time in the MVA-MUC1/IL-2-transduced cultures was most likely a consequence of known MVA-mediated cytopathic effects that can occur in infected human cell types, including DC [14, 16]. To confirm that DC cell death was attributable to the MVA vector and not overtly influenced by expression of MUC1 or IL-2, cells receiving either MVA-MUC1/IL-2 or a wild-type MVA virus lacking the transgenes (MVA-wt) were compared for the extent of cell death. Figure 4 shows FACS analysis of apoptotic and necrotic DC 48 h after vector transduction (MOI 0.1). Apoptosis was indicated by Annexin V staining, while necrosis was determined by propidium iodide (PI) staining. Relative to the non-transduced DC population, both the MVA-wt and MVA-MUC1/IL-2 transduced DC cultures exhibited significant numbers of cells that appeared to have experienced apoptosis, followed by necrosis based on dual staining by both Annexin V and PI (MVA-wt, 17%; MVA-MUC1/IL-2, 15%). Moreover, both populations contained higher levels of apoptotic cells at this time point, as indicated by Annexin V staining only (MVA-wt, 18%; MVA-MUC1/IL-2, 16%). With respect to viable cells that were negative for Annexin V and PI staining, the MVA-wt-transduced culture displayed only slightly fewer viable cells than the MVA-MUC1/IL-2 population (MVA-wt, 49% viable; MVA-MUC1/IL-2, 59% viable). Overall, the observed cytopathic effects appeared to be mediated by the MVA viral vector with no obvious effects of MUC1/IL-2 transgene expression on DC viability.

Functional activity of MVA-transduced DC

The ability of DC to induce proliferation of allogeneic PBMC has served as a reliable indicator of DC immunostimulatory function [21]. Recent studies have reported that transduction with a wild-type vaccinia virus vector can inhibit the ability of DC to stimulate allogeneic PBMC proliferation [19, 30]. The functional properties of non-transduced DC and DC transduced with the various MVA vectors (MVA-wt; MVA-MUC1:

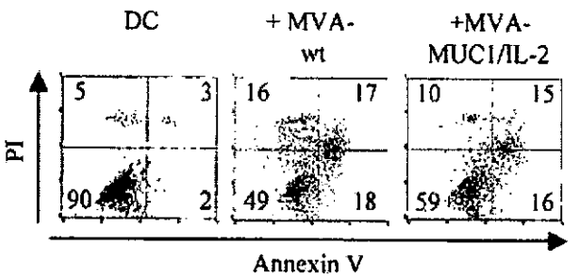

Fig. 4 MVA-mediated cell death in DC cultures. DC were transduced with either MVA-MUC1/IL-2 or MVA-wt (MOI 0.1) and analyzed 48 h later. Apoptotic and necrotic cells were determined by staining with FITC-Annexin V and propidium iodide (PI) followed by FACScan analysis

MVA-MUC1/IL-2) were compared in an allogeneic MLR assay. DC cultures were transduced at an MOI of 0.1, followed by the addition of allogeneic PBMC at a DC:PBMC ratio of 1:5. Cultures were assessed 5 days later for induced PBMC proliferation. Analysis of separate aliquots of the DC cultures at 24 h post-transduction indicated 32% and 30% MUC1-positivity in populations exposed to the MVA-MUC1 and MVA-MUC1/IL-2 vectors, respectively. Controls included non-transduced DC cultures plus PBMC co-cultivated in 100 IU/ml of IL-2, as well as PBMC alone with or without exogenous IL-2 addition. As shown in Figure 5A, comparable levels of allogeneic PBMC proliferation were observed in MVA-transduced and non-transduced cultures. Neither the IL-2 expressed by the MUC1/IL-2 transgene nor exogenous IL-2 influenced proliferative responses. Most likely, this reflects the highly stimulatory nature of the allogeneic DC; allo-PBMC proliferation would not necessarily be further enhanced by IL-2 addition. PBMC alone exhibited minimal proliferation, which was augmented by the addition of exogenous IL-2. Even though, the overall level of proliferation remained far less than cultures containing DC. These findings indicate that MVA-transduced DC cultures in general, and those expressing MUC1 and IL-2 in particular, are functionally capable of stimulating an allogeneic PBMC response.

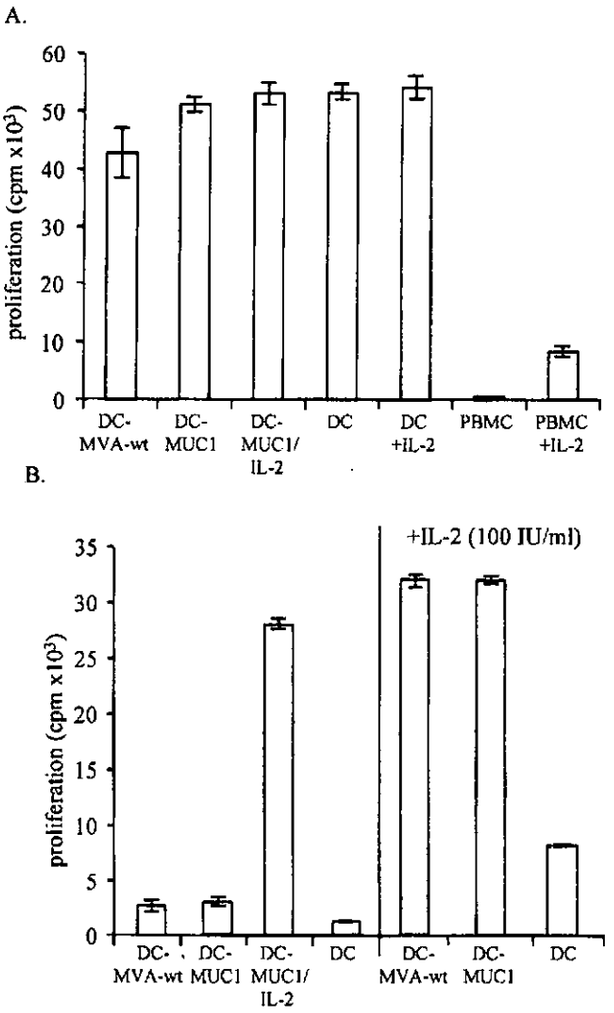

Fig. 5A, B Functional activities of MVA-transduced DC, as indicated by MLR assays. A DC were transduced at an MOI of 0.1 with the MVA viral vectors (MVA-wt; MVA-MUC1; MVA-MUC1/IL-2). Allogeneic PBMC (2×10^5 cells) were cultured in the absence or presence of the DC populations (4×10^4 cells). Recombinant human IL-2 (100 IU/ml) was added as indicated (+IL-2). [^{3}H]-thymidine uptake was subsequently measured 5 days after co-cultivation. B An autologous MLR assay was performed as described in A. Data are reported as mean counts per minute (cpm) of triplicates ± SD

The concept of including the IL-2 cDNA insert in the MVA vector was to provide further immunostimulatory support to autologous lymphocytes that would be exposed to the MVA-MUC1/IL-2-transduced DC in vivo. With this consideration, proliferation of autologous PBMC cultured in the presence of DC transduced with the MVA vectors was assessed in an autologous MLR assay. PBMC were mixed with the respective DC cultures at a ratio of 5:1 immediately following the 1.5-h transduction period. In separate cultures maintained in the absence of added PBMC, the MVA-MUC1/IL-2 DC secreted IL-2 at 228 IU/10^6 cells by 24 h post-transduction. MUC1 positivity was 31% and 28% in the MVA-MUC1 and MVA-MUC1/IL-2 DC cultures, respectively. The proliferative activity of autologous PBMC cultured in the presence of MVA-MUC1/IL-2 DC was markedly higher than that observed in samples receiving non-transduced DC or DC transduced with MVA-wt or MVA-MUC1 vector (Fig. 5B). The addition of exogenous IL-2 (100 IU/ml) to reactions containing DC transduced with MVA or MVA-MUC1 increased PBMC proliferation to levels comparable to the MVA-MUC1/IL-2 cultures (Fig. 5B). Although exogenous IL-2 addition improved proliferation of PBMC exposed to non-transduced DC, the effect was ~4-fold less than that observed in the MVA-transduced cultures. Similar results have been observed using DC and PBMC derived from a second donor (data not shown). These observations demonstrate that IL-2, either provided by transgene expression or exogenous addition, stimulates the proliferation of autologous PBMC upon exposure to MVA-transduced DC. Possibly, the donor PBMC are responding to MVA antigens.

MVA vector transduction of DC matured in the presence of TNF-α

We examined whether transduction with the MVA-MUC1/IL-2 vector would alter the maturation of DC exposed to TNF-α. This cytokine is known to induce DC maturation and, thereby, augment antigen-specific T cell responses [6, 9, 21]. Moreover, TNF-α-matured DC have been applied in cancer vaccine trials in which the DC appear to stimulate antigen-specific CTL responses [10, 37]. DC derived from two separate donors were exposed

to the MVA-MUC1/IL-2 virus (MOI 0.1) and cultured with or without TNF-α addition for 48 h. Comparable levels of MUC1 and IL-2 were observed in the presence or absence of TNF-α (Fig. 6A). As indicated by assessment of the levels of CD83 expression, a primary indicator of DC maturation [21], virus transduction did not appear to affect TNF-α-induced maturation (Fig. 6A). CD83 expression was upregulated 3–6-fold in both non-transduced and transduced cultures.

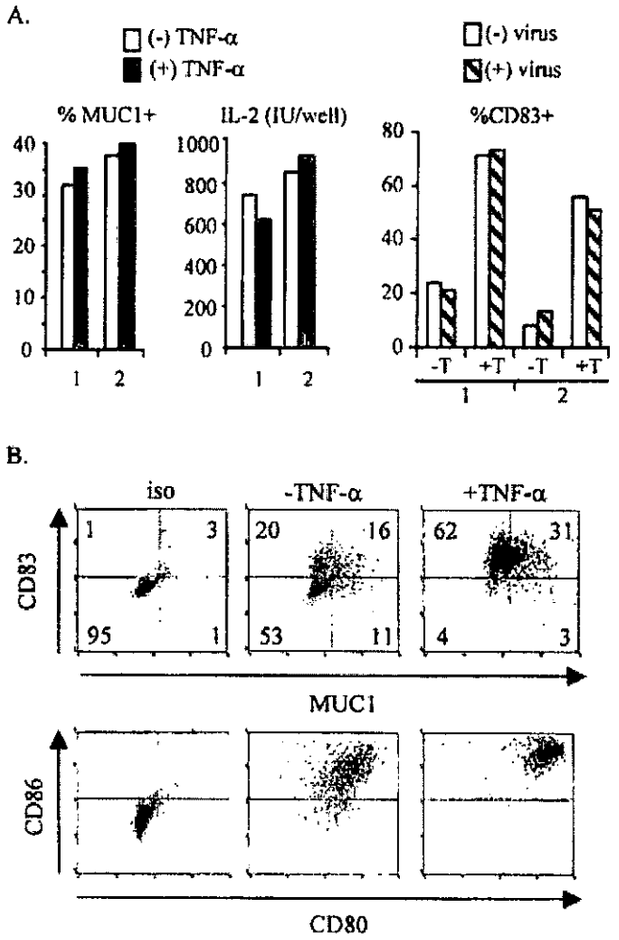

Fig. 6A, B Effect of MVA transduction on TNF-α-induced DC maturation. **A** DC populations derived from two separate donors (1 and 2) were transduced with the MVA-MUC1/IL-2 vector (MOI 0.1) and cultured for 48 h in the presence of GM-CSF and IL-4 cytokines with or without the addition of TNF-α (200 IU/ml). MUC1 expression was determined by immunostaining with the HMFG-1 antibody followed by FACS analysis. ELISA analysis of cell supernatants was used to monitor IL-2 expression and accumulation during the 48-h incubation period. Surface expression of the CD83 maturation marker was monitored by immunostaining and FACS analysis of both non-transduced and transduced cultures, with or without the addition of TNF-α (−T, +T). **B** MVA-MUC1/IL-2 DC, cultured in the presence or absence of TNF-α for 48 h, were dual immunostained and analyzed for MUC1 expression and markers of DC maturation. Analysis of staining with control, isotype antibodies is also shown (*iso*). *Upper panel*, co-staining for MUC1 and CD83. *Numbers* represent percentages of cells present in each quadrant based on FACScan analysis: *upper left*, $CD83^+$ only; *upper right*, $CD83^+$ $MUC1^+$; *lower right*, $MUC1^+$ only; *lower left*, $CD83^-$ $MUC1^-$. *Lower panel*, co-staining for CD80 and CD86 maturation markers. Note that TNF-α induced an increase in intensity of cells expressing both markers

In a separate experiment, dual flow cytometry was performed to confirm that matured DC displaying CD83 also expressed the MUC1 transgene. As shown in Fig. 6B, DC transduced and cultured in the absence of TNF-α exhibited relatively low levels of the CD83 marker (36% positive), as expected, with MUC1 expression detected in both CD83-positive (16% MUC1 positive) and -negative cells (11% MUC1 positive). Transduced DC that were subsequently matured in the presence of TNF-α displayed an overall higher level of CD83 expression with the majority of cells (93%) displaying CD83. The majority of cells exhibiting MUC1-positivity were of the $CD83^+$ mature phenotype (31%). As is well known for maturing DC populations [21], the co-stimulatory molecules CD80 and CD86 were also substantially upregulated by TNF-α treatment (Fig. 6B), along with enhanced expression of the MHC II molecule HLA-DR (data not shown). Non-transduced DC showed a similar upregulation of these markers upon TNF-α exposure (data not shown). Taken together, these results indicate that MVA-MUC1/IL-2 transduction and gene expression are not inhibitory to TNF-α-induced maturation. Conversely, TNF-α maturation does not modify expression of the MVA-encoded transgenes.

With respect to MVA-mediated cell death, Annexin-V and PI co-staining demonstrated that infection followed by TNF-α exposure results in a loss in viability, as observed for immature DC populations exposed to virus. By 48 h post-transduction with either MVA-wt or MVA-MUC1/IL-2 virus, ~50% of the cells remained viable (data not shown). TNF-α maturation of previously transduced DC did not appear to impact the cytopathic effects of the MVA virus.

If DC cultures were instead first matured in the presence of TNF-α for 48 h followed by MVA-MUC1/IL-2 exposure (MOI 0.1), expression levels of the MUC1 and IL-2 transgenes were comparable to immature, transduced DC (Fig. 7). Moreover, virus transduction and expression did not substantially alter levels of the CD83 marker induced by prior TNF-α exposure. Further FACS analysis revealed no effects of virus transduction on the upregulated expression of HLA-DR, CD80 and CD86 molecules (data not shown). Overall, TNF-α-matured DC were as susceptible to MVA virus infection and transgene expression as immature DC. Based on DC marker evaluations, the MVA-MUC1/IL-2 virus did not affect the DC maturation status.

Discussion

DC are attractive cancer vaccine agents, based on their ability to efficiently present TAAs and prime CTL anti-tumor responses [6, 21, 41]. Transduction of DC with

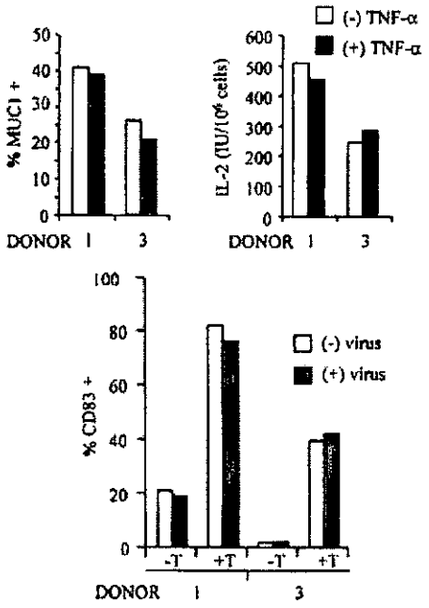

Fig. 7 MVA-MUC1/IL-2 transduction of TNF-α-matured DC. DC populations were cultured in the presence of GM-CSF and IL-4 with or without TNF-α (200 IU/ml) for 48 h prior to exposure to the MVA-MUC1/IL-2 virus (MOI 0.1). Cells were analyzed for MUC1, IL-2 and CD83 expression at 24 h post-transduction as described in Fig. 6A

recombinant virus vectors is considered an efficient means of loading DC with TAA for DC immune display of TAA antigenic peptides [34]. Herein, we have characterized the transduction of monocyte-derived DC with an MVA vector expressing genes for both the MUC1 TAA and the immunostimulatory cytokine IL-2. Moreover, we have investigated biological aspects of MVA vector-DC interactions that could influence clinical application of the MVA-MUC1/IL-2-transduced DC.

Thus far, reports of DC transduced with recombinant MVA vectors have been limited [16, 17], although there have been several studies applying recombinant VV vectors derived from conventional virus strains (Western Reserve, Copenhagen) [19, 49, 18, 30]. An MVA vector encoding the melanoma TAA tyrosinase has been shown to express in monocyte-derived DC; however, potential virus-related effects on the target DC were not addressed [17]. In a second study, MVA-mediated gene transfer into $CD34^+$ stem cells or $CD34^-$-derived DC was investigated rather than DC derived from monocytes [16].

With respect to transgene expression in MVA-MUC1/IL-2-tranduced DC cultures, an MOI of 0.1 provided significant expression of both MUC1 and IL-2, with the levels of IL-2 secretion consistently reflecting the MUC1 positivity. Following transduction with either the MVA-MUC1 or MVA-MUC1/IL-2 vector, MUC1 expression levels were virtually identical, indicating that the MUC1/IL-2 dual-expression vector is of a favorable design and that IL-2 co-expression does not alter the level of MUC1 production. A co-regulation of the MUC1 and IL-2 transgenes is anticipated, as the MUC1 and IL-2 transgenes are each driven by similar promoter elements that carry both early and late transcriptional signals (pHR5 and p7.5, respectively). In studies with other VV strains, early promoters have been shown to retain activity in monocyte-derived DC, while late promoter activity is suppressed, along with virus replication [18, 19, 30]. Consequently, known replicative strains of VV are phenotypically similar to MVA in that virus production is attenuated in DC cultures.

MVA-MUC1/IL-2-transduced DC predominantly display fully glycosylated MUC1, comparable to that found on normal epithelia. There is only low-level expression of under-glycosylated forms that are typical of tumor cells, including the MCF-7 breast cancer cells in this study [12, 13]. As a non-malignant cell type, DC would not be expected to exhibit changes in glycosyltransferase activities that are known to give rise to tumor-associated glycoforms of MUC1 [51]. Our results are compatible with one other study in which $CD34^-$ cells were transduced with a retroviral vector encoding MUC1 and subsequently differentiated into DC; underglycosylated MUC1 molecules were only weakly detected [27]. In theory, the glycosylation status of MUC1 expressed by DC should not affect MHC class I peptide display, because class I molecules are loaded with peptide in the ER before transport and glycosylation in the Golgi apparatus [51]. Moreover, vaccination with DC transfected with human MUC1 RNA induces MUC1-specific CTL and anti-tumor immunity in mice bearing tumors expressing human MUC1 [35]. Although the MUC1 glycosylation status was not determined, this result indicates that DC expressing MUC1 are capable of processing and displaying MUC1 peptides in the context of MHC class I molecules.

The significant loss in DC expressing the MUC1/IL-2 transgenes over a 3-day period post-transduction correlates with enhanced cell death. Comparable percentages of apoptotic and necrotic cells were observed in cultures transduced with either MVA-wt or the MVA-MUC1/IL-2 vector, indicating that the loss in cell viability is MVA-related. Similarly, MVA-associated toxicity has been observed in transduced $CD34^+$-derived DC cultures [16]. The occurrence of cells staining for both Annexin-V and PI suggests that our MVA-transduced cells die via apoptosis followed by necrosis, a phenomenon previously seen in DC cultures transduced by a standard VV strain (Western Reserve) [19, 49]. MVA-induced DC death does not necessarily obviate the application of such cultures as a cancer vaccine. Previous findings have demonstrated that necrotic cell debris and apoptotic bodies derived from either DC or tumor cells can be phagocytosed by viable DC that subsequently cross-prime $CD4^+$ and $CD8^+$ antigen-specific T cells [3, 20, 29, 46].

Due to the extensive cell death observed in the MVA-transduced DC cultures, impairment of the allostimulatory capacity might be expected. However, DC cultures transduced with either the MVA-wt, MVA-

MUC1 or MVA-MUC1/IL-2 vectors displayed immunostimulatory activities equivalent to non-transduced DC. Most likely, the delayed cell death that occurs over several days provides ample time for the PBMC to mount a strong allo-proliferative response. Furthermore, neither the presence of IL-2 expressed by the MVA-MUC/IL-2 transgene nor the addition of exogenous IL-2 enhanced allo-PBMC proliferation. Because the lymphocyte response to allogeneic MHC antigens is extraordinarily robust and results in T cell secretion of immunostimulatory cytokines (including IL-2) [1], additional IL-2 would not necessarily further augment proliferation. For our MLR analyses, immature DC generated in the presence of GM-CSF and IL-4 were used. In similar studies of immature DC transduced with non-attenuated VV, both enhanced and reduced allo-MLR responses have been observed [18, 30]. These differences have been attributed to variances in individual donor lymphocyte responses [18].

In autologous MLR assays, PBMC proliferation was strongest in cultures containing MVA-MUC1/IL-2 transduced DC or upon addition of IL-2 to DC transduced with the MVA-wt or MVA-MUC1virus. These results indicate that the predominant PBMC response is against vaccinia virus antigens, as suggested by others applying VV-transduced DC [18]. Because our donors were vaccinated in childhood against smallpox, these individuals most likely possess low levels of vaccinia-specific, memory lymphocytes that are primed by the MVA-transduced DC and further expanded by IL-2 supplementation. In general, our findings portend well for the use of a recombinant MVA vector encoding IL-2 to support the outgrowth of low-frequency T cells.

Precursor lymphocytes recognizing MUC1 are rare, but can be detected in PBMC populations derived from at least some MUC1-vaccinated patients [10, 47]. Multiple in vitro stimulations with MUC1 peptide-pulsed DC have been shown to generate tumor-reactive CTL from PBMC of only a limited number of healthy donors [9]. Further experimentation will clarify presumed MVA-specific T cell responses and determine whether the MVA-MUC1/IL-2-transduced DC can prime T cell reactivity against MUC1. We do have promising preliminary results in mice immunized with DC transduced by the MVA-MUC1/IL-2 vector; vaccinated animals injected with human MUC1-expressing mouse tumor exhibit improved, tumor-free survival (manuscript in preparation).

Important issues for clinical development of MVA-MUC1/IL-2-transduced DC are whether TNF-α maturation influences recombinant MVA transgene expression and, conversely, whether MVA transduction would interfere with TNF-α induced maturation. Immature DC efficiently process antigen for MHC display, while matured DC initiate stronger antigen-specific T cell responses due to upregulation of MHC molecules, co-stimulatory molecules (such as CD80, CD86 and CD40) and certain chemokine receptors [21]. Thus, immunization with DC that have been transduced and subsequently matured would prove more effective in sensitizing anti-MUC1 T cells in vivo. Moreover, recent studies in humans have suggested that ex vivo maturation of DC is essential for the immune efficacy of DC [15, 32]. As indicated by known markers of maturation, MVA-MUC1/IL-2 transduction does not alter the potential of DC to undergo TNF-α-induced maturation or modify the maturation status. Furthermore, the levels of MUC1and IL-2 produced in immature and mature DC cultures are approximately the same.

Our results are in distinct contrast to previous findings of DC infected with non-attenuated VV strains. VV infection prior to maturation dramatically inhibits the upregulation of such molecules as HLA-DR, CD83 and the T cell co-stimulatory molecules CD80 and CD86. Maturation followed by VV transduction results in a loss of CD83, CD86 and CD80 expression [19, 30]. Consistent with the marker phenotype, the functional capacity of VV-transduced DC to stimulate PBMC responses is also reduced [19, 30]. Possibly, our results are accounted for by the type of culture media employed or the TNF-α maturation method, both of which differ from previous VV-DC studies. A more plausible explanation is that conventional VV strains, unlike MVA, express known "immune evasion genes" encoding functional receptors for TNF-α, IFN-γ and IFN-α/β [5, 7] that could well attenuate cytokine-induced DC maturation. Because MVA infection does not interfere with DC maturation, we would speculate that MVA-MUC1/IL-2 transduced DC would be more efficient in generating anti-MUC1 tumor responses than DC infected with conventional, non-attenuated VV vectors. Although further analyses are required to define the complex effects of MVA-derived vectors on target DC cells, vaccination with MVA-MUC1/IL-2-transduced DC may well elicit effective anti-tumor T cell responses and prove broadly applicable for the treatment of a wide number of known MUC1$^+$ tumor types.

Acknowledgments This work was supported by funds from the University of Arizona Medical Center, Tucson, Arizona, and the Arizona Disease Control Research Commission (contract no. 9931).

References

1. Abbas AK, Lichtman AH, Pober JS (1997) Cellular and molecular immunology. Saunders, Philadelphia
2. Acres B, Apostolopoulos V, Balloul JM, Wreschner D, Xing PX, Ali-Hadji D, Bizouarne N, Kieny MP, McKenzie IF (2000) MUC1-specific immune responses in human MUC1 transgenic mice immunized with various human MUC1 vaccines. Cancer Immunol Immunother 48: 588
3. Albert ML, Pearce SF, Francisco LM, Sauter B, Roy P, Silverstein RL, Bhardwaj N (1998) Immature dendritic cells phagocytose apoptotic cells via $\alpha_v\beta_5$ and CD36, and cross-present antigens to cytotoxic T lymphocytes. J Exp Med 188: 1359
4. Anderson PM, Bach FH, Ochoa AC (1988) Augmentation of cell number and LAK activity in peripheral blood mononuclear cells activated with anti-CD3 and interleukin-2. Cancer Immunol Immunother 27: 82

5. Antoine G, Scheiflinger F, Dorner F, Falkner FG (1998) The complete genomic sequence of the modified vaccinia Ankara strain: Comparison with other orthopoxviruses. Virology 244: 365
6. Banchereau J, Briere F, Caux C, Davoust J, Lebecque S, Liu YJ, Pulendran B, Palucka K (2000) Immunobiology of dendritic cells. Annu Rev Immunol 18: 767
7. Blanchard TJ, Alcami A, Andrea P, Smith, GL (1998) Modified vaccinia virus Ankara undergoes limited replication in human cells and lacks several immunomodulatory proteins: implications for uses as a human vaccine. J Gen Virol 79: 1159
8. Bronte V, Carroll MW, Goletz TJ, Wang M, Overwijk WW, Marincola F, Rosenberg SA, Moss B, Restifo NP (1997) Antigen expression by dendritic cells correlates with the therapeutic effectiveness of a model recombinant poxvirus tumor vaccine. Proc Natl Acad Sci USA 94: 3183
9. Brossart P, Heinrich KS, Stuhler G, Behnke L, Reichardt VL, Stevanovic S, Muhm A, Rammensee HG, Kanz L, Brugger W (1999) Identification of HLA-A2-restricted T-cell epitopes derived from the MUC1 tumor antigen for broadly applicable vaccine therapies. Blood 93: 4309
10. Brossart P, Wirths S, Stuhler G, Reichardt VL, Kanz L, Brugger W (2000) Induction of cytotoxic T-lymphocyte responses in vivo after vaccinations with peptide-pulsed dendritic cells. Blood 96: 3102
11. Burchell JM, Durbin H, Taylor-Papadimitriou J (1983) Complexity of expression of antigenic determinants recognised by monoclonal antibodies HMFG-1 and HMFG-2 in normal and malignant human mammary epithelial cells. J Immunol 131: 508
12. Burchell J, Gendler S, Taylor-Papadimitriou J, Girling A, Lewis A, Millis R, Lamport D (1987) Development and characterization of breast cancer reactive monoclonal antibodies directed to the core protein of the human milk mucin. Cancer Res 47: 5476
13. Carr-Brendel V, Markovic D, Ferrer K, Smith M, Taylor-Papadimitriou J, Cohen EP (2000) Immunity to murine breast cancer cells modified to express MUC-1, a human breast cancer antigen, in transgenic mice tolerant to human MUC-1. Cancer Res 60: 2435
14. Carroll MW, Moss B (1997) Host range and cytopathogenicity of the highly attenuated MVA strain of vaccinia virus: propagation and generation of recombinant viruses in a nonhuman mammalian cell line. Virology 238: 198
15. Dhodapkar MV, Steinman RM, Krasovsky J, Munz C, Bhardwaj N (2001) Antigen-specific inhibition of effector T cell function in humans after injection of immature dendritic cells. J Exp Med 193: 233
16. Di Nicola M, Siena S, Bregni M, Longoni P, Magni M, Milanesi M, Matteucci P, Mortarini R, Anichini A, Parmiani G, Drexler I, Erfle V, Sutter G, Gianni AM (1998) Gene transfer into human dendritic antigen-presenting cells by vaccinia virus and adenovirus vectors. Cancer Gene Ther 5: 350
17. Drexler I, Antunes E, Schmitz M, Wolfel T, Huber C, Erfle V, Rieber P, Theobald M, Sutter G (1999) Modified vaccinia virus Ankara for delivery of human tyrosinase as melanoma-associated antigen: induction of tyrosinase- and melanoma-specific human leukocyte antigen A*0201-restricted cytotoxic T cells in vitro and in vivo. Cancer Res 59: 4955
18. Drillien R, Spehner D, Bohbot AL, Hanau D (2000) Vaccinia virus-related events and phenotypic changes after infection of dendritic cells derived from human monocytes. Virology 268: 471
19. Engelmayer J, Larsson M, Subklewe M, Chahroudi A, Cox WI, Steinman RM, Bhardwaj N (1999) Vaccinia virus inhibits the maturation of human dendritic cells: A novel mechanism of immune evasion. J Immunol 163: 6762
20. Ferlazzo G, Semino C, Spaggiari GM, Meta M, Mingari MC, Melioli G (2000) Dendritic cells efficiently cross-prime HLA class I-restricted cytolytic T lymphocytes when pulsed with both apoptotic and necrotic cells but not with soluble cell-derived lysates. Int Immunol 12: 1741
21. Fong L, Engleman EG (2000) Dendritic cells in cancer immunotherapy. Annu Rev Immunol 18: 245
22. Gilewski T, Adluri S, Ragupathi G, Zhang S, Yao TJ, Panageas K, Moynahan M, Houghton A, Norton L, Livingston PO (2000) Vaccination of high-risk breast cancer patients with mucin-1 (MUC1) keyhole limpet hemocyanin conjuate plus QS-21. Clin Cancer Res 6: 1693
23. Girling A, Bartkova J, Burchell J, Gendler S, Gillett C, Taylor-Papadimitriou J (1989) A core protein epitope of the polymorphic epithelial mucin detected by the monoclonal antibody SM-3 is selectively exposed in a range of primary carcinomas. Int J Cancer 43: 1072
24. Gong J, Chen D, Kashiwaba M, Manome Y, Tanaka T, Kufe D (1997) Induction of antigen-specific antitumor immunity with adenovirus-transduced dendritic cells. Gene Ther 4: 1023
25. Gong J, Chen D, Kashiwaba M, Li Y, Chen L, Takeuchi H, Qu H, Rowse GJ, Gendler SJ, Kufe D (1998) Reversal of tolerance to human MUC1 antigen in MUC1 transgenic mice immunized with fusions of dendritic and carcinoma cells. Proc Natl Acad Sci USA 95: 6279
26. Goydos JS, Elder E, Whiteside TL, Finn OJ, Lotze MT (1996) A Phase I trial of a synthetic mucin peptide vaccine: induction of specific immune reactivity in patients with adenocarcinoma. J Surg Res 63: 298
27. Henderson RA, Nimgaonkar MT, Watkins SC, Robbins PD, Ball ED, Finn OJ (1996) Human dendritic cells genetically engineered to express high levels of the human epithelial tumor antigen mucin (MUC-1). Cancer Res 56: 3763
28. Henderson RA, Konitsky WM, Barratt-Boyes SM, Soares M, Robbins PD, Finn OJ (1998) Retroviral expression of MUC-1 human tumor antigen with intact repeat structure and capacity to elicit immunity in vivo. J Immunother 21: 247
29. Inaba K, Turley S, Yamaide F, Iyoda T, Mahnke K, Inaba M, Pack M, Subklewe M, Sauter B, Sheff D, Albert M, Bhardwaj N, Mellman I, Steinman RM (1998) Efficient presentation of phagocytosed cellular fragments on the major histocompatibility complex class II products of dendritic cells. J Exp Med 188: 2163
30. Jenne L, Hauser C, Arrighi JF, Saurat JH, Hugin AW (2000) Poxvirus as a vector to transduce human dendritic cells for immunotherapy: abortive infection but reduced APC function. Gene Ther 7: 1575
31. Jerome KR, Bu D, Finn OJ (1992) Expression of tumor-associated epitopes on Epstein-Barr virus immortalized B-cells and Burkitt's lymphomas transfected with epithelial mucin complementary DNA. Cancer Res 52: 5985
32. Jonuleit H, Schmitt E, Schuler G, Knop J, Enk AH (2000) Induction of interleukin 10-producing, nonproliferating $CD4^+$ T cells with regulatory properties by repetitive stimulation with allogeneic immature human dendritic cells. J Exp Med 192: 1213
33. Karanikas V, Hwang LA, Pearson J, Ong CS, Apostolopoulos V, Vaughan H, Xing PX, Jamieson G, Pietersz G, Tait B, Broadbent R, Thynne G, McKenzie IF (1997) Antibody and T cell responses of patients with adenocarcinoma immunized with mannan-MUC1 fusion protein. J Clin Invest 11: 2783
34. Kirk CJ, Mule JJ (2000) Gene-modified dendritic cells for use in tumor vaccines. Hu Gene Ther 11: 797
35. Koido S, Kashiwaba M, Chen D, Gendler S, Kufe D, Gong J (2000) Induction of antitumor immunity by vaccination of dendritic cells transfected with MUC1 RNA. J Immunol 165: 5713
36. Kotani H, Newton PB, Zhang S, Chiang YL, Otto E, Weaver L, Blaese RM, Anderson WF, McGarrity GJ (1994) Improved methods of retroviral vector transduction and production for gene therapy. Hum Gene Ther 5: 19
37. Kugler G, Stuhler G, Walen P, Zoller G, Zobywalki A, Brossart P, Trefzer U, Ullrich S, Muller CA, Becker V, Gross AJ, Hemmerlein B, Kanz L, Muller GA, Ringert RH (2000)

Regression of human metastatic renal cell carcinoma after vaccination with dendritic cell hybrids. Nat Med 6: 332
38. Lees CJ, Apostolopoulos V, Acres B, Ramshaw I, Ramsay A, Ong CS, McKenzie IF (2000) Immunotherapy with mannan-MUC1 and IL-12 in MUC1 transgenic mice. Vaccine 19: 158
39. Miles DW, Taylor-Papadimitriou J (1999) Therapeutic aspects of polymorphic epithelial mucin in adenocarcinoma. Pharmacol Ther 82: 97
40. Minev, BR, Chavez FL, Mitchell MS (1999) Cancer vaccines: novel approaches and new promise. Pharmacol Ther 81: 121
41. Morse MA, Lyerly HK (2000) Clinical applications of dendritic cell vaccines. Curr Opin Mol Ther 2: 20
42. Nishimura N, Nishioka Y, Shinohara T, Sone S (2000) Centrifugal enhancement of adenovirus-mediated gene transduction into human dendritic cells. Mol Ther 1: S56
43. Quinn ER, Lum LG, Trevor KT (1998) T cell activation modulates retrovirus-mediated gene expression. Hum Gene Ther 9:1457
44. Rowse GJ, Tempero, RM, VanLith, ML, Hollingsworth MA, Gendler SJ (1998) Tolerance and immunity to MUC1 in a human MUC1 transgenic murine model. Cancer Res 58: 315
45. Rughetti A, Biffoni M, Sabbatucci M, Rahimi H, Pellicciotta I, Fattorossi A, Pierelli G, Scambia G, Lavitrano M, Frati L, Nuti M (2000) Transfected human dendritic cells to induce antitumor immunity. Gene Ther 7: 1458
46. Sauter B, Albert ML, Francisco L, Larsson M, Somersan S, Bhardwaj N (2000) Consequences of cell death: Exposure to necrotic tumor cells, but not primary tissue cells or apoptotic cells, induces the maturation of immunostimulatory dendritic cells. J Exp Med 191: 423
47. Scholl SM, Balloul J-M, Le Goc G, Bizouarne N, Schatz, C, Kieny MP, Von Mensdorff-Pouilly S, Vincent-Salomon A, Deneux L, Tartour E, Fridman W, Pouillart P, Acres B (2000) A recombinant vaccinia virus encoding human MUC1 and IL-2 as immunotherapy in breast cancer patients. J Immunother 23: 570
48. Spehner D, Drillien R, Proamer F, Houssais-Pecheur C, Zanta M-A, Geist M, Dott K, Balloul J-M (2000) Enveloped virus is the major virus form produced during productive infection with the modified vaccinia virus Ankara strain. Virology 273: 9
49. Subklewe M, Chahroudi A, Schmaljohn A, Kurilla MG, Bhardwaj N, Steinman RM (1999) Induction of Epstein-Barr virus-specific cytotoxic T-lymphocyte responses pulsing dendritic cells pulsed with EBNA-3 A peptides or UV-inactivated, recombinant EBNA-3 A vaccinia virus. Blood 94: 1372
50. Sutter G, Moss B (1992) Nonreplicating vaccinia vector efficiently expresses recombinant genes. Proc Natl Acad Sci USA 89: 10847
51. Taylor-Papadimitriou J, Burchell J, Miles DW, Dalziel M (1999) MUC1 and cancer. Biochim Biophys Acta 1455: 310
52. Treon SP, Mollick JA, Urashima M, Teoh G, Charuhan D, Ogata A, Raje N, Hilgers JH, Nadler L, Belch AR, Pilarski LM, Anderson KC (1999) MUC1 core protein is expressed on multiple myeloma cells and is induced by dexamethasone. Blood 93: 1287

PALL Life Sciences

Scientific & Technical Report

PN 33289

Diafiltration: A Fast, Efficient Method for Desalting, or Buffer Exchange of Biological Samples

By Larry Schwartz, Senior Technical Manager, Pall Life Sciences

Diafiltration is a technique that uses ultrafiltration membranes to completely remove, replace, or lower the concentration of salts or solvents from solutions containing proteins, peptides, nucleic acids, and other biomolecules. The process selectively utilizes permeable (porous) membrane filters to separate the components of solutions and suspensions based on their molecular size. An ultrafiltration membrane retains molecules that are larger than the pores of the membrane while smaller molecules such as salts, solvents and water, which are 100% permeable, freely pass through the membrane.

This article will cover the concepts of protein concentration and diafiltration. It will compare different ways of performing diafiltration and their impact on process time, volume, product stability, and recovery.

CONCENTRATION

The solution retained by the membrane is known as the concentrate or retentate. The solution that passes through the membrane is known as the filtrate or permeate.

A membrane for concentration is selected based on its rejection characteristics for the sample to be concentrated. As a general rule, the molecular weight cut-off (MWCO) of the membrane should be 1/3rd to 1/6th the molecular weight of the molecule to be retained (3-6X Rule). This is to assure complete retention. The closer the MWCO is to that of the sample, the greater the risk for some small product loss during concentration. The risk increases if diafiltration will also be used since the relative loss depends on the total volume of filtrate that will be generated. Membrane flux rate (filtrate flow rate per unit area of membrane) is related to pore size. The smaller the pores, the lower the flux rate for the same applied pressure. Therefore, when selecting a membrane for concentration / diafiltration, one must consider the time factor versus product recovery. In most biological applications, recovery outweighs the time consideration. The process time can always be reduced by increasing the amount of membrane area used.

Figure 1 below provides an example of concentration. The sample is placed in a device containing a suitable ultrafiltration membrane that will retain the large molecules. Pressure is applied until half the volume has passed through the membrane. The large molecules are retained in half the original volume (concentrate), which also contains half of the salt molecules. The filtrate contains the other half of the salt molecules but none of the large molecules. Therefore, the large molecules are concentrated as liquid and salt are removed. The salt molecule to volume ratio in the concentrate remains constant so the ionic strength of the concentrated solution remains relatively constant.

Figure 1.
2X Concentration of Sample by Ultrafiltration

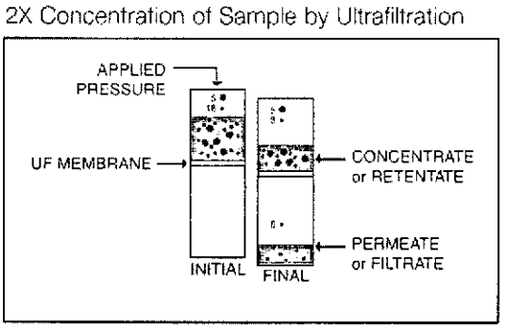

- Large molecules – bigger than pores in membrane
- Small molecules – salts or solvent

The ionic strength of the concentrate (retentate) solution can subsequently be reduced by "washing" the remaining salt out with water, a process called diafiltration. This is essentially a dilution process and is performed in conjunction with a concentration process. Water is added while filtrate is removed. If the washing solution is another buffer instead of water, the new buffer salt will replace the initial salt in the sample.

For simplicity, the above and subsequent examples use a direct flow filtration device such as a centrifugal concentrator. The same principles apply to cross flow filtration devices such as cassettes and hollow fibers where the retentate is recirculated.

BENEFITS OF DIAFILTRATION

Conventional techniques used for salt removal or buffer exchange such as membrane dialysis and column-based gel filtration can be effective but have limitations. Dialysis procedures can take up to several days, require large volumes of water for equilibration and risk product loss through manual manipulation of the dialysis bags. Gel filtration results in a dilution of the sample and often requires an additional ultrafiltration step to concentrate it back. Adding steps to a process can risk sample loss or possible contamination. With diafiltration, salt or solvent removal as well as buffer exchange can be performed quickly and conveniently. Another big advantage of diafiltration is that the sample is concentrated on the same system, minimizing the risk of sample loss or contamination.

There are several ways to perform diafiltration. While the end result may be the same, the time and volume required to complete the process may vary considerably. It is important to understand the differences in the methods used and when to choose one over the other.

CONTINUOUS DIAFILTRATION

The technique of continuous diafiltration (also referred to as constant volume diafiltration) involves washing out the original buffer salts (or other low molecular weight species) in the retentate (sample) by adding water or a new buffer to the retentate at the same rate as filtrate is being generated. As a result, the retentate volume and product concentration does not change during the diafiltration process. If water is used for diafiltering, the salts will be washed out and the conductivity lowered. If a buffer is used for diafiltering, the new buffer salt concentration will increase at a rate inversely proportional to that of the species being removed.

The amount of salt removed is related to the filtrate volume generated, relative to the retentate volume. The filtrate volume generated is usually referred to in terms of "diafiltration volumes". A single diafiltration volume (DV) is the volume of retentate when diafiltration is started. For continuous diafiltration, liquid is added at the same rate as filtrate is generated. When the volume of filtrate collected equals the starting retentate volume, 1 DV has been processed.

Using continuous diafiltration, greater than 99.5% of a 100% permeable solute can be removed by washing through 6 retentate volumes (6DV) with the buffer of choice.

Molecules that are larger than salts and solvents, but which are still smaller than the pores in the membrane, can also be washed out. The permeability of these molecules, however, may be less than 100%. In such cases, it will take more liquid, i.e. more DV's, to completely wash a partially permeable molecule through the membrane, compared to a 100% permeable molecule. Typically, the larger the molecule, the lower the permeability and the greater the wash volume required.

The permeability of a molecule through a specific membrane can be determined by measuring the concentration of the molecule in the filtrate compared to the concentration in the retentate under specified conditions.

$$\% \text{ permeability} = (\text{Conc.}_{\text{FILTRATE}} / \text{Conc.}_{\text{RETENTATE}}) \times 100$$

Permeability is often described in terms of "Rejection Coefficient" of the membrane, i.e. the membrane's ability to hold back or reject a given molecule from passing through.

$$\text{Rejection Coefficient} = 1 - (\text{Conc.}_{\text{FILTRATE}} / \text{Conc.}_{\text{RETENTATE}})$$

A rejection coefficient of 1 equals 0% permeability

A rejection coefficient of 0 equals 100% permeability

Permeability will be affected by such factors as transmembrane pressure (TMP), crossflow rate, retentate concentration, pH, and ionic strength, and gel layer formation (concentration polarization). Therefore, the permeability may change during the process.

Table 1 shows the relationship between permeability through a membrane and the number of diafiltration volumes required for removal of permeating species. As noted earlier, a greater volume of buffer is required to remove a molecule that is partially retained. To remove 99.9% of a molecule that is 25% permeable to the membrane requires 9 DV's, while for a 100% permeable species, only 7 DV's are required.

Table 1:
Continuous (Constant Volume) Diafiltration

Diafiltration Volumes	Permeability 100% Rejection Coefficient = 0	Permeability 75% Rejection Coefficient = 0.25
1	63%	53%
2	86%	77%
3	95%	89%
4	98.2%	95%
5	99.3%	97.6%
6	99.7%	98.9%
7	99.9%	99.4%
8		99.7%
9		99.9%

0% - Salts, solvents, buffers, etc.

25%- Molecules lower in MW than MWCO of membrane but bigger than salts

DISCONTINUOUS DIAFILTRATION – Sequential Dilution

Discontinuous diafiltration by sequential dilution involves first diluting the sample with water or replacement buffer to a predetermined volume. The diluted sample is then concentrated back to its original volume by ultrafiltration. This process is repeated until the unwanted salts, solvents, or smaller molecules are removed. Each subsequent dilution removes more of the small molecules.

As shown in Figure 2, the sample is generally diluted with an equal volume of buffer (1DV). Alternatively, multiple volumes can be added at once, provided the process tank is large enough to hold the entire volume. Diluting the sample usually lowers the viscosity, which may increase the filtrate flux rate.

Figure 2.
Discontinuous Diafiltration – Sequential Dilution

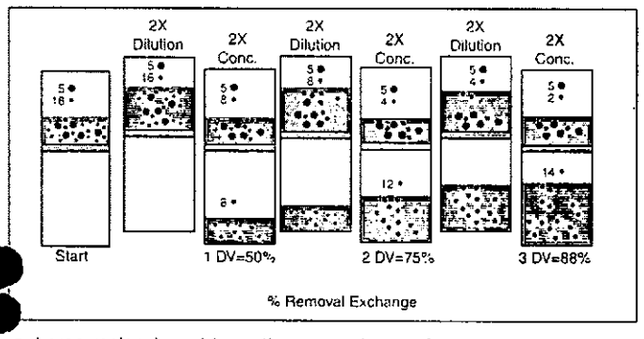

- Large molecules – bigger than pores in membrane
- Small molecules – salts or solvent

DISCONTINUOUS DIAFILTRATION – Volume Reduction

Discontinuous diafiltration by volume reduction reverses this procedure. The sample is first concentrated to a predetermined volume, and then diluted back to its original volume with water or replacement buffer. This is repeated until the unwanted salts, solvents, or smaller molecules are removed. Each subsequent concentration and dilution removes more of the small molecule (Figure 3).

Figure 3.
Discontinuous Diafiltration with Volume Reduction

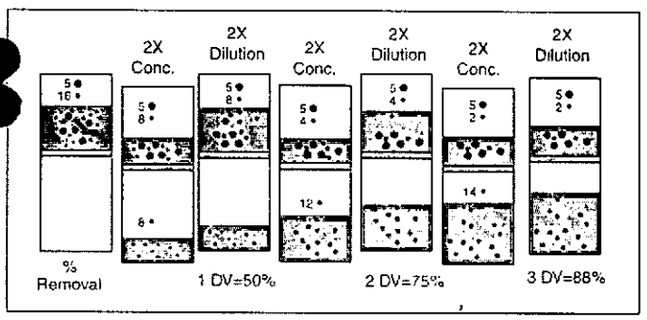

- Large molecules – bigger than pores in membrane
- Small molecules – salts or solvent

After the last buffer addition to complete diafiltration, the sample may be concentrated before analysis or the next purification step is performed.

The final product, after diafiltration by either method (discontinuous 2X volume reduction or sequential dilution) is at the same volume and concentration as when diafiltration started. The salt concentration has been equally reduced in both examples. However, the volume of diafiltration buffer used by the volume reduction method was half that used in sequential dilution. This is because the initial concentration step reduced the volume in half. A diafiltration volume is equal to the volume where dilution occurs. Therefore, half the volume was required.

This being the case, it would seem that concentrating before diafiltration, by either discontinuous sequential dilution or constant volume diafiltration, should reduce the required diafiltration buffer volume and save time. And in most cases this is true. The factor we have not accounted for is filtrate flux rate, which equates to process time. As the product becomes concentrated, viscosity increases and the filtrate flux rate decreases. The filtrate flux rate varies inversely as the log of the concentration factor.

$$J = k \ln(C_G / C_B)$$

Where

J = Filtrate Flux Rate

k = constant

C_G = gel layer concentration

C_B = retentate (bulk flow) concentration

This becomes very significant as the product concentration (C_B) increases above a few percent and is dependent on the characteristics of the specific molecules that make up the sample. So, although it might take significantly less volume to diafilter a concentrated sample, it could take considerably more time compared to a less concentrated sample. Simple protocols are available to find optimum conditions to maximize productivity.

Table 2.
Salt Reduction from Sample using Volume Reduction or Constant Volume Diafiltration

Diafiltration Volumes	2X Volume Reduction		Continuous Diafiltration (Constant Volume)	
	100% Permeable 0% Retention*	75% Permeable 25% Retention*	100% Permeable 0% Retention*	75% Permeable 25% Retention*
1	50%	41%	63%	53%
2	75%	65.%	86%	77%
3	88%	79%	95%	89%
4	94%	88%	98.2%	95%
5	96.9%	93%	99.3%	97.6%
6	98.4%	95.6%	99.7%	98.9%
7	99.2%	97.4%	99.9%	99.4%
8	99.6%	98.4%		99.7%
9	99.8%	99.0%		99.9%
10	99.9%	99.4%		

*Retention of smaller molecules

0% - Salts, solvents, buffers, etc.

25%- Molecules lower in MW than MWCO of membrane but bigger than salts

CONTINUOUS OR DISCONTINUOUS DIAFILTRATION - WHICH TECHNIQUE SHOULD BE USED?

When deciding which technique to use and where in the process to perform diafiltration, consider the following factors:

1) Initial sample volume, concentration and viscosity

2) Required final sample concentration

3) Stability of sample at various concentrations

4) Volume of buffer required for diafiltration

5) Total processing time

6) Reservoir size available

7) Economics

The choice of which method to use must be based on several criteria. Scale is an important consideration. What we will do at laboratory scale may be very different than at process scale, especially if the process is automated. At lab scale discontinuous diafiltration is often used for simplicity. Continuous diafiltration requires a pump or equipment to add the diafiltration solution at a constant rate. Both techniques can be automated for process applications. If we eliminate the equipment issue and focus on the process, we can compare the differences.

The ionic strength, buffer composition and stabilizer concentration can affect stability of the sample. Diafiltration may remove salts or stabilizing molecules, resulting in protein product denaturation and aggregation. The process of concentrating and diluting a protein solution can also affect molecular interactions resulting in denaturation or aggregation as well as subsequent precipitation and product loss. It is necessary to evaluate the effect of concentration on the product to determine where diafiltration is best performed relative to concentration effects.

Continuous diafiltration offers an advantage over discontinuous diafiltration in that the retentate concentration remains constant. It is often seen as a more gentle process relative to the stability of the product.

WHEN TO PERFORM DIAFILTRATION - BEFORE OR AFTER CONCENTRATION?

We have already seen that concentrating a sample first can significantly reduce the volume of diafiltration solution required. We have also seen that continuous diafiltration takes less volume than discontinuous diafiltration with sequential dilution. Therefore, if the sample is first concentrated to the final concentration required and then continuous diafiltration performed, acceptable results should be obtained.

However, above a certain concentration, filtrate flux rates may become prohibitively slow. It may actually takes longer to diafilter the concentrated sample than it would if the sample were first diluted to reduce the concentration. In this situation, even though continuous diafiltration of the diluted sample requires a greater diafiltration volume, the total processing time would be less due to the faster filtrate flux rate. (Process Time = Filtrate flow rate x Volume)

In general, the optimum retentate concentration for performing (continuous) diafiltration is at:

$\ln (C_G/C_R) = 1$ or $C_{R\ (optimum)} = C_G/e = 0.37C_G$ *

Where

C_G = gel layer concentration

C_R = retentate concentration.

$C_{R(Optimum)}$ = highest retentate concentration where diafiltration should be performed

The C_G value for a sample can be determined from experimentation by concentrating a sample on a membrane and recording and plotting data for filtrate flux rate vs. log concentration (or concentration factor). The curve can then be extrapolated to filtrate flux rate = "0". The C_G value will be the same for this product regardless of the starting concentration or filtrate flux rate.

Figure 4.
Determination of the C_G Value for a product

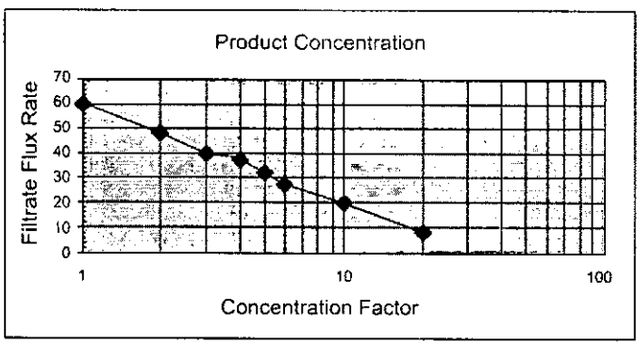

In this example (Figure 4) the C_G value is a concentration factor of approximately 33X. Therefore the optimal concentration to perform diafiltration would be $0.37C_G$ = 12.2X. If the starting product concentration is 5mg/mL, then diafiltration should be performed when the concentration reaches 61mg/mL. If the final concentration will be less than 61mg/mL, then diafiltration should be performed after concentration, unless it is necessary to remove a specific molecule prior to concentration.

The ultrafiltration product selected may dictate choice of continuous or discontinuous diafiltration. Stirred cells and centrifugal devices are best suited for discontinuous diafiltration because of their mode of operation. Tangential flow devices have the advantage of being useful for either diafiltration technique.

Summary

Diafiltration is a fast and effective technique for desalting or buffer exchange of solutions. It can be performed in a continuous or discontinuous mode. Continuous diafiltration usually takes less volume to achieve the same degree of salt reduction as discontinuous diafiltration with sequential dilution and can be easier to perform.

Continuous diafiltration is also perceived as a kinder and gentler process on active biomolecules. On the other hand, discontinuous diafiltration with volume reduction takes less volume than continuous diafiltration. Concentrating the sample before diafiltration usually reduces the required filtrate volume and saves time. However if the sample viscosity becomes too great, the filtrate flux rate decreases and the process time can increase substantially. Determining the C_G for the sample can help answer the question - At what concentration should I perform diafiltration?

Initial volumes from a few milliliters up to thousasnds of liters can be processed using Pall's Tangential Flow Filtration (TFF) products. Pall's tangential flow systems allow easy addition of membrane surface area, providing the flexibility to reduce processing time or scale up the process. This range of devices and systems provides scalability as well as the flexibility to work with almost any sample volume. Pall's highly selective OMEGA™ polyethersulfone (PES) membranes with narrow pore size distribution and high flow rates provide fast processing time and efficient separation for diafiltration.

* Industrial Ultrafiltration Design and Application of Diafiltration Processes, Beaton & Klinkowski, J. Separ. Proc. Technol., 4(2) 1-10 (1983)

Glossary

Diafiltration: Diafiltration is a technique that uses ultrafiltration membranes to completely remove or lower the concentration of salt or solvent, or to replace buffer salts from solutions containing proteins and other large molecules,

Diafiltration Volume: One diafiltration volume equals the initial volume in which the molecule of interest is suspended. The number of diafiltration volumes required depends on whether the permeating species is freely passing (salts, buffers, solvents) or partially retained.

Continuous Diafiltration: The technique of continuous diafiltration (also referred to as constant volume diafiltration) involves washing out the original buffer salts (or other low molecular weight species) in the retentate (sample) by adding water or a new buffer to the retentate at the same rate as filtrate is being generated

Discontinuous Diafiltration-Sequential Dilution: Discontinuous diafiltration by sequential dilution involves first diluting the sample to a predetermined volume, then concentrating the sample back to its original volume with water or replacement buffer. This is repeated until the unwanted salts, solvents, or smaller molecules are removed. Each subsequent dilution removes more of the small molecules

Discontinuous Diafiltration-Volume Reduction: Discontinuous diafiltration by volume reduction involves first concentrating the sample to a predetermined volume, then diluting the sample back to its original volume with water or replacement buffer. This is repeated until the unwanted salts, solvents, or smaller molecules are removed. Each subsequent concentration and dilution removes more of the small molecule.

PALL® Life Sciences

Pall Life Sciences
600 South Wagner Road
Ann Arbor, MI 48103-9019 USA

800.521.1520 toll free in USA
734.665.0651 telephone
734.913.6114 fax

United Kingdom
Europa House
Havant Street
Portsmouth, Hampshire
PO1 3PD

023 92 302600 telephone
023 92 302601 fax

*Filtration. Separation. Solution.*SM

Australia – Lane Cove, NSW
Tel: 02 9425-2333
1800 635-082 (in Australia)
Fax: 02 9425-5610
Austria – Wien
Tel: 043-1-49 192-0
Fax: 0043-1-49 192-400
Canada – Ontario
Tel: 905-542-0330
800-263-5910 (in Canada)
Fax: 905-542-0331
Canada – Québec
Tel: 514-332-7255
800-435-6268 (in Canada)
Fax: 514-332-0996
800-808-6268 (in Canada)
China – P. R., Beijing
Tel: 86-10-8458 4010
Fax: 86-10-8458 4001
France – St. Germain-en-Laye
Tel: 01 30 61 39 92
Fax: 01 30 61 58 01
Lab-FR@pall.com

Germany – Dreieich
Tel: 06103-307 333
Fax: 06103-307 399
Lab-DE@pall.com
India – Mumbai
Tel: 91-22-5956050
Fax: 91-22-5956051
Italy – Milano
Tel: 02-47796-1
Fax: 02-47796-394
or 02-41-22-985
Japan – Tokyo
Tel: 3-3495-8319
Fax: 3-3495-5397
Korea – Seoul
Tel: 2-569-9161
Fax: 2-569-9092
Poland – Warszawa
Tel/Fax: 22-635 83 83
Russia – Moscow
Tel: 095 787-76-14
Fax: 095 787-76-15

Singapore
Tel: (65) 389-6500
Fax: (65) 389-6501
Spain – Madrid
Tel: 91-657-9876
Fax: 91-657-9836
Sweden – Lund
Tel: +46 (0)46 158400
Fax: +46 (0)46 320781
Switzerland – Basel
Tel: 061-638 39 00
Fax: 061-638 39 40
Taiwan – Taipei
Tel: 2-2545-5991
Fax: 2-2545-5990
United Kingdom – Portsmouth
Tel: 023 92 302600
Fax: 023 92 302601
Lab-UK@pall.com

Visit us on the Web at www.pall.com

E-mail us at Lab@pall.com or Lab-UK@pall.com

2/03, 2.5k, GN02.0629 PN33289